THE STRUCTURAL AND STRATIGRAPHIC SETTING OF THE ROSH PINAH ZINC-LEAD DEPOSIT WITHIN THE GARIEP TROUGH

by

DENNIS JOHN ALCHIN

THESIS PRESENTED IN PARTIAL FULFILMENT OF THE REQUIREMENTS
FOR THE DEGREE OF MASTER OF SCIENCE
AT THE UNIVERSITY OF STELLENBOSCH

STUDY LEADER: Prof. I. W. Hälbich December 1993

"VERKLARING

Ek die ondergetekende verklaar hiermee dat die werk in hierdie tesis vervat, my eie oorspronklike werk is wat nog nie vantevore in die geheel of gedeeltelik by enige ander universiteit ter verkryging van 'n graad voorgelê is nie.

Handtekening

Datum

17/2/94

Samevatting

DIE STRUKTURELE EN STRATIGRAFIESE PLASING VAN DIE ROSH PINAH SINK-LOOD AFSETTING IN DIE GARIEP TROG.

'n Geologiese ondersoek in die Rosh Pinah, Obib, Pickelhaube en Namuskluft-Dreigratberg omgewings het die strukturele en stratigrafiese plasing van die Rosh Pinah lood-sinkafsetting in die Gariep Trog aangedui. Die sedimentêre evolusie van die Pan-Afrika Gariepgordel het begin met wydverspreide vorming van slenkdale, en die oopmaak van 'n oseaan (die Adamastoroseaan) met die skepping van 'n kontinentale rand. Afsetting van die basale klastiese Stinkfonteinopeenvolging as breë alluviale waaiers en kuslynsedimente het plaasgevind in 'n transgressiewe see.

Daarna is die Kaigas diamiktiete en vulkanoklastiese gesteentes van die Formasie Rosh Pinah as massavloei-afsettings gevorm in lokaal ontwikkelde grabens. Gedurende die finale fases van transgressie is sinsedimentêre ertslae in stiller waters neergelê terwyl rifkarbonate langs die kuslyn gevorm het. Hierdie sedimente is uiteindelik bedek deur mariene klastiese en karbonaat fasies wat afgeset is in 'n marginale see. Na die opheffing van die kraton het wydverspreide basiese gange en plate al hierdie sedimente geïntrudeer. Hulle word hier gegroepeer in die Formasie Rosh Pinah.

Gedurende die seevloeruitbreidingsfase van kontinentale evolusie is die klastiese en karbonatiese gesteentes van die Hildaopeenvolging afgeset in water van vlak tot intermediêre diepte. Die basale Wallekraalkonglomerate is as lokale waaiers met ondergeskikte puinstortings neergelê en word onderlê deur die karbonate van die Formasie Dabieriviér.

Hierna vind regressie plaas en is gestreepte ysterklip formasies afgeset in vlak depressies terwyl die glasiogene Numeesopeenvolging se diamiktiete onkonform oor die Hilda en die ysterklip neergelê is. Hulle word opgevolg deur die klastiese diepseegesteentes van die Holgatopeenvolging. Die Witputsopeenvolging oorlê die Numeesopeenvolging onkonform langs die kontak met vloergesteentes in

die ooste, en word gesien as 'n afgeleë vlakwater ekwivalent van die Holgatopeenvolging.

Gravitasietektoniek het 'n belangrike rol gespeel in die aanvanklike strukturele ontwikkeling van die Gariepgordel. Massavloeie en versakkingsstrukture vertoon prominent in half-grabenstrukture gedurende die slenkdalvormingsfase. Die sluiting van die Pan-Afrika Adamastoroseaan as gevolg van kontinentale botsing het egter gelei tot 'n periode van intense en uitgerekte SE-gerigte transpressie wat meeste gravitasiestrukture uitgewis het.

Die D_1 transpressiewe fase het NNW-strekkende vloeroorskuiwings gedurende 'n SE-gerigte tektoniese hoof-gebeurtenis veroorsaak. Dit het uiting gevind in 'n aantal tektoniese pulse om boogvormige nappe-strukture te vorm (bv. die Marmora-, Schakalsberg- en moontlik ook die Rosh Pinah-nappe) wat as skubbe oormekaar op die dekgesteentes ingeplaas is. Oorskuiwings het gepaard gegaan met oos-noordoos vergerende F_1 plooie met asse wat subparallel aan die D_1 vervoerrigting asook aan die strekking van 'n deurdringende en weshellende S_1 transposisie kliewing gerig is.

Gedurende die D_1-transpressiewe fase het die Schakalsberg oorskuiwing wat nou in die Schakalsberge dagsoom, 'n dik laag van digte basiese gesteentes met ofiolitiese eienskappe op 'n voorland oorgeskuif. Gravitasionele onstabilitiet het gevolglik in die kors ontstaan en 'n waaier van listriese takverskuiwings is gevorm aan die voorlandkant van die oorliggende en uitbreidende massa.

Soos die komplekse tektoniet vervolgens verder ontwikkel kon dit verskeie vervormingspaaie gevolg het. Drie gedeeltelik nie-kolineêre fases van vervorming sluit in: skuins opritte, terugskuiwing en terugplooiing.

Die Annisfontein antiklinorium kon gevorm het as 'n D_1 vloer oorskuiwing wat oor opritte geplooi is as gevolg van voortgesette druk vanuit die weste. Gedurende hierdie puls is ander D_1 strukture ook sub-ko-aksiaal herplooi deur nie-sillindriese WSW vergerende F_2 skuifskeurplooie as gevolg van oos-gerigte druk oor NNW strekkende opritte. Sulke strukture is blootgestel as terugplooie in die

Namuskluft-Dreigratberg omgewing en word ook afgelei vir die dieper vlakke van die westelike gebied.

Die semi-allochtone Formasie Rosh Pinah met die Rosh Pinah ertsliggame in die tipe gebied is herplooi gedurende D_2 in 'n hinterland vergerende antiklinorium as gevolg van sy nabyheid aan die groot skuinsopritte. Dit was ook verantwoordelik vir die steil opskuiwings in die Rosh Pinah-Namuskluft-Dreigratberg gebied, wat waarskynlik omgekeerde, hoogs vervormde graben en horst strukture verteenwoordig.

Op die oostelike flank van die Annisfontein antiklinorium het 'n hinterland-hellende dupleks uit opeengestapelde strukturele waaiers ontstaan bo-op die vervormde en oorgeskuifde sedimente (die Pickelhaube duplekstruktuur). Dit is die gevolg van die vasdruk en versteiling van opritte teen die vloergesteentes. Voortdurende opwaartsboggeling van die Annisfontein antiklinorium, of as gevolg van opstapeling van oorskuiwing, of as gevolg van veelvuldige opritte gevorm langs 'n oorspronklike vloerongelykheid, veroorsaak dat die oos-hellende dele van die Rosh Pinah-nappe gede-aktiveer is.

In die ooste mag beperkte laat (post-kompressie) gravitasionele gly van die oorgeskuifde sedimente in die dak van die Rosh Pinah-nappe die terugplooiing van oorgeskuifde Hildalitologieë aangehelp het.

Die feit dat litologieë skuins opgery het teen die kratoniese rand en dalk ook teen dieper gesetelde opritte, verklaar heel moontlik die D_3 strukture. As gevolg van differensieële beweging is hierdie F_3 plooie soms effens oorgeplooi na die suid-ooste. Sodoende het gly plaasgevind langs kliewingsvlakke om kleinskaalse oorskuiwing met 'n NE-SW strekking skuins tot die ouer strukture te vorm. Die interferensie van hierdie plooifase met die ouer strukture is verantwoordelik vir die noord-suid golwing van alle sigbare strukture en daarmee die landskap as sulks, soos gesien vanuit die ooste.

Die laat, laterale transtensiewe fases D_4-D_5 het gevolg op die intrusie van die Kuboos-Swartbank plutone en is nie goed verteenwoodig in hierdie studie area nie.

Die Gariepgordel was onderhewig aan 'n verlengde periode van laer groenskisfasies metamorfose (M_1), gevolg deur 'n tweede en lokale kontakmetamorfe episode (M_2) wat veroorsaak is deur die intrusie van die Kuboos en Swartbank plutone in die Richtersveld.

ABSTRACT

THE STRUCTURAL AND STRATIGRAPHIC SETTING OF THE ROSH PINAH ZINC-LEAD DEPOSIT WITHIN THE GARIEP TROUGH

A geological investigation in the Rosh Pinah, Obib and Pickelhaube Peaks and Namuskluft-Dreigratberg areas has established the structural and stratigraphic setting of the Rosh Pinah zinc-lead deposits within the Gariep Trough. The sedimentary evolution of the Pan-African Gariep Belt was initiated by widespread rifting and opening of an ocean (the Adamastor Ocean) along a continental margin. Deposition of the basal clastic Stinkfontein Sequence as broad alluvial fans and strandline sediments took place in the transgressive sea.

The mass flow Kaigas Formation diamictites and volcaniclastics of the Rosh Pinah Formation were subsequently deposited in locally developed grabens. Syn-sedimentary ore beds of hydrothermal origin (including Rosh Pinah orebodies) were precipitated on the sea floor while reef carbonates formed along the coast line during the final stages of transgression. These sediments were eventually covered by a marginal marine clastic and carbonate facies with widespread intrusion of basic sills and dykes following uplift of the craton. These rocks are here grouped within the Rosh Pinah Formation.

During the sea floor spreading stage of continental evolution the clastic-carbonates of the Hilda Sequence were deposited in a shallow to moderately deep-water environment. The Wallekraal conglomerates were deposited as local submarine fans with minor debris flows and are overlain by the Dabie River Formation carbonates.

During regression banded iron formations were deposited in shallow depressions and the glaciogenic Numees Sequence diamictites were deposited unconformably above the Hilda Sequence and iron formations. These in turn are overlain by the deep-water clastics of the Holgat Sequence. The Witputs Sequence, which unconformably overlies the Numees Sequence along the basement in the east is seen as a proximal shallow water equivalent of the distal Holgat Sequence.

Gravity tectonics played an important role during the early structural evolution of the Gariep Belt. Mass flow and slump structures featured prominently in half graben structures formed during the rifting stage. However, the closing of the Pan-African Adamastor Ocean as a result of subduction and continental collision led to a single, very intensive and protracted period of SE directed transpression, which largely obliterated all gravity deformation characteristics.

The D_1 transpressive phase produced NNW-trending basement-involved oblique ramps during a major SE-directed tectonic event, which culminated in several deformation pulses. Arcuate nappe structures were formed, e.g. the Marmora, Schakalsberg and possibly the Rosh Pinah Nappes as a result of the oblique emplacement of thrust slices over the cover rocks. Thrusting was accompanied by east-northeast-verging F_1 folds with axes rotated sub-parallel to the D_1 transport direction, and a penetrative westerly dipping S_1 transposition cleavage.

The master Schakalsberg Thrust emplaced a thick slice of dense basic rock with ophiolitic affinities onto a foreland situated in the Schakalsberg mountains during the D_1 transpressive phase. Gravitational instability was thereby caused in the crust, and an imbricate fan of listric splay faults formed in front of the overlying spreading mass.

Several deformation paths for the complicated tectonite containing three partly non-colinear phases of deformation can be envisaged from here which includes oblique ramping, backthrusting and backfolding. The Annisfontein anticlinorium may have formed as a D_1 basement thrust ramped up section and folded due to continued pressure from the W. During this pulse D_1 structures were sub-coaxially refolded by non-cylindrical WSW-verging F_2 shear folds because of E-directed compression across NNW trending ramps. This is displayed in the Namuskluft-Dreigratberg area and is also inferred for the deeper levels of the western areas, and leads to backfolding over most of the area.

The semi-allochthonous Rosh Pinah Formation containing the Rosh Pinah orebodies in the type area was refolded during D_2 into a hinterland-verging anticlinorium because of its proximity to the

major oblique ramps, which are also responsible for the steeply dipping thrusts in the Rosh Pinah-Namuskluft-Dreigratberg area, and which probably represent highly deformed earlier graben and horst structures.

On the eastern limb of the Annisfontein anticlinorium, a hinterland-dipping duplex of imbricate fan sheets developed on the deformed and overthrust sediments (the Pickelhaube Duplex Structure) as a result of ramping and steepening against the basement. Continued upward bulging of the Annisfontein anticlinorium due to either antiformal thrust stacking or multiple ramping along an initial basement irregularity on the footwall resulted in east-dipping parts of the Rosh Pinah Nappe Thrust being inactivated.

Late, limited gravitational gliding of the overthrust sediments along the Rosh Pinah Nappe Thrust towards the east may have followed contractional deformation to enhance backfolding of thrust slices of Hilda lithologies in the duplex zone. The oblique ramping of lithologies against the cratonic margin and possible deeper seated ramps finally also accounts for D_3 structures.

Due to differential movement these F_3 folds may be slightly overturned towards the southeast, with slip occurring along cleavage planes to outline minor thrusting oblique to the previous events and trending NE-SW. This folding phase resulted in the present day north-south undulation of the structures and the landscape.

The late lateral transtensive phases D_4-D_5 resulted from the emplacement of the Kuboos-Swartbank plutons and are not well represented in this area.

The Gariep Belt has been subject to a protracted period of lower greenschist facies metamorphism (M_1), followed by a second local contact-thermal event (M_2) which resulted from the emplacement of the Kuboos and Swartbank plutons in the Richtersveld.

INDEX

LIST OF FIGURES

LIST OF TABLES

APPENDIX

LIST OF FIGURES

LIST OF TABLES

1. INTRODUCTION

1.1 Objective of Study

Mapping by Von Veh (1988) has indicated the complex stratigraphic and structural relationships of the Gariep Belt rocks south of the Orange River, which resulted from extensive regional thrusting.

Against this background the stratigraphic and structural relationships in the Rosh Pinah area (Fig. 1) were studied along two traverses, and the basement/cover relationships were also examined in the Namuskluft-Dreigratberg area (Fig. 2).

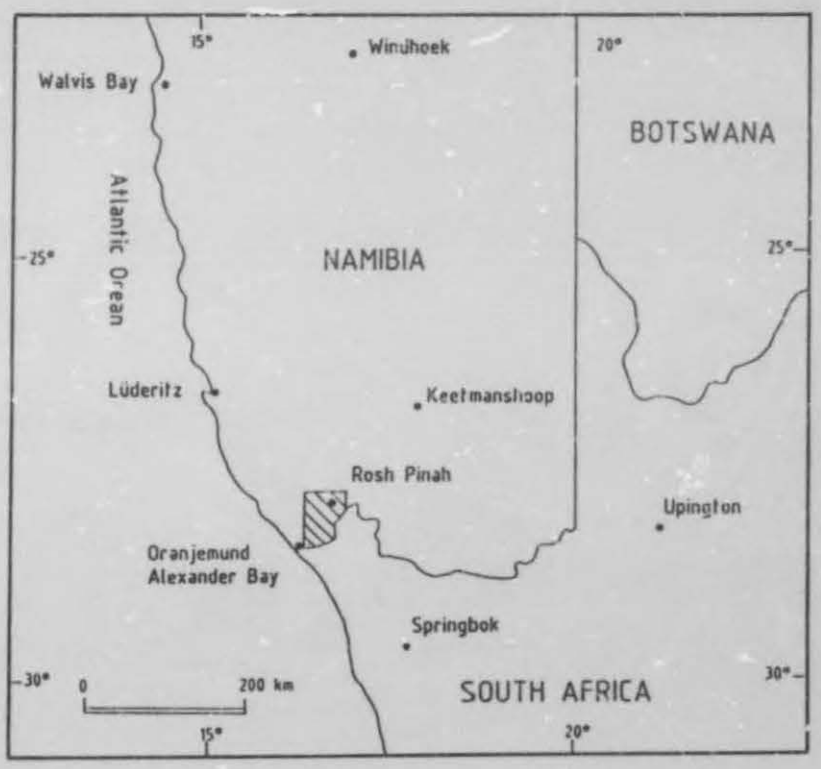

Fig. 1 Locality plan of study area.

Apart from a structural tectonic analysis to expand and amplify on the work of Von Veh (1988), the ultimate aim of the study was to try to clarify the stratigraphic and structural position of the economically important Rosh Pinah Formation within the broader Gariep Trough. These results

have implications for further exploration of the area but are not discussed in this study.

1.2 Location and Physiography

Detailed geological mapping covered 290 square kilometres along specific traverses in the area south and west of Rosh Pinah and in parts of Diamond Area No 1 (Fig. 2).

A large sandy plain extending N-S forms the central part of the region, and is bounded by Gariep rocks forming the Obib and part of the Namuskluft mountains. Elevations vary from a maximum of 902m at Obib Peak, to 50m at the Orange River. The main access to the area is via a gravel road leading from Rosh Pinah to the State Water Scheme (Fig. 2) at the Orange River. Several tracks give adequate access to the outcrops on Namuskluft, while valleys between the hills in the Sperrgebiet can comfortably be negotiated by four wheel drive vehicle.

The climate is arid with an average annual rainfall of only 72mm and sparsely distributed xerophytic shrubs and hardy grass grow along dry watercourses. The well-known Kokerboom (Aloe dichotoma) and the characteristic Halfmens (Pachypodium namaquensis) are prominent on many of the koppies and hills. Part of this area has been proclaimed as a nature and recreational reserve.

1.3 Previous research

While extensive investigations have been undertaken on the South African side of the Orange River (the barren Richtersveld), the area in southwestern Namibia has received less attention as it is partially covered by the prohibited diamond area (Sperrgebiet).

The first reconnaissance survey on the South African side of the Orange River was undertaken during 1915 by Dr A.W. Rogers, and was followed by an extensive mapping program by De Villiers and Söhnge during 1959. Since 1963 the Precambrian Research Unit of the University of Cape Town has been studying the crustal evolution in the southwestern part

GEOLOGICAL MAP OF THE SENDELINGSDRIF - ROS

LOCALITY MAP

NUMAISSPITZE

(RPNT)

ROSH PINAH NAPPE THRUST

ROSH PINAH ANTIFORM

ROSH PINAH

OBIB WATERHOLE

OBIB WATERHOLE THRUST

OBIB MOUNTAINS

OBIB

OBIB PEAK THRUST

VALLEY THRUST

GUMCHAVIB THRUST (GT)

PICKELHAUBE

ANNEXURE 3

MAJOR F3 SYNFORM

GAMSKONTEIN ANTICLINORIUM

GOMTSAWIS MOUNTAIN

LEGEND

- Surficial Cover
- Karoo Dolerite
- Amphibolite
- Dolomite, limestone, schist, conglomerate, arkose — Witputs Sequence
- Diamictite, ferruginous schist, banded iron formation — Numees Sequence
- Dolomite, marble, limestone (partly brecciated) — Dabie River Formation
- Feldspathic grit, quartzite, conglomerate; Schist, phyllite, minor conglomerate — Wallekraal Formation
- Dolomitic limestone, minor chert — Pickelhaube Formation — Hilda Sequence
- Quartz-biotite-muscovite schist; Dolomitic limestone, calcareous quartzite; Acid volcanics, arkoses, quartzites, minor argillite — Rosh Pinah Formation
- Quartzite, arkose, minor limestone and felsic volcanics — Gumchavib Formation — Stinkfontein Sequence
- Garieb Belt
- Granodiorite, leucogranite — Vioolsdrif Suite
- Mafic and felsic volcanics — Orange River Group

KEY

- Lithological contact
- Dip & strike of bedding
- Major overthrust (Teeth on overriding block)
- F-F Fault
- Fault (inferred)
- F1 F2 F3 Antiform
- Synform
- Outline of Annexure 1
- Outline of Annexure 2 & 3
- Trigonometrical beacon
- Mine or mineral prospect
- Road or track
- Settlement
- E-F N-S section line
- OT Obib Peak thrust
- OWT Obib Waterhole thrust
- GT Gumchavib thrust

Scale 1 : 100 000

0 1 2 3 4 5 6 7 8 9 10 Km

16° 45'

Compiled and drawn by D.J. Alchin (1990-1992)
Based on the 1:100 000 map of M.D. McMillan (1968) and strip mapping

AP OF THE SENDELINGSDRIF - ROSH PINAH AREA

FIG. 2.

NUMAISSPITZE

ROSH PINAH

ROSH PINAH NAPPE THRUST

ROSH PINAH ANTIFORMORIUM

NUMEES THRUST

MAJOR F3 STRUCTURE?

ANNEXURE 1

ANNEXURE 2

ANNEXURE 3

ROSH PINAH VALLEY

NAMUSKLUFT

NAMUSKLUFT THRUST

NAMUSKLUFT SYNCLINORIUM

NUMEES ANTICLINE

SOLE THRUST

DREIGRATBERG THRUST

DREIGRATBERG NORTH

DREIGRATBERG

DREIGRATORIF

LORELEI

DREIGRATBERG SYNCLINE

SENDELINGSDRIF SYNCLINORIUM

ORANGE RIVER ANTICLINE

STATE WATER SCHEME

IAKKALSBERG THRUST

ORANGE RIVER

SENDELINGSDRIF

OBIB MOUNTAINS

OBIB WATERHOLE

OBIB WATERHOLE THRUST

OBIB

OBIB PEAK THRUST

VALLEY THRUST

GUMCHAVIB THRUST (GT)

GUMCHAVIB

GOMTSAWIB MOUNTAIN

PICKELHAUBE

ANNAFONTEIN ANTICLINORIUM

(RT-NT)

(VT)

(OT)

(OWT)

(GT)

Gariep Belt

Vioolsdrif Suite

Orange River Group

E-F N-S section line

OT Obib Peak thrust

OWT Obib Waterhole thrust

GT Gumchavib thrust

Scale 1 : 100 000

0 1 2 3 4 5 6 7 8 9 10 Km

28° 00'

16° 45'

of the African continent (Martin, 1965). Several mapping projects have been undertaken, the most recent being the research of Von Veh (1988).

The discovery of the Rosh Pinah orezone in southern Namibia during regional mapping by McMillan in 1963 generated interest in this area. Mining and prospecting activities (Page and Watson, 1976; Page and Kindl, 1978; Van Vuuren, 1986; Siegfried, 1990) broadened the local geological knowledge.

The geology of the Western Richtersveld and adjacent coastal areas was revised by A. Kröner in 1969-1970,. and several researchers worked in the area during this period (Kröner and Germs, 1971; Kröner and Rankama, 1972; Kröner, 1972, 1974, 1977a, 1977; Kröner and Welin, 1973; Kröner and Jackson, 1974; Kröner and Blignault, 1976; Kröner and Hawkesworth, 1977; Kröner et al., 1980; Von Veh, 1988).

1.4 Present research

Kröner (1974), differed from McMillan's (1968) regional geological interpretation and set out to remap the Rosh Pinah-Obib hills area but never completed the project. This and the general lack of a modern tectonic analysis served as a stimulus to study the area more closely.

This study combined photogeological mapping with structural, stratigraphic and minor sedimentological data gathering and interpretation. The method used in this polyphase deformed area was to carefully document and analyze all large and small scale structures and try to relate them to each other as far as style and attitude were concerned, and as far as possible over areas homogeneous at least with respect to one major structural element.

Special attention was paid to the following features:

a) varying bedding attitudes

b) fold interference patterns

c) deformation of older planar and linear structures

In the field a Breithaupt Coclar structural compass was used and fabric elements were plotted as poles on equal area lower hemisphere stereographic projections (Schmidt net) by utilizing the Pascal computer program written by C. Stowe (1988) of the Precambrian Research Unit, University of Cape Town. The direction and angle of dip or plunge of planar or linear fabric elements respectively are indicated.

Finite strain analysis of certain rocks in the area was undertaken by measuring deformed particles within the Numees diamictite, and conglomerate pebbles within the Wallekraal Formation. The Rf/θ method of Ramsay (1967) was applied using the standard theta graphs of Lisle (1985).

Petrographic examinations were undertaken on thin sections to record metamorphic minerals and paragenesis, and to study their relationships to microstructures. Twenty rock samples were also analyzed by X-ray diffraction to define the mineralogy. Fourteen thin sections were stained with a solution of Alizarin red and potassium ferricyanide to differentiate between calcite and dolomite.

1.5 Regional Setting

The Gariep Belt is an arcuate north-south trending tectonic unit straddling the Orange River and stretching from south of Kleinzee in the north-western Cape to due south of Luderitz Bay in south-western Namibia.

The Gariep sediments were originally deposited in a coastal geosyncline, which includes the Saldanian, Gariep, Damaran, and West Congo fold-thrust belts, all of which were formed during the upper Proterozoic/lower Palaeozoic Pan-African event (Clifford, 1967; Stowe et al., 1984; Fig. 3).

The Gariep Trough has a strike length in the order of 400 km with an inland extension of up to 80km, and the sediments lie unconformably on the metavolcanics (De Hoop and Haib Subgroups) and metasediments (Rosyntjieberg Formation) of the

early Proterozoic (Kibaran-age) Orange River Group of the Richtersveld Subprovince (De Villiers and Söhnge 1959).

The metavolcanics have been intruded on a large scale by the cogenetic ≈ 1900-1730 Ma Vioolsdrif Granitoid Suite (Blignault, 1977; Reid, 1977, 1979, 1982). Highly metamorphosed and deformed suites of granites and gneisses of the Bushmanland and Gordonia Subprovince of the Namaqua Province lie in contact with the Richtersveld Subprovince.

Previously the Gariep cover rocks were seen as a geosynclinal assemblage containing an eastern "miogeosynclinal" and a western "eugeosynclinal" unit. (Martin, 1965; McMillan, 1968; Kröner, 1972, 1974, 1975). Currently it is interpreted as a tectonostratigraphic sequence and has been named the "Gariep Complex" (South African Committee for Stratigraphy, (SACS, 1980), "Gariep Arc" (Davies and Coward, 1982), "Cariep Province" (Tankard et al., 1982) and "Gariep Belt" (Von Veh, 1988).

The belt can be divided into two structural entities, viz. an eastern "Port Nolloth Zone" and a western "Marmora Terrane" which are separated by the Schakalsberg thrust fault (Stowe et al., 1984; Hartnady et al., 1985). The Port Nolloth Assemblage (Von Veh, 1988) is considered a para-autochthonous unit located on the western edge of the Kalahari Craton, while the Marmora Terrane is seen as an allochthonous ophiolite terrane.

The late Precambrian-Cambrian clastic-carbonate lithologies of the Nama Group have been deposited within a foreland basin to the east. Major units of the group are the lower Kuibis, overlain by the Schwarzrand and finally the Fish River Subgroups (Germs 1972, 1974). Germs (1983) relates the deposition of the Nama above the Gariep to a single major geotectonic cycle with the deposition of the upper Schwarzrand and Fish River Subgroups occurring during uplift associated with the Damaran orogeny.

A number of pre-, syn-, and post-tectonic intrusions provide age limits for the Gariep Belt. The largest of the

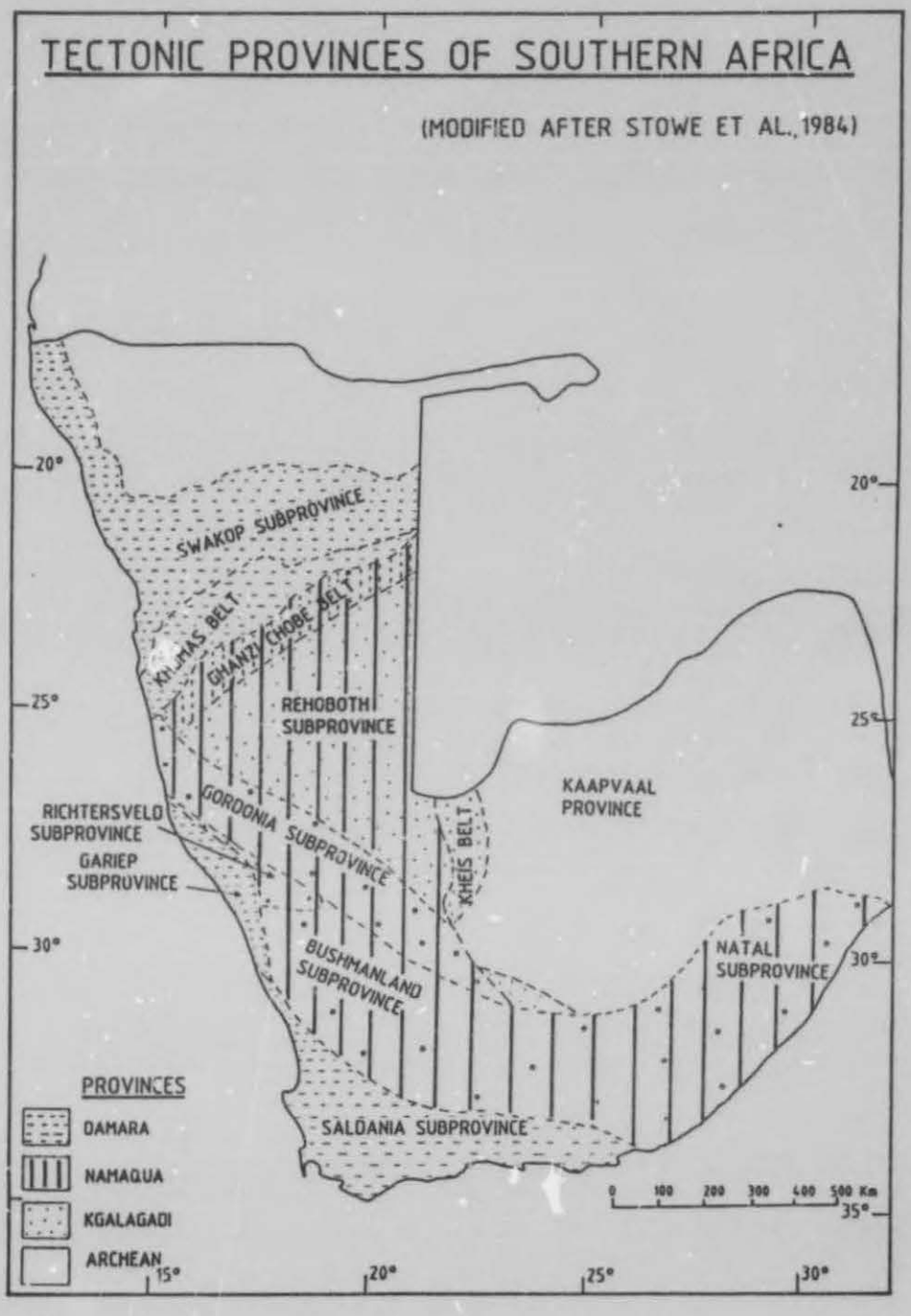

Fig. 3 *Tectonic provinces of Southern Africa (modified after Stowe et al., 1984).*

intrusions consists of a large batholith (the Kuboos pluton) and two smaller plutons of granite and leucogranite (Van Biljon, 1939; Söhnge and De Villiers, 1948), and the Gannakouriep dyke swarm defined by northeast trending mafic

and ultramafic rocks (De Villiers & Söhnge, 1959; Middlemost, 1964; Kröner & Blignault, 1976; Reid, 1979).

A late set of aplite, granite porphyry, basic and bostonite dykes of early Phanerozoic age cut the plutons (Kröner & Hawkesworth, 1977).

The Namib desert dunes cover most of the western part of the Gariep Belt over a considerable area and no detailed mapping has been undertaken here.

1.6 Geochronology

Dating of the Gariep Belt rocks has been very unsuccessful up to the present as radiometric ages obtained cannot be interpreted with certainty as primary ages. The presence however, of several syntectonic and post-tectonic intrusives have yielded primary radiometric ages, which can be correlated with episodes of the later Gariep history (Tankard et al., 1982).

Fig. 4 is modified after Von Veh (1988) and summarizes dates and tectonic events. The sedimentation stage of the Gariep Belt rocks can be placed in the period 630-900 Ma as confirmed by several age measurements e.g. the intrusion of pre-Gariep alkali granites and syenites of the Richtersveld Igneous Suite at ± 900 Ma (Allsopp et al., 1979) which marks the lower limit.

The Gannakouriep dykes intrude the Richtersveld Igneous Suite as well as the lower part of the Stinkfontein Sequence and define a minimum age of 717±11 Ma for the base of the Gariep Belt (Reid et al., 1991). Other age limits for Gariep intrusive Gannakouriep Dyke Suite, e.g. ^{40}A[illegible]s falling in the range 500-550 Ma (Reid, 1977; similar ages of 543 ± 15 Ma as stated in De Villiers [illegible], and 542 ± 4 Ma in Onstott et al. (1986), are thought to be reset ages.

The minimum age of the Gariep Belt is confirmed by the age of the post-tectonic Kuboos-Bremen line of plutonic intrusives with Rb-Sr dates of 500-550 Ma (Nicholayson and

Burger, 1965). This age can be compared to the age of Damara deformation at 650-550 Ma, (Kröner, 1982; Downing and Coward, 1981), and the Gariep and Damara Belts are therefore interpreted to form part of the widespread Pan-African tectono-thermal event (Kennedy, 1964).

In the Rosh Pinah area felsites have been dated by Rb-Sr methods at 719 ± 28 Ma by Welke (in De Villiers, 1968) and 683 ± 32 Ma by Allsopp et al., (1979). Köppel (1987) established model $^{207}Pb/^{208}Pb$ ages for Rosh Pinah lead ores but concluded that the values of 1065 to 1145 Ma appeared to be too old.

The minimum age for the basement rocks to the Gariep Belt (the Orange River Group) is defined by the radiometric age for the intrusive Vioolsdrif Suite at 1731-1900 Ma (Reid, 1979), which are cogenetic and temporally closely related.

2. REGIONAL STRATIGRAPHY

The most recent stratigraphic classification (modified after Von Veh, 1988) is outlined in Table 1. Minor adjustments and extensions to the lithostratigraphy and some rearranging of certain formations, e.g. the Rosh Pinah Formation are made here.

2.1. Basement Complex

2.1.1 Distribution and stratigraphy

The Richtersveld Subprovince is underlain by the volcano-sedimentary sequence of the Orange River Group (ORG) and the co-genetic intrusive Vioolsdrif Suite, which form the basement to the rocks of the Gariep Belt. The Orange River Group appears as steeply dipping, NNW-striking wedges of volcanic rocks, in contrast to the Namaqua Mobile Belt pegmatite belts and shear zones, which generally strike oblique to this direction towards the NW.

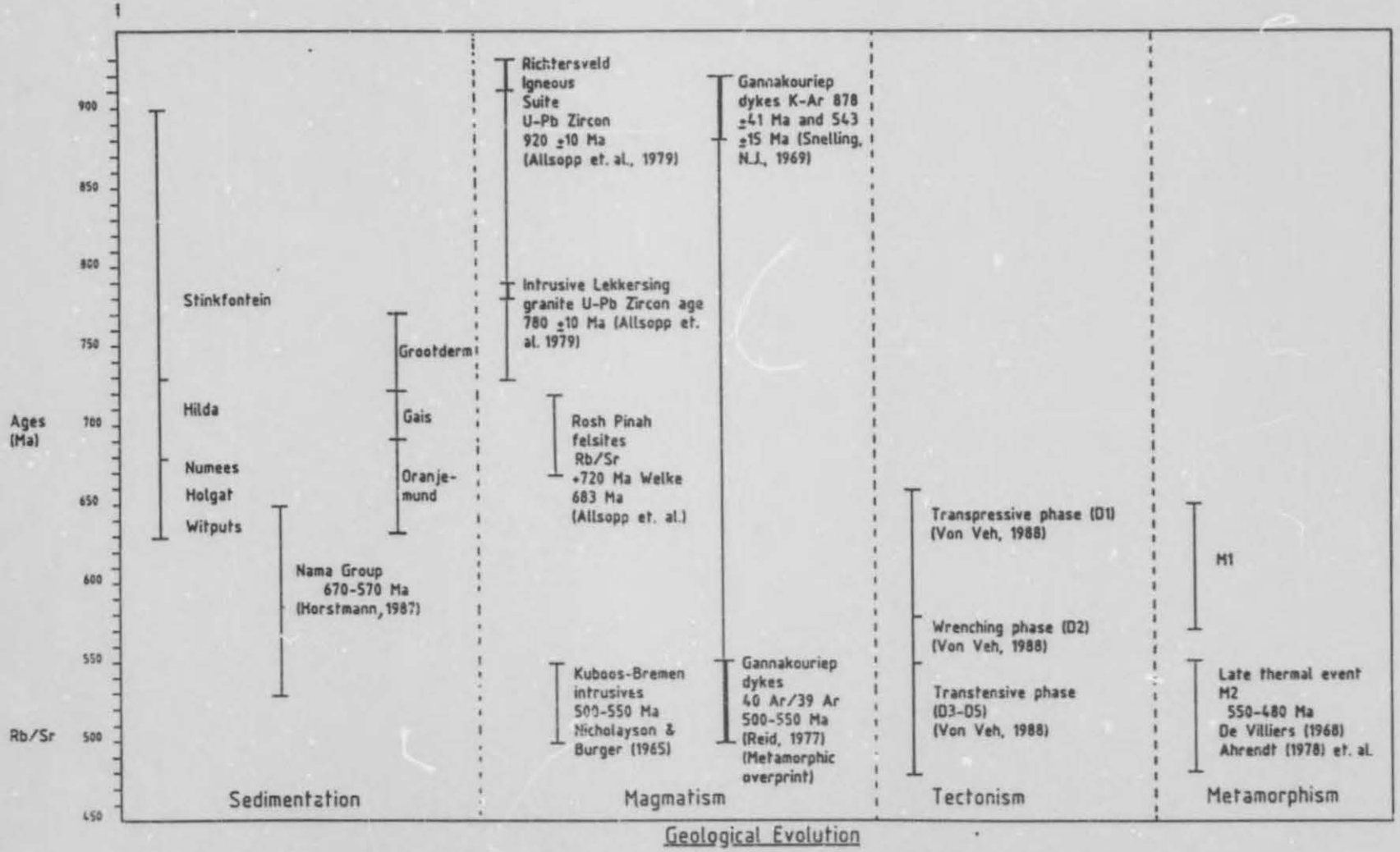

Fig. 4 Interpreted chronological evolution of the Gariep Belt (modified after Von Veh, 1988). Some key dates of intrusive phases (outlined by thick bar) which place relative dates on the different sequences are given.

Blignault (1977) has divided the ORG into three units as follows:

Orange River Group
- Haib Subgroup (Wilgenhoutdrif Series)
- Rosynebos Formation (Kaaien Series)
- De Hoop Subgroup (Marydale series)

He recognized three volcanic units within the De Hoop Subgroup, which forms the lowermost exposed portion of the basement rocks. These units are a leucocratic quartz feldspar porphyry, which structurally overlies a darker feldspar porphyry, which in turn is overlain by a mesocratic mafic aphanite. On the farm Aussenkjer the mafic De Hoop volcanics were recognized with intercalated lenses of volcanic breccia. These volcanic rocks are unconformably overlain by the Rosyntjieberg Formation (formerly the Rosynebos Formation), which is a very distinct unit constituting all the sediments in the ORG.

The main members of the unit are ortho- and feldspathic quartzites, ripple marked iron formation and iron rich psammites and pelites (Shimron, 1987). The upper Haib Subgroup can be divided into a mafic Nous Formation and a felsic Tsams Formation (Blignault, 1977).

The Orange River Group rocks have been subjected to the almandine-amphibolite facies of metamorphism. No basement to the ORG has ever been recognised.

2.1.2 Lithology

In the study area only the De Hoop Subgroup is exposed and consists dominantly of dark green chlorite-biotite schists containing quartz and feldspar phenocrysts. These rocks are fine-grained and well-foliated and are intercalated with fine-grained grey quartz-sericite schists containing feldspar phenocrysts.

The intrusive Vioolsdrif Suite (grey gneissic granite of De Villiers & Söhnge, 1959) is a general name for numerous types of intrusions including basic-ultrabasic complexes, diorites, tonalites, granodiorites, adamellites, leucogranites and minor amounts of mineralized porphyritic intrusives (Minnit, 1992). In the Rosh Pinah area prominent outcrops of this suite underlie low hills due east of the Gariep Belt (Fig. 2).

The granodiorite rocks are grey-brown, mesocratic and medium to coarse-grained with occasional lenticular mafic inclusions. They consist of quartz, plagioclase, K-feldspar and mafic minerals, which include hornblende and biotite. Accessory amounts of sphene, rutile, leucoxene, zircon and opaque minerals are also present (Minnit, 1992).

2.1.3 Depositional environment

Blignault (1977) has established that the De Hoop Subgroup is composed mostly of dacite, although the full range from andesitic to rhyolitic lavas are present. The Orange River Group therefore constitutes a differentiated lava suite with a predominant dacite and andesite character. These rocks form part of a calc-alkaline series (Reid, 1974).

Due to intense deformation the volcanic breccias and tuffs of the Haib Subgroup lack primary structures, which could indicate subaqueous deposition. No pillow structures have been identified, and Blignault (1977) uses this as evidence for a subareal environment.

2.2 The Stinkfontein Sequence

2.2.1 Distribution and stratigraphy

Von Veh (1988), groups the lithologies immediately overlying the basement in the Annisfontein anticlinorium (Annexure 3) within the Stinkfontein Sequence and names them the Gumchavib Formation after a prominent peak 1 km north of the Orange River. He stratigraphically places this formation at the top of the Stinkfontein Sequence above the Lekkersing Formation.

SACS (1980), Tankard et. al. (1982)		Von Veh (1988)			Current study		
Miogeosynclinal facies	Eugeosynclinal facies	Port Nolloth Assemblage		Marmora Terrane	Port Nolloth Assemblage		Marmora Terrane
			Kuboos-Bremen line			Kuboos-Bremen line	
NAMA GROUP			Nama Group			Nama Group	
		Holgat Sequence			Witputs Sequence	Namuskluft Formation	
Numees Formation		Numees Sequence	Sendelingsdrif Formation Jakkalsberg Formation		Numees Sequence	Sendelingsdrif Formation Jakkalsberg Formation	
Hilda Suite	Holgat Suite	Hilda Sequence	Dabie River Formation Wallekraal Formation Pickelhaube Formation		Hilda Sequence	Dabie River Formation Wallekraal Formation Pickelhaube Formation	Oranjemund Suite
	Oranjemund Suite			Oranjemund Suite			
Stinkfontein Formation	Grootderm Suite	Stinkfontein Sequence	Kaigas Formation Gumchavib Formation Vredefontein Formation Lekkersing Formation	Grootderm Suite	Stinkfontein Sequence	Rosh Pinah Formation Gumchavib Formation Vredefontein Formation Lekkersing Formation	Grootderm Suite
		Basement Complex			Basement Complex		

TABLE 1: STRATIGRAPHIC CLASSIFICATION OF THE GARIEP BELT (POST 1980)

Observations of Haughton (1961, 1963), indicate that Gannakouriep dykes intrude only Stinkfontein beds but not other Gariep lithologies and that members of the latter are absent in places where basement and Stinkfontein rocks are in proximity to one another. A similar situation occurs in the Obib mountains.

The Stinkfontein Sequence was originally subdivided into 4 members by Van Biljon (1939) from the top to the base:

Vetberg quartzites and schists
Klein Dwarsberg quartzites
Gelykwerf grits, quartzites and thin conglomerates
Dwarsberg group of quartzites with alternating schists

Joubert & Kröner (1972, p.48), however proposed a two fold sub-division based on lithological differences:

Upper Stinkfontein Formation
Lower Stinkfontein Formation

These two formations were changed to the Lekkersing and Vredefontein Members by SACS (1980).

The Vredefontein Member (Lower Stinkfontein Formation) has an interbedded relationship with an upper diamictite-dolomite unit, the Kaigas Member (Kröner, 1974). Von Veh (1988) interprets this member as consisting of all the diamictite-grit units immediately overlying the Lekkersing and Vredefontein Members as well as the basement complex.

According to Von Veh (1988) the Numees Prospect diamictite (the original type locality of the Numees Formation) is thus interbedded in the Kaigas. This redefinition does away with the enigmatic multiple repetitions of diamictite-dolomite units of previous authors, e.g. Kröner (1974), leaving only two horizons viz. the Kaigas and Numees diamictites.

The major part of the diamictites occurring north of Dreigratberg are therefore interpreted by Von Veh (1988) as the Kodas beds of the Kaigas Formation. The relationship

with the overlying dolomites of the Dreigratberg and Five Sisters is described as interfingering.

The Stinkfontein lithologies in the study area (the Rosh Pinah and Gumchavib Formations) occur along an elongated zone striking from south of the Orange River to due west of Rosh Pinah, forming parts of the Obib and Gumchavib mountains, and in the Rosh Pinah area. These rocks were originally grouped within the Hilda Sequence (McMillan, 1968).

Evidence for a meaningful correlation of the Rosh Pinah Formation (previously the Kapok Formation) is scarce. It has been correlated by the Geological Survey (Dr. P. Hugo, pers. com. to SACS, 1978) with the upper Stinkfontein Formation of the Richtersveld. Structural considerations obtained during the current study confirm this interpretation and correlate the Rosh Pinah Formation with the central to upper parts of the Gumchavib Formation of the Stinkfontein Sequence.

The correlation is also favoured for the following reason:- both formations contain similar lithologies e.g. the feldspathic quartzites/arkoses and felsic volcanics. The latter are however, more prevalent in the Rosh Pinah Formation. Outcrops of felsite occur due east of the Valley Thrust near Obib Peak (Annexure 3) in the Gumchavib Formation, and thin horizons of quartz-sericite schists may also be interpreted as felsites.

Other speculative correlations have been with the Wallekraal Formation (Von Veh, 1988, and Hoffmann, 1989), who see the Rosh Pinah Formation as either a local turbidite facies occurring at the base of the Hilda Sequence, or as a facies of the middle Wallekraal Formation.

A correlation of the Rosh Pinah and Wallekraal Formations is rejected because lithologies such as felsic volcanics, basic and/or amphibolitic dykes, and continuous dolomite bands are not found in the Wallekraal Formation. No continuous outcrops between the two formations can be found. On the southern boundary of the farm Zebrafontein to the northeast of the study area the Rosh Pinah Formation unconformably overlies the Vioolsdrif Suite along a basal conglomerate.

2.2.2 Lithology

The Gumchavib rocks consists of a monotonous sequence of massive or cross-bedded grits, arkoses and calcareous quartzites, which unconformably overlie the basement. North-south trending amphibolite dykes and sills are intrusive in the sequence and could possibly be correlated with the Gannakouriep Dyke Swarm. Similar amphibolite dykes are also present within the Rosh Pinah Formation.

McMillan (1968), recognized two lithostratigraphic units with a gradational contact within the Hilda Sequence (here interpreted as Stinkfontein lithologies) north of the Orange River (the G_{2Qc1} and G_{2Qc2} units). The upper unit consists of blue-grey clastic carbonate beds with intercalated calcareous quartzite beds up to 50m thick. This upper unit is here placed in the Rosh Pinah Formation. The lower quartzite unit may be up to 1000m thick, but has suffered thrust duplication and is placed within the Gumchavib Formation.

In the Rosh Pinah area the Rosh Pinah Formation consists mainly of a thick sequence of arkosic to feldspathic quartzite with intercalated argillites, amphibolite, porphyritic felsite, limestone and minor conglomerate horizons as well as local carbonate mudflow deposits in the upper parts.

2.2.3 Depositional environment

Deposition of the sedimentary rocks took place during the Pan-African cycle of geosynclinal filling and deformation, and is thought to be related to a rifting phase. Most previous workers agree that the Stinkfontein sediments have been deposited as an alluvial fan or as several broad coalescing fans in a proximal to distal braid plain environment (Middlemost, 1966; De Villiers & Söhnge, 1959; Tankard et al., 1982, Von Veh, 1988). Sediments were eroded from an uplifted region to the east.

The Gumchavib arenites were deposited under quieter submerged conditions (Von Veh, 1988) as conglomerates are virtually

absent, crossbedding is scarce and beds are thin. Intercalated calcareous quartzites confirm these conditions.

These types of alluvial fans prograde across the basin axis, away from the faulted or uplifted basin margin. A possible analogue may be drawn with parts of the Newark basin (Arguden & Rudolfo, 1986), in which the following deposits were identified: debris flow deposits (matrix – supported conglomerates), streamflood deposits (clast – supported conglomerates), braided stream strata (coarse pebbly sandstones), sheetflood deposits (medium-to fine-grained sandstone) and a waning-flood facies (thin mudstones). Towards the final phases of filling of the basin, several thin dolomite horizons were formed.

Within the Rosh Pinah Formation the presence of widespread extrusions of felsic lavas together with basic lavas are evidence of a very unstable crust weakened through repeated stretching. These weak zones eventually ruptured and formed elongated conduits for voluminous outpouring of lavas. Rapid deposition of immature feldspathic sediments preceded as well as postdated the volcanic extrusions, and deposition seems to have ended when the rift sediments were covered by the so-called drift sediments (Hilda Sequence).

Some relevant Stinkfontein outcrops in the Gariep Belt (Von Veh, 1988) which have a stratigraphic relationship to outcrops north of the Orange River will be discussed briefly.

Numees Prospect beds

This locality was the original type area for the Numees Group, and a correlation with the Stinkfontein Sequence (Von Veh, 1988) therefore merits a discussion.

De Villiers & Söhnge (1959) recognized a four-fold subdivision in the Numees beds:

Upper Stage	Upper dolomites
	Arkoses, grits etc.
	Lower dolomites
Lower stage	Tillite

Van Veh (1988) claims that a correlation of these Numees Prospect diamictites with the Sendelingsdrif diamictites (Numees Sequence) is incorrect for the following reasons:

1. The Numees Prospect beds rest on basement rocks and Stinkfontein quartzites, whereas the Sendelingsdrif beds are underlain by Hilda sediments.

2. The Numees Prospect beds are interbedded with grit, arenite and phyllite, while the Sendelingsdrif Numees is unbedded and massive.

3. The Numees Prospect beds do not contain a near basal iron formation or ferruginous zone (the Jakkalsberg Formation).

4. Carbonate erratics are conspicuously absent in the Numees Prospect beds, but are present in the Sendelingsdrif diamictite.

5. The overlying beds do not resemble each other.

Von Veh (op. cit.) therefore assigns the Numees Prospect beds to the older Stinkfontein Sequence as the Kaigas diamictite.

The distribution of the Kaigas diamictic beds are attributed to a debris flow deposition mechanism (Von Veh, 1988) as inferred from:

a) limited geographic distribution
b) sharp upper and lower bedding contacts
c) massive internal structure
d) correlation between clast sizes and bedding thickness
e) rapid westward decrease in clast sizes.

The diamictites near Dreigratberg north (Fig. 2) which overlie the basement contain varved beds (Fig. 5) and quartzites at their base (Fig. 6) together with carbonate clasts suggesting a correlation with the Sendelingsdrif Formation of the Numees Sequence rather than the debris flow deposited Kaigas Formation. Large scale bedding features are also present (Fig. 7).

Fig. 5 *Varved ripple-marked siltstone of the Sendelingsdrif Formation with some prominent dropstones. The locality is 0,5 km southwest of Lorelei Mine. Photo lens for scale.*

2.3 The Hilda Sequence

2.3.1 Distribution and stratigraphy

The Hilda rocks were initially described as the Kaigas Series by Rogers (1915). Kröner (1974) however, established that the Hilda rocks are younger than the Stinkfontein Formation and considered them equivalent to the Holgat Formation.

The Hilda rocks were redefined by Von Veh (1988) and their distribution reduced as compared with the classification of previous authors (Kröner, 1982). They unconformably overlie the Stinkfontein Sequence and consist of a mixed sequence of limestones, dolomites, schists, quartzites, grits and conglomerates.

Fig. 6 *Ripple-laminated quartzite at the base of the Numees diamictite of the Sendelingsdrif Formation (at same locality as above). Geological hammer for scale.*

The relationship of the Hilda Sequence to the Rosh Pinah Formation has been interpreted as a facies change (Davis & Coward, 1982), and Von Veh (1988), but McMillan (1968 p.64) interprets the contact as unconformable as he has located a thin talus conglomerate containing felsite pebbles, limestone, grit and dolomite overlying two small hills of felsite along his major Namuskluft Fault (Jakkalsberg Thrust, Fig. 2).

A threefold subdivision of the Hilda rocks based on lithological characteristics (Von Veh, 1988) has been made as follows:

Lower carbonate unit (Pickelhaube)
Mixed rudite-argillite unit (Wailekraal)
Upper dolomite unit (Dabie River)

Von Veh (1988) limits the Hilda to four exposures in the Richtersveld:

1.Anniskop beds of the Annisfontein anticlinorium
2.Knubus beds

3.The Helskloof Pass beds
4.The Hakiesdoring beds

Fig. 7 *Large scale bedding within the Sendelingsdrif Formation diamictites near Namuskluft synclinorium. The thickness of the near vertical darker coloured unit is approximately 30m (Locality P/11, Annexure 1).*

The beds relevant to this study are briefly discussed below.

Anniskop beds

The Anniskop beds are found in the Annisfontein anticlinorium where these dolomitic limestone beds of the Pickelhaube Formation rest conformably on and interfinger with the Gumchavib arenite. In the study area these rocks are grouped within the Rosh Pinah Formation as they contain numerous amphibolite sills and dykes.

The overlying Wallekraal Formation is a 1400m thick sequence of arenite and rudite, alternating with mica schists and phyllite with only poorly developed carbonate.

Khubus beds

In the Richtersveld the Pickelhaube Formation is represented by a thin marble on the eastern limb of the Sendelingsdrif synclinorium (Von Ven, 1988).

In the study area Hilda beds occur in the southern Namuskluft syncline, and along the eastern limb of the Annisfontein anticlinorium (Fig. 2).

2.3.2 Lithology

The Pickelhaube dolomitic limestone in the study area is a fine-grained, blue-grey rock containing thin laminations, which are here mostly interpreted as an intense bedding parallel tectonic fabric. The thin lenses of grey to reddish brown arkoses and grey-white phyllite, which are occasionally interbedded south of the Orange River (Von Veh, 1988) are here regarded as the upper part of the Rosh Pinah Formation. Quartz and calcite veins are abundant in the dolomitic limestone.

The major rock types of the Wallekraal Formation north of the Orange River are light-brown to blue-grey quartzites and arkosic grits with numerous intercalated lenses of conglomerates. The conglomerates are made up of a variety of boulders, cobbles and pebbles in a light-coloured gritty or quartzitic groundmass.

The clasts range from well-rounded to angular and have been flattened tectonically. The texture is clast-supported and the constituents consist essentially of vein-quartz and quartzite, with lesser amounts of gneissic granite, granodiorite, quartzitic sandstone, grit, micaschist, phyllite and minor dolomite. Intercalated feldspathic grits and arenites range in colour from beige-brown or reddish-blue in the south to dark-grey in the northern outcrops.

Isolated irregular to subrounded and angular masses of dolomite up to several tens of metres in diameter are found throughout the Wallekraal Formation. These bodies are

usually very dark-coloured and unbedded and probably represent bioherms.

The Wallekraal lithologies are poorly sorted, with both normal and inverse grading. In certain instances the inverse bedding was found to occur on the overturned limbs of east-verging isoclinal F_1 folds (Fig. 8).

Fig. 8 *East-verging isoclinal F_1 fold in Wallekraal conglomerates truncated by D_1 thrust. The locality is approximately 4km to the east of Pickelhaube Peak.*

Different clast size ranges are present within different lenses but the largest clasts are always dolomitic and were subject to the most intense tectonic deformation. Numerous rip-up fragments of the Wallekraal schists are present in the conglomeratic units.

The conglomerates and grits form sharp contacts with green-grey fine-grained schists (the Wallekraal schists) or may grade into this rock with some large feldspar grains along the contact. The schists are fine to medium-grained, silvery blue-grey to greenish-grey laminated rocks. In thin section (specimen NT 128) the schists consist essentially of quartz and muscovite, with accessory biotite, chlorite, feldspar and

opaque minerals. The well-cleaved rocks are often also graphitic.

Shearing within the schists is shown by small brown-coloured sandstone units, which have been attenuated to form strings of eye-like lenses up to 20cm in length and 5cm thick.

2.3.3 Depositional environment

The Pickelhaube Formation was probably deposited in a relatively shallow water to moderately deep water carbonate shelf paleo-environment. Von Veh (1988) ascribes the calcitic composition of the carbonates, the lateral persistence of beds, presence of parallel laminations, absence of stromatolites, and relatively high argillaceous and graphitic content to a moderately deep water environment. The presence of graded beds may be added to this list.

The better rounded clasts of mainly quartzitic rocks indicate a high energy depositional environment for the Wallekraal Formation in what could have been a submarine fan environment. The presence of angular clasts of e.g. dolomites suggest a contribution by local slumping from bioherms.

The lateral discontinuity of the conglomerate and quartzite units suggests deposition in channels in the upper fan or in suprafan lobes in the midfan region (Von Veh, 1988). A moderate to deep water euxinic environment is inferred as suggested by the presence of fine-grained carbonaceous sediments. The presence of near shore biogenic structures within the Dabie River carbonates suggest deposition as a barrier bar or shelf lagoon within a shallow water carbonate platform environment (Von Veh, 1988).

The complex Pickelhaube dolomite contact relationship with the underlying Stinkfontein Sequence (as seen in the interfingering with the Kaigas diamictite at Five Sisters and at Dreigratberg by Von Veh, 1988) cannot be confirmed here. The Dreigratberg dolomites are here grouped within the much younger Witputs Sequence, which is correlated with the Holgat

Sequence, as they stratigraphically overlie the Numees diamictites (Table 1).

2.4 The Numees Sequence

2.4.1 Distribution and stratigraphy

The non-genetic term diamictite will be used here in preference to mixtite, tillite etc. All diamictitic rock types north of the Orange River, which fill two thoroughly deformed north-westerly trending synclinoria that line up over a strike distance of some 120 km have been grouped together as the Numees Formation (SACS 1980). These rocks conformably overlie the Hilda Sequence (Kröner, 1974 p.24) in the Richtersveld.

Kröner (1974) described a highly ferruginous zone along the contact of the Hilda Sequence with the Numees Sequence, which Von Veh (1988) subsequently named the Jakkalsberg Formation.

Von Veh (1988) has subdivided the diamictitic rocks to the south of the Orange River into an older Kaigas Group within the Dreigratberg syncline and the younger Numees Sequence within the Sendelingsdrif synclinorium (Annexure 1). The redefined Numees Sequence of Von Veh (1988), would then consist only of the main Sendelingsdrif diamictites and the Bloeddrif beds around the hinge of the Annisfontein anticlinorium.

Within the Witputs Trough the Numees is paraconformably overlain by Nama beds and the two formations locally show concordant folding.

2.4.2 Lithology

Previous researchers have grouped an upper dolomitic unit within the Numees Sequence (McMillan, 1968) in the Namuskluft and Witputs areas, but Van Veh (1988) found evidence that these rocks belong to the dolomitic Holgat Sequence. This study confirms a younger age for the upper dolomitic unit and defines them as the Witputs Sequence (Table 1).

In the study area the Numees Sequence consists of interbeds of magnetite-quartzites, iron rich- and iron poor-schists, arkoses and diamictites. The schists are usually dark-green, well-cleaved chlorite bearing rocks forming sharp contacts with the other lithologies and are interpreted as original submarine muds. Numerous dropped-in pebbles and boulders, mostly of granitic origin are present in the latter (Fig. 9).

Fig. 9 Granitic dropstone within dark green chloritic diamictite of the Jakkalsberg Formation. The locality is near the western slope of Dreigratberg (Q/17, Annexure 1).

Banded magnetite-quartzites (iron formations) are prominent near the eastern limb of the Dreigratberg syncline in the study area where they are duplicated by thrusting. The overlying diamictitic unit has been named the Sendelingsdrif Formation by Von Veh (1988), who subdivided it into the Nabab River and the Bloeddrif beds respectively in the Richtersveld.

The 700m thick Nabab River beds have a markedly disconformable basal contact along the western limb of the Sendelingsdrif synclinorium (Fig. 2). This disconformity may have an entirely tectonic origin as the basal contact is

paraconformable where it is unfaulted north of Khubus (Von Veh, 1988).

North of the Orange River the contact is also faulted (Fig. 2). The Jakkalsberg banded ironstone and iron-rich quartzite and schist beds are located a few metres above the unconformity.

The Bloeddrif beds in the Richtersveld lie along the western limb of the Annisfontein anticlinorium, and have a thickness of only 100m. These beds are para-conformable with the underlying beds, but become extensively imbricated towards the north with the overlying dolomites. In the study area they crop out in the area of the upthrust granites in the vicinity of Gumchavib Peak (Annexure 2) where they unconformably overlie the Wallekraal Formation.

2.4.3 Depositional environment

Deposition of the Numees Sequence took place on an uneven terrain as several small basins are still preserved over a wide area. Most of the previous researchers favour a glacial origin (Rogers, 1915; De Villiers & Söhnge, 1959; Martin, 1965; McMillan, 1968; and Von Veh, 1988) although alternative depositional models have been proposed.

Kröner & Rankama (1972, p.14) proposed a subaqueous setting whereby glaciogenic material became partly incorporated into turbidites through processes of reworking. Davies & Coward (1982) favour a model with the diamictite forming as a molasse-type deposit in a foreland basin during regional overthrusting. If the latter applies more clasts of Gariep lithologies would be expected.

Certain features, e.g. the occurrence of dolomites and banded iron formations within the sequence are incompatible with a glacial origin, but have been explained by the alternate precipitation of iron and silica through the admixture of cold oxygenated water or as a result of convective overturn related to tidewater glaciers (Young, 1982, p.733). The laminated (varved) siltstones or shales with dropped-in

pebbles and unsorted boulder and pebble beds are taken as evidence of a glacial deposition.

The extensive lateral distribution and relative textural homogeneity of clasts implies a widespread source area rather than point sources (Hoffman, 1983). The presence of outsized extrabasinal lonestones and clusters of clasts of particular lithologies in groups can be taken as evidence of ice-rafting processes (Von Veh, 1988). Glacial deposition was preceded by a period of fluvial deposition as indicated by cross-bedded sandstone and grit lenses. During the waning period of glaciation till material bound in large ice rafts melted and was deposited in glacial lakes.

The periods of glaciation culminated in brief warmer periods during which limestone and dolomite beds were formed e.g. the lenticular dolomite units north of the Dreigratberg (Fig. 2).

As granitic lithologies dominate in the eastern Richtersveld, a source region in this area seems likely but minor lithologies of the underlying Hilda Sequence suggest that these rocks were already lithified at the time of Numees glaciation and that glacial movement took place over the basin edge. The basin shoaled towards the east and north as indicated by widespread varved shales, e.g. forming the base of the Numees diamictite on Namuskluft (N/6, Annexure 1).

2.5 The Witputs Sequence

2.5.1 Distribution and stratigraphy

A sequence of clastic and carbonate rocks are exposed along the escarpment in the study area trending from northeast of the Namuskluft farmstead to the Orange River. This sequence unconformably overlies the Numees along the escarpment and in the Witputs graben (McMillan, 1968).

These lithologies were originally grouped within the Numees Formation (McMillan, 1968), but they are classified here as the Witputs Sequence following Hoffman (1989) who proposed the name Witputs Group. The term "sequence" is preferred as

it is used to define rock units bounded by major faults or unconformities.

Kröner (1974) observed that the top of the Numees in the above mentioned area is always composed of cream-yellow dolomite followed by greenish siltstone, which is similar to the stratigraphy on Dreigratberg (Fig. 10) and which is here correlated with the Witputs Sequence.

Fig. 10 Dolomitic rocks of the Witputs Sequence within the Dreigratberg forming a sharp contact with the Sendelingsdrif diamictites (darker coloured).

The rocks have suffered extensive thrusting and may represent more than one sequence. Their correlation with other Gariep rocks is not always clear. An alternative stratigraphic placing of these rocks has been given by Kröner (1982), who suggested that they may form part of the basal Rosh Pinah Formation with the diamictite forming a lower member of the sequence. Hoffman (1989) states that the group consists of four as yet informal units but does not elaborate. As the Sendelingsdrif diamictites form a continuous sequence south and north of the Orange River, these rocks are excluded from the Witputs Sequence.

Stratigraphic relationships observed in the Namuskluft area (Annexure 1) indicate that the rocks of the Witputs Sequence unconformably overlie the Numees diamictites. These lithologies have also been thrust over the underlying Precambrian volcanic and granitic basement rocks of the Orange River Group and Vioolsdrif Suite respectively (Annexure 1).

2.5.2 Lithology

The sequence consists of a variety of light-grey, cream-coloured, pinkish to blue-grey dolomites and limestones with intercalated argillites and conglomerates. From the base upwards a blue-grey limestone is conformably overlain by a cream-coloured dolomite. This is followed by a chloritic schist, which is again overlain by cream-coloured dolomite. On this follows a carbonate mudflow bed followed by a pinkish limestone sequence, which is finally overlain by an intermittent quartzite/arkose unit.

A pisolitic dolomite occurs near the Orange River. The lowest cream-coloured dolomite has lenses of a light-yellow to brown and dark-grey banded to conglomeratic limestone at its base. Banding is present on a 5-10cm scale and elongated clasts of yellowish carbonate are enclosed in a snow-white carbonate matrix. The overlying chlorite schist (originally a siltstone) is similar to the Wallekraal schists and is characterized by the presence of small sheared grit bands. A sliver of tectonised carbonaceous shale along the contact to the basement may represent remnants of an older sequence that contains pre-tectonic amphibolite dykes.

2.5.3 Depositional environment

A shallow to moderate deep water euxinic platform type environment of deposition is inferred for the Witputs Sequence as indicated by the presence of pisolitic and dolomitic carbonates with possible stromatolitic structures, carbonaceous schists and tabular crossbedded sandstones. The Witputs Sequence is regarded as a proximal basin edge equivalent of the distal Holgat Sequence.

2.6 The Holgat Sequence

2.6.1 Distribution and stratigraphy

A group of poorly exposed and intensely deformed clastic-carbonate beds occur on the western side of the Gariep Belt. These rocks have a diachronous contact with the other formations of the Gariep Belt, and Von Veh (1988) places this Holgat Sequence stratigraphically above the Numees Sequence. He has discovered a thin horizon of Numees diamictite with its characteristic near-basal ferruginous quartzite that underlies the Holgat beds in the area east of the Goms and Omkeer trigonometrical beacons.

Hoffmann (1989) correlates the Holgat Formation with the 'Upper Dolomite' of the Numees Sequence (here redefined as the Witputs Sequence). This is unconformably overlain by the basal Dabis Formation quartzite of the Kuibis Subgroup of the Nama Group in the Witputs escarpment.

The characteristic pink or cream-coloured dolomite of the Holgat Sequence could be similar to the pink dolomites located on Namuskluft (P/10, Annexure 1) along the track leading to the old Lorelei Mine. Therefore, and because it is in a similar stratigraphic position, the Witputs Sequence is correlated with the Holgat Sequence.

2.6.2 Lithology

The Holgat lithologies consist of a thick sequence of arkoses, schists and greywackes, which are usually either blue-grey to brown-grey in colour. Blue-grey dolomitic and calcitic marbles are intercalated and the rocks are characterized by an intense deformational lamination, which commonly obliterates the original bedding trace.

2.6.3 Depositional environment

The greywackes were probably deposited by turbidity currents in a deep water environment as indicated by the presence of a very thick sequence of fine-grained quartzites and schists,

with minor intercalated carbonates and coarse clastics (Von Veh, 1988).

3. THE GANNAKOURIEP DYKE SUITE

3.1 Distribution and geology

The Gannakouriep Dyke Suite comprise intrusions of Namibian age, consisting of various swarms of mafic and ultramafic dykes and sills.

They outline a distinct evolutionary event of the Late Precambrian geosyncline (Kröner, 1974) and are seen as the final episode in the Richtersveld Igneous Province (Kröner & Blignault, 1976). These rocks are intrusive into the Stinkfontein as well as the basement complex to the east as either concordant sills or form cross-cutting dykes (Kröner, 1974). They follow the arcuate shape of the late Precambrian Belt and their strike is almost everywhere parallel to the intruded sediments.

Basic dykes within the Vioolsdrif Granitoid Suite in the Lorelei Mine area (S/14, Annexure 1) and the numerous amphibolite dykes and sills within the Rosh Pinah and Gumchavib Formations (Annexure 3) in the present area of investigation are possibly correlated with this suite. Along the basement contact (P/10, Annexure 1) and in the Obib mountains the basic sills and dykes are pre-tectonic in age. They usually have fine-grained chill zones.

A swarm of vertical diorite dykes regionally pervade the Ai-Ais area in southern Namibia and continue south into the Richtersveld (Blignault, 1974). These dykes are usually melanocratic and medium rather than fine-grained. South-east of Rosh Pinah the dykes trend in a NNE direction but change towards N-S in the Richtersveld, being commonly associated with faulting and shearing.

The main Gannakouriep dyke has a strike length of at least 90 km and forms a layered complex along the Fish River. The other Gannakouriep dykes usually consist of a single diorite phase.

Petrographically the mafic rocks consist essentially of **plagioclase + clinopyroxene + ore + chlorite + hornblende + epidote.** Pyrite is often an accessory mineral while chlorite is formed by the breakdown of the clinopyroxene. The plagioclase is essentially andesine with rare labradorite (Blignault, 1977).

Kröner (1974) states that all these intrusions occurred prior to the final phase of the deformation within the Gariep Group and are thus older than the post-tectonic Kuboos granite pluton dated at between 585 and 550 Ma, which cuts them.

4. STRUCTURAL SYNOPSIS

4.1 Introduction

The following structural nomenclature is used throughout this study and is defined as follows;

D_{1-3} = deformation phases
F_{1-3} = fold phases
S_{1-3} = planar elements
L_{1-3} = linear elements.

Numerous conspicuous structural features are exposed in the mountainous terrain of the Richtersveld and southern Namibia. Major structures were originally outlined in detail by De Villiers & Söhnge (1959).

Joubert & Kröner (1972) defined four deformational phases with distinct folding styles during their study of the Stinkfontein Succession east and south-east of Port Nolloth.

The oldest structures (F_1) were identified as small westward plunging gravity induced folds, while the main phase of folding (F_2) is characterized by two slightly diverging trends of linear structures ranging from NNE to NNW. These folds are largely symmetric with a penetrative axial planar cleavage. The mild north-south trending open and mainly monoclinal folds (F_3) with related faults are assigned to a period of cataclastic deformation. The final phase of deformation is related to the emplacement of the Kuboos

pluton and is expressed as ubiquitous east-west or SE-striking fractures, which are sometimes accompanied by small brittle faults. Small crenulations and kink folding (F_4) are also present.

Kröner (1974) did a comprehensive structural investigation of the western Richtersveld. He recognised two major tectonic domains in which the eastern miogeosynclinal domain was subjected to continuous vertical movement in the basement, which resulted in mild gravity induced folding. The western eugeosynclinal domain was characterized by intense compressional deformation, and both these events he related to only one regional orogenic event.

A detailed structural analysis of the area between Sendelingsdrif and Annisfontein was undertaken by Von Veh (1988). He recognizes five deformational phases, the first (D_1) of which is related to major south-east directed overthrusting accompanied by open to asymmetric eastward verging folds.

The second phase (D_2) is characterized by abundant closed non-cylindrical F_2 folds trending in a NNW direction and verging towards the west. Minor NNW-SSE trending normal faults with rare open small scale F_3 gravity folds define the third deformational phase (D_3). The intrusion of the Kuboos pluton outlines the fourth deformation phase (D_4) and is accompanied by reverse faults, conjugate and box folds with E-W and WNW trending axes. The final deformation phase (D_5) has formed ESE-WNW striking normal faults, dykes, veins, fractures and joints.

Gresse (1993) investigated strain partitioning in the southern Gariep Arc. He concluded that F_1 strain is partitioned between the outer and inner arc. F_1 folds and thrusts reflect sinistral transpression caused by southeasterly transport in the northern inner and east-verging outer arc, while in the southern outer arc frontal ramp conditions resulted in south-east vergent folds and thrusts.

In the area north of the Orange River no detailed structural analysis has so far been undertaken. Although many structural features were noted by McMillan (1968), e.g. major thrusts in the Obib Peak area, he did not relate all these structures to specific deformation episodes. Davies & Coward (1982), confirmed McMillan's (op. cit.) findings from structural studies in the Chamais Bay and Witputs-Rosh Pinah area, and identified two major nappes, viz. the Marmora Nappe and the Schakalsberg Nappe.

Several detailed structural studies were undertaken over small areas around the Rosh Pinah mine by students of Cape Town and Stellenbosch Universities (I'ons and Light, 1971; Hodgson et al., 1972; Hälbich, 1971, 1972, 1973).

4.2 Discussion

The current investigation shows that a major phase of spreading tectonics coupled with minor gravity tectonics produced the structures of this area. Certain distinct characteristics (Fig. 11) of each phase have been listed by Shack Pedersen (1987).

Gravity tectonics have:

1. listric normal faults and extensional fault imbrication

2. flat-lying coherent thrust sheets disturbed by extensional graben faulting

3. diverticulation phenomena whereby upper stratigraphic units are displaced further than the lower units

4. exposure of a peel off regime in the rear part of the thrust fault region

For spreading tectonics :

1. an imbricate fan formed by listric splay faults in front of the overlying spreading mass

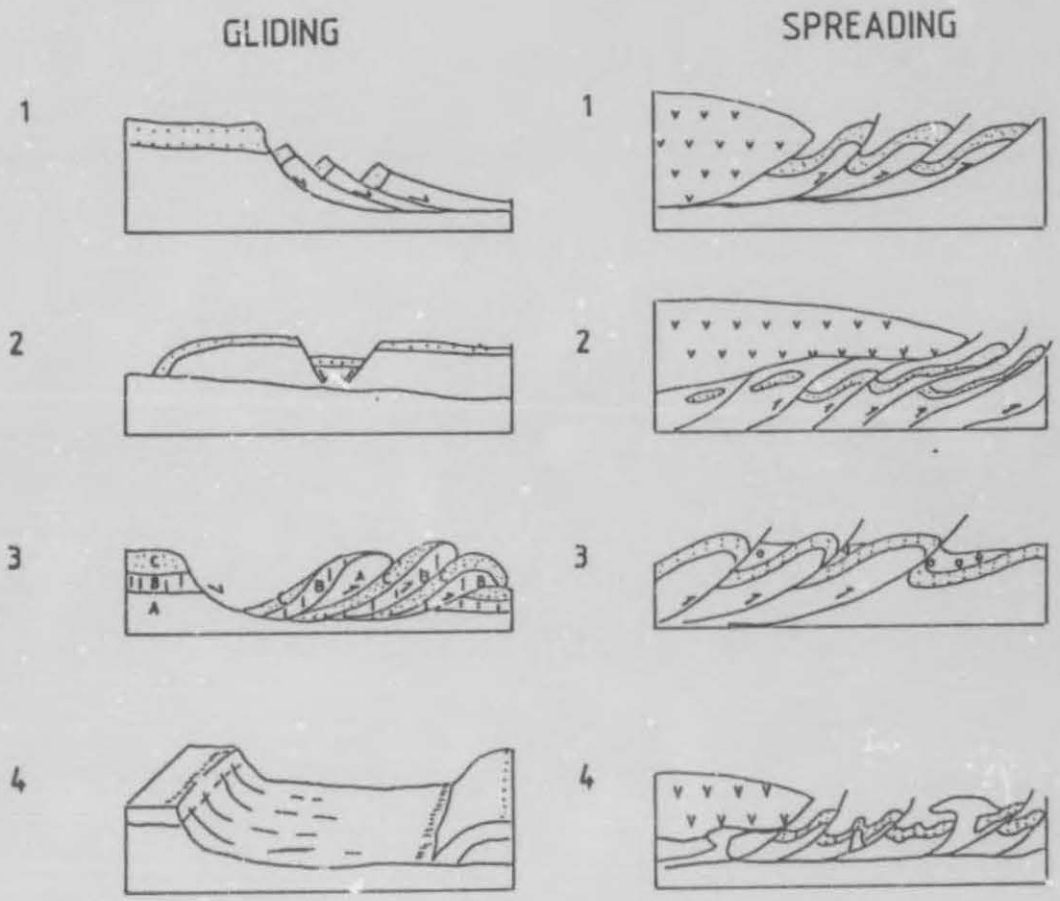

Fig. 11 *Characteristic features of gravity gliding and gravity spreading tectonics (after Schack Pedersen, 1987). See text below for description of features.*

2. a duplex of imbricate fan sheets developed on the deformed and overthrust sediments. Due to loading, boudins may be formed beneath the spreading unit

3. in the frontal part of the gravity-spreading deformation system, syn-tectonic basins are formed with progressively younger sediments away from the spreading mass

4. due to increasing fluid dynamic overpressure on the decollement unit water escape structures and mud diapirs occur in the frontal region of the gravity spreading system.

Wet, unconsolidated sediment deformation is also present e.g. slump folding in the Rosh Pinah Mine argillites and syn-sedimentary brecciated sediments in Dreigratberg. These structural features occur without definite hard rock micro- and meso-structures such as vein arrays, slickensided surfaces, recrystallization cleavages and kink bands.

Some important characteristic features of sediment slumping (Pickering, 1987) can be described as follows:

1. Sediments fold without a related cleavage.

2. Curvilinear fold hinges are present.

3. Continuous layers/beds laterally becoming totally disrupted and chaotic over distances of centimetres to decimeters.

4. Layers of chaotic brecciated sediments occur.

5. Detached fold hinges are present with liquefied sediment flow structures, both within hinge zones and attenuated fold limbs.

Bryant et al., (1969) have undertaken a study on the significance of lineations and minor folds near major thrust faults in the southern Appalachians and the British and Norwegian Caledonides.

Near the sole of the thrust sheet around the Grandfather Mountain window in North America numerous small tight or isoclinal folds are found with fold axes subparallel to an intense penetrative cataclastic 'a' lineation and axial planes parallel to foliation in the thrust sheet. These folds seem to have formed by tightening, flattening and passive rotation of earlier more open folds originally formed perpendicular to the direction of transport. A prominently developed penetrative cataclastic lineation is defined by parallel alignment of mineral aggregates, sometimes elongated, detrital quartz grains, and by streaking and grooving. The lineation decreases in prominence away from

the sole of the thrust and is parallel to the regional direction of tectonic transport, the 'a' direction.

A similar pattern was observed in the Moine thrust belt of Scotland by Lindström (1961) where an alignment of mineral lineation and axes of tight folds are present.

This study includes investigations on the orientation of fold axes and elongation lineations, which have been rotated parallel or subparallel to the tectonic transport direction.

5. METAMORPHISM

The process of metamorphism can be defined as the structural and mineralogical adjustments of solid rocks to physical and chemical conditions, which differ from those under which the different rock types were originally deposited or emplaced.

5.1 Introduction

Various types of metamorphism have been recognised which can be related to temperature, confining pressure, deformation or directed stress, and metamorphic fluid composition. The physical and chemical adjustments in rocks may either lead to the formation of an assemblage of higher temperature minerals (prograde metamorphism) or may form lower grade minerals (retrograde metamorphism).

In the Gariep Belt rocks an early or S_1 fabric is present which gives rise to a marked mechanical and chemical anisotropy in the rocks. Mimetic growth of minerals along the pre-existing anisotropy may take place (Turner & Weiss, 1963; Etheridge & Hobbs, 1974).

During the evolution of an orogenic province there may be several episodes or periods of metamorphism. The relationship between mineral growth and deformation may be established. For this purpose the microstructure or texture, which defines the size of the component grains, their shape, distribution and orientation in a metamorphic rock is studied. These studies also establish the metamorphic mineral assemblage, and facilitate comparisons of the

microstructure in thin section to the meso-structures observed in the field.

The study of inclusion trails in porphyroblasts (S_i) and the external fabric (S_e) helps to clarify whether mineral growth has been pre-, syn-, or post-tectonic with regard to that particular deformational event (Whitten, 1966, Spry, 1969).

In the study area the Gariep rocks have been subject to the ≈ 550-500 Ma Pan African tectonothermal events.

5.2 The determination of metamorphic grade

A limited study of thin sections was undertaken to determine the metamorphic grade and to establish whether medium-grade metamorphism has or has not been attained locally within this low-grade metamorphic zone.

Metapelites from the low - grade zone, which consists of phengite ("muscovite"), quartz, and chlorite ± chloritoid are the best indicators to show the change from low-grade to medium-grade metamorphism. Valuable positive indicators outlining a change to medium grade are the first appearance of cordierite and/or staurolite (Winkler, 1976).

The negative indicator 'chloritoid-out', can only be used if the phyllites in the low-grade zone contain this mineral and it is likely that rocks of the same bulk composition continue into the medium-grade metamorphic terrain. Winkler (1976), lists the other negative indicators as 'no chlorite touching muscovite' which could be potentially of much more use as most pelitic rocks, greywackes, and most igneous rocks of low metamorphic grade contain chlorite and muscovite. Chlorite which is not in contact with muscovite may persist to considerably higher temperatures. The muscovite and chlorite assemblage disappears in medium grade rocks if the chlorite is not too rich in Mg.

The formation of zoisite or clinozoisite characterizes the beginning of low-grade metamorphism and the assemblage zoisite/clinozoisite + chlorite + muscovite is diagnostic of the complete range of low-grade metamorphism. Unfortunately,

chlorite may easily form as a secondary product from biotite or hornblende e.g. in the Orange River Group volcanics, but the nature of the chlorite can be established if it can be observed under the microscope to be an alteration product of the host mineral.

The study of selected thin sections along the traverse lines indicate that only mineral assemblages of the lower greenschist facies are present within pelitic zones. Mineral assemblages of the classic Barrovian chlorite and biotite zones are located in two areas.

Along the basement contact on Namuskluft (Annexure 1) the chlorite zone assemblages are defined by the presence of chlorite-muscovite schists (specimens NT 2). Assemblages of the biotite zone seem to be confined to the Stinkfontein rocks, e.g. in the Rosh Pinah and Obib Peak areas, or in the northern Numees diamictites. These biotite- chlorite-muscovite assemblages are best defined in specimen NT 111.

A sample of the greenschist below Obib Peak has been analyzed for this study by H. Frimmel of the University of Cape Town. A representative analysis is as follows:

SiO_2	=	42,48%
TiO_2	=	0,22%
Al_2O_3	=	14,00%
Cr_2O_3	=	0,00%
Phi	=	17,58%
MnO	=	0,17%
MgO	=	9,76%
CaO	=	11,65%
Na_2O	=	1,79%
K_2O	=	0,26%
TOTAL		97,91%

The high Al- and high Ca-content indicates that the amphibole present is hornblende, and not actinolite as originally optically determined. This indicates that a metamorphic grade in the upper greenschist facies, or albite-epidote hornblende facies (H. Frimmel, personal comm.) has been

obtained. The temperature reached here would be around 500°C.

No chloritoid or staurolite has been identified in the study area and chlorite lies persistently in contact with muscovite, and these criteria can be used to indicate that medium-grade metamorphism has not been attained.

This study confirms the presence of a hydrothermal phase (McMillan, 1968 p.162) as indicated by the presence of tourmaline, barite, hornblende, chlorite and epidote (especially in the area surrounding Obib Peak, and Rosh Pinah). In thin section quartz replaces skeletal grains of magnetite and feldspar and the silicification of the Rosh Pinah Formation quartzites and arkoses are evidently related to the mineralizing event. The presence of numerous quartzo-feldspathic veins can also be grouped within this phase.

Only one regional prograde metamorphic event, M_1 is outlined by the biotite-chlorite-muscovite mineral assemblages established above. It attained greenschist facies grade (Kröner, 1974; Von Veh, 1988, and this study) and culminated in the growth of syn- to post-D_1 biotite porphyroblasts. Retrograde effects occurred at a later stage e.g. the formation of retrograde chlorite.

5.3 The first regional metamorphic event (M_1)

a) Microstructural characteristics

i) Quartz fabric

Sedimentary quartz grains are major constituents of the metasediments of the Gariep Belt, but well-rounded grains are virtually no longer recognizable, except within certain rocks of the Witputs Sequence.

During the first metamorphic event grains have been annealed and recrystallized. They now have concavo-convex, straight or serrated boundaries and overgrowths and indentations can be observed. Later deformational events have elongated and strained the quartz grains into lens shaped blades or

ribbons. Undulatory extinction and mica beards are present. A late phase of silicification is evident where silica replacement of various other mineral grains, e.g. feldspar can be observed.

ii) Microstructures of sheet silicates

A strong preferred orientation of sheet silicates is observed especially in the micaceous rocks (e.g. Wallekraal schist) of the Gariep Belt. They form a distinct, penetrative S_1 foliation with mica (001) parallel to the various S-planes in the rock and parallel to the axial planes of F_1 isoclinal folds.

Chlorite, biotite and muscovite are the most common sheet silicates to crystallize along a mimetic cleavage parallel to bedding and to a local S_1 cleavage as a result of load and/or prograde syntectonic metamorphism. Bending, shearing and rupturing of the S_1 cleavage has occurred to outline a secondary cleavage, S_2.

Idioblastic biotite porphyroblasts truncate the older aligned micas and confirm that favourable conditions were present towards the end of the first deformation event for the growth of the latter (Specimen NT 161, NT 162). These idioblasts have a prismatic habit with a typical poikiloblastic texture, with quartz and feldspar inclusions dominating. They may easily be confused with staurolite as twinned biotite crystals may have a typical hour glass texture (Fig. 12).

A distinct mineral elongation lineation is formed by the growth of hornblende, biotite and muscovite needles along low pressure zones. These structures are prominent below the Obib Peak Thrust (Annexure 3).

Muscovite and biotite fish probably form when larger massive grains are boudinaged by a combination of brittle and plastic processes acting on the rock (Eisenbacher, 1970). The presence of these shear-sense indicators reveal the extensive tectonic deformation the rocks have suffered.

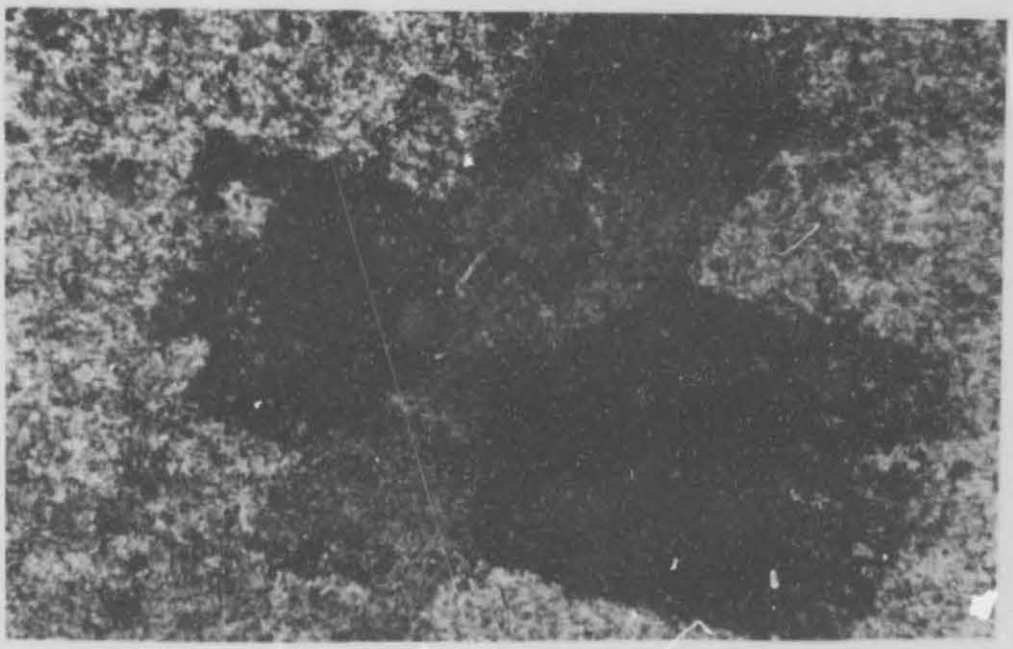

Fig. 12 Twinned biotite porphyroblasts with typical hour glass texture (uncrossed nichols; scale 1cm ≈250 µm)

b) Mineral Paragenesis

The M_1 mineral assemblages in the Gariep lithologies of the study area cover the low to intermediate range (chlorite to biotite zone) of the greenschist facies. In pelitic lithologies a mineral paragenesis of **muscovite-chlorite-quartz-albite ± biotite ± calcite ± epidote** is present. The chlorite may be either of a prograde or retrograde origin, while accessory minerals are apatite, zircon, sphene and oxide minerals. Albite and epidote form minor constituents in the paragenesis.

(i) The paragenesis in the arenaceous rocks

The assemblage in the arenaceous rocks consists of **quartz-muscovite ± feldspar ± biotite ± dolomite** e.g. NT 39, NT 53, NT 67. The feldspars are mostly of detrital origin and include plagioclase, microcline and microperthite.

(ii) The paragenesis in other Gariep Group lithologies

In dolomitic marbles west of Obib Peak (specimen NT 90) the following paragenesis has been established:
dolomite-calcite + quartz + biotite ± talc.

The marble is usually very pure, and consists almost entirely of calcite and dolomite. The paragenesis mentioned above remains unaffected at very low-grade metamorphism (Winkler, 1976) i.e. the lower greenschist facies.

Von Veh (1988) established the following mineral paragenesis for the area south of the Orange River:

calcite-dolomite ± quartz ± talc ± muscovite ± chlorite.

The paragenesis in the greenschist (Grootderm volcanics and Stinkfontein lavas), which are absent from the study area was established as follows by Von Veh (op. cit.):

albite-chlorite-calcite-actinolite-epidote-opaques ± biotite.

The paragenesis present in the amphibole-chlorite schists below Obib Peak (NT 139) are constituted as follows:

albite-hornblende-quartz-biotite-opaques ± calcite ± epidote.

These rocks are therefore interpreted as an altered dyke or sill.

c) Temperature

Von Veh (1988) has found no evidence to verify Kröner's (1974, p.101) assertion of a westward increase in temperature from the **quartz-albite-muscovite-chlorite** subfacies to the **quartz-albite-epidote-biotite** subfacies of the greenschist facies.

In the Rosh Pinah area biotite is ubiquitous in argillites of the Rosh Pinah Formation as well as in rocks near Obib Peak. This may indicate that dynometamorphism largely

influences the distribution of metamorphic grades in these rocks.

Von Veh (1988) interprets the blue-green hornblende, plagioclase with an oligoclase-andesine composition and the presence of almandine garnet reported by McMillan (1968) to have probably been present in specimens collected in basement gneisses and schist. The present study however, verifies the presence of garnets in the country rocks along the contacts of some amphibolite sills. These garnets can be related to contact metamorphism as a fine-grained chill zone is present. Tremolite needles are present in some Pickelhaube carbonates northeast of Pickelhaube Peak.

For the Rosh Pinah area only low grade minerals have been described (Page and Kindl, 1978; Watson, 1980) but it should be noted that there is a sharp increase in the presence of biotite and pyrrhotite in coexistence with pyrite.

Mineral paragenesis indicates that the higher temperature range of the greenschist facies has not been reached, therefore the M_1 temperatures probably did not exceed 450°C, except for amphibole schists below Obib Peak where the temperature range is 500°C.

d) Pressure

In contrast to the temperature the pressure regime was found to be quite high (Von Veh, 1988) and to have increased in a westerly direction. Both Beetz (1926, p.199, 202) and Kröner (1974, p.101) have reported high pressure minerals (glaucophane and other Na-amphiboles) from the central parts of the Gariep Belt in the proximity of or on the contact between the Grootderm volcanics and the underlying greywacke.

The presence of these minerals would represent strong evidence for the presence of a major plate collision event (Frimmel & Hartnady, 1992). Their presence could, however not be verified by the latter researchers, who established that the blue sodic amphiboles recorded previously, can be classified as magnesio-riebeckites.

Ritter (1980, p.202) reports a mean b_0-value of 9,04664 for white micas for his Gariep samples, which is a typical value for intermediate pressure Barrovian-type metamorphism (Sassi and Scolari, 1974) as quoted by Von Veh (1988).

Estimates of pressure conditions between ≈ 6-7kb. (Hartmann et al., 1983) for the Southern Marginal Zone of the Damara orogen is accepted by Von Veh (1988) and seems a reasonable value.

e) The relationship of porphyroblast to D_1

Porphyroblasts often contain inclusions with a preferred alignment representing the trend of a pre-existing foliation. Temporal relationships are elucidated from the relationship between the internal (S_i) and external (S_e) s-surfaces, and between porphyroblast margins and S_e.

In the study area M_1 biotite porphyroblast (specimen NT 161, NT 162) can be seen to overgrow the internal (S_i) and external (S_e) s-surfaces (Fig. 13).

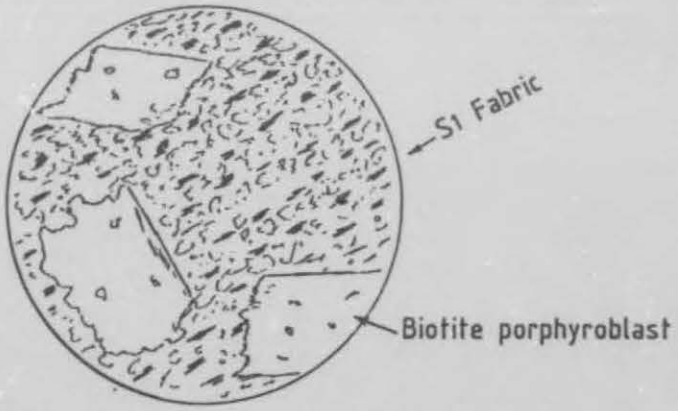

Fig. 13 Randomly orientated biotite porphyroblasts overgrowing the internal (S_i) fabric. (Sample NT 161).

The long axes of the blasts are randomly orientated and the internal trails are continuous with S_i of the matrix. Von Veh (1988, p.113) outlines textural evidence to indicate that the M_1 biotite porphyroblast grew after D_1, but before D_2 e.g.

as seen in the overgrowing of the S_1 cleavage, and deflection of S_2 cleavage etc.

5.4 The contact metamorphic event (M_2)

The second metamorphic event M_2, is associated with the D_4 emplacement of the Kuboos-Swartbank plutons (Von Veh, 1988) and is very localised. Contact metamorphic minerals can be observed in the contact aureole of the ≈500 Ma Kuboos pluton. No effects of this recrystallization event were observed in any thin sections of the study area, which can be explained by the distance from the pluton.

6. THE GEOLOGY AND STRUCTURE OF THE NAMUSKLUFT-DREIGRATBERG AREA

6.1 Basement Complex

6.1.1 Distribution and stratigraphy

The De Hoop volcanics of the Orange River Group (ORG) in the vicinity of the old Lorelei Mine have a complex relationship with the surrounding rocks. They are here underlain by a large granodiorite batholith. Sandwiched between these two units there is a distinct ripple-marked quartz arenite of Gariep affinity, which grades into a diamictite unit. This anomalous stratigraphic relationship can be explained by thrusting of the basement volcanics over the much younger diamictite, which originally overlay the latter (Annexure 1).

6.1.2 Lithologies and petrography

A petrographic examination (NT 70) indicates that along the higher part of this volcanic formation there are rocks of possible sedimentary origin. The rock consists of rhythmic alternating sericite and quartz bands, sericite with disseminated garnet grains, followed by a garnet bearing chlorite zone, and finally quartz-magnetite bands. Some sericitized feldspar porphyroblasts are also present (NT 74) while a fault gouge and a flattening fabric indicates extensive tectonic disturbance. The rock can be described as a banded quartz-magnetite-garnet-chlorite schist (banded iron formation).

The mineralogy of these rocks suggest that they are either thrust-in slivers of the basal rocks of the Numees Sequence (the Jakkalsberg Formation) which has attained a higher metamorphic grade (almandine-amphibolite facies), or form remnants of the Rosyntjieberg Formation unconformably overlying the Haib Subgroup.

Locally some rocks which look similar to arkoses are present within the ORG (NT 55, NT 71). They consist mostly of quartz, feldspar and calcite grains with minor amounts of strongly aligned amphibole needles. The feldspars are extensively sericitized and saussuritized, and the rock is interpreted as altered and sheared granodiorite.

Other rocks in this group are fine-grained grey to greenish feldspar and quartz-sericite schists. The sericitic matrix constitutes up to 90% of these rocks, which are interpreted as original felsic volcanics. Some brown, slightly gossanous calc-silicate material is incorporated in the volcanic rocks and consists essentially of fine- to coarse-grained dolomite with minor quartz. Accessory calcite and muscovite are also present and thin acicular textured amphibole needles have been identified as actinolite-tremolite (NT 69).

Near the granite contact in the Lorelei Mine area pervasive epidotization is present as a result of the breakdown of hornblendes to form biotite and epidote. Numerous concordantly emplaced quartz veins also host widespread epidotization features which are largely absent in the younger Gariep rocks.

The youngest intrusive phase of the Vioolsdrif Suite is present as leucogranites near Lorelei Mine. In thin section (NT 75) the rock is a medium-grained massive unit containing quartz grains with polygonal contacts. Accessory minerals include minor microperthite, biotite and some sericite. Plagioclase, and K-feldspar together with minor chlorite may also be present.

These leucogranites can be grouped within the L_2-type leucogranites (Minnit, 1992) and occur as sinuous veins or elongate bodies. Small lenticular inclusions of the ORG

volcanics are incorporated within the granite, indicating the intrusive nature of the latter.

A dark green amphibolite dyke intrudes the granodiorite at this locality (S/14, Annexure 1) and is correlated with the Gannakouriep Dyke Suite. In thin section this rock consists largely of biotite and aegirine augite, together with minor quartz, rutile and opaque minerals (NT 76). No preferred orientation of any minerals is present.

A major unconformity separates the ORG from the Gariep Belt, and is defined by a thin basal conglomerate preserved locally on the farm Namuskluft (P/11, Annexure 1). It is a polymict matrix supported unit with approximately 90% of the clasts consisting of well-rounded to subrounded pebbles of quartzite. Minor granodiorite and Orange River Group volcanics make up the remainder of the clasts but carbonates are notably absent. The matrix of the conglomerate is dark-grey, quartzitic to arkosic. Along the major part of the contact, however, the cover rocks have been thrust over the older basement volcanics.

6.2 The Stinkfontein Sequence

6.2.1 Distribution, stratigraphy and lithology.

A possible Stinkfontein lithology that outcrops in this area is a thin sliver of argillitic and carbonatic rocks occurring along the basement contact on Namuskluft from M/4 up to O/8, Annexure 1). The other diamictite beds in this study area are here interpreted as thrust imbricates of the Numees Sequence and the older Kaigas diamictites are therefore (with the possible single exception mentioned below) absent from the area north of the Orange River.

A dark-grey to black and massive dolomite unconformably overlies the basement, and form a sheared and brecciated contact with the basement granites (M/4, Annexure 1) as indicated by their lenticular and intercalated nature (samples NT 7, NT 11, NT 24). The mineral paragenesis is **calcite-dolomite ± quartz ± talc ± muscovite ± chlorite ± biotite.** Quartz vein stockworks occur throughout. The

contact between the Orange River Group volcanics and the dolomite is marked by a thin basal conglomerate (e.g. P/10, Annexure 1).

The overlying incompetent black to dark-grey argillitic unit is partly calcareous and strongly foliated. It consists mainly of calcite and quartz grains (NT 5) with minor muscovite and accessory chlorite. Near the Namuskluft farmstead dolomite and calcite dominate the rock with quartz and chlorite as accessory minerals. Some thin carbonate bands within the unit consist of a banded quartz and dolomite sequence (NT 6). Accessory actinolite is also observed. Further towards the south (P/7, Annexure 1) the argillite unit consists almost entirely of kinkbanded chlorite, with minor intercalated lenticular quartz grains (NT 19). Calcite and dolomite are minor constituents here. Deformed quartz veins, often isoclinally folded and excessively attenuated form a tectonic melange in several zones in the argillite near the basement contact.

Locally a sandy, blue-grey carbonate (similar to the Pickelhaube) lies in contact with the black argillite. The latter (NT 12) is intensely altered with chlorite, muscovite, biotite and sericite forming the cleavage planes surrounding calcite grains and has been subject to some silicification. The presence of pre-tectonic amphibolite sills (P/9, Annexure 1) leads to a correlation with the older sequences e.g. the upper Stinkfontein in this study.

In area S/14, S/15 (Annexure 1) intensely folded diamictite non-conformably overlying the granite grades upwards into a ripple-marked arenite unit with a sheared upper contact. This contact with the overlying ORG is interpreted as a thrust boundary.

The Kaigas diamictite has a similar lithology to that of the Numees diamictites. However, Von Veh (1988) points out the absence of carbonate clasts and banded ferruginous quartzite or schists as a distinguishing criterium.

Although the iron formation or ferruginous beds are absent at S/14,15, Annexure 1, single carbonate clasts are

conspicuous in these rocks. This occurrence is therefore interpreted as a thrust inlier of transgressive Numees diamictite over which a stack of ORG volcanics has been thrust (see also section EF, Annexure 1).

6.3 The Hilda Sequence

6.3.1 Distribution and stratigraphy

A marked change in stratigraphy is evident towards the south along the Namuskluft synclinorium, which is sliced obliquely by the Namuskluft Thrust (NKT) and the Rosh Pinah Nappe Thrust (RPNT), (R/15, Annexure 1). Arenaceous and rudaceous lithologies absent from the Namuskluft area are exposed near the Orange River in the Namuskluft Valley (Fig. 2).

These lithologies together with boudined dolomite zones are interpreted as tectonised remnants of the Hilda Sequence as they are similar to the rocks of the Wallekraal and Dabie River Formations. They locally interfinger with the Numees diamictites.

In the Jakkalsberg area south of the Orange River, Von Veh (1988) describes similar interfingering of conglomerates and grits with pebbly schists and diamictites. Kröner (1974, p.23) interprets this interfingering as a large scale facies change.

6.3.2 Lithology and petrography

The Hilda Sequence here consists of a thick series of quartzites and grits with several intercalated conglomerates lenses. The lenses are generally not thicker than 5m, and are clast supported with originally well-rounded and sorted clasts of mainly vein quartz and a minor component of carbonate. At the Orange River the clasts have an average diameter of approximately 3 cm and are tectonically flattened. Locally the matrix is ferruginous and clasts of ferruginized material were also recorded.

A band of light-brown weathering dark-grey to black dolomite is intercalated and grades into a typical blue-grey

Wallekraal schist unit. The dolomites are characterized by extensive brecciation and large scale boudinage. Shearing is extensive and is manifested by ubiquitous quartz veins with a right lateral sense of displacement and interspersed lenses of diamictite. These rocks are here correlated with the Dabie River Formation.

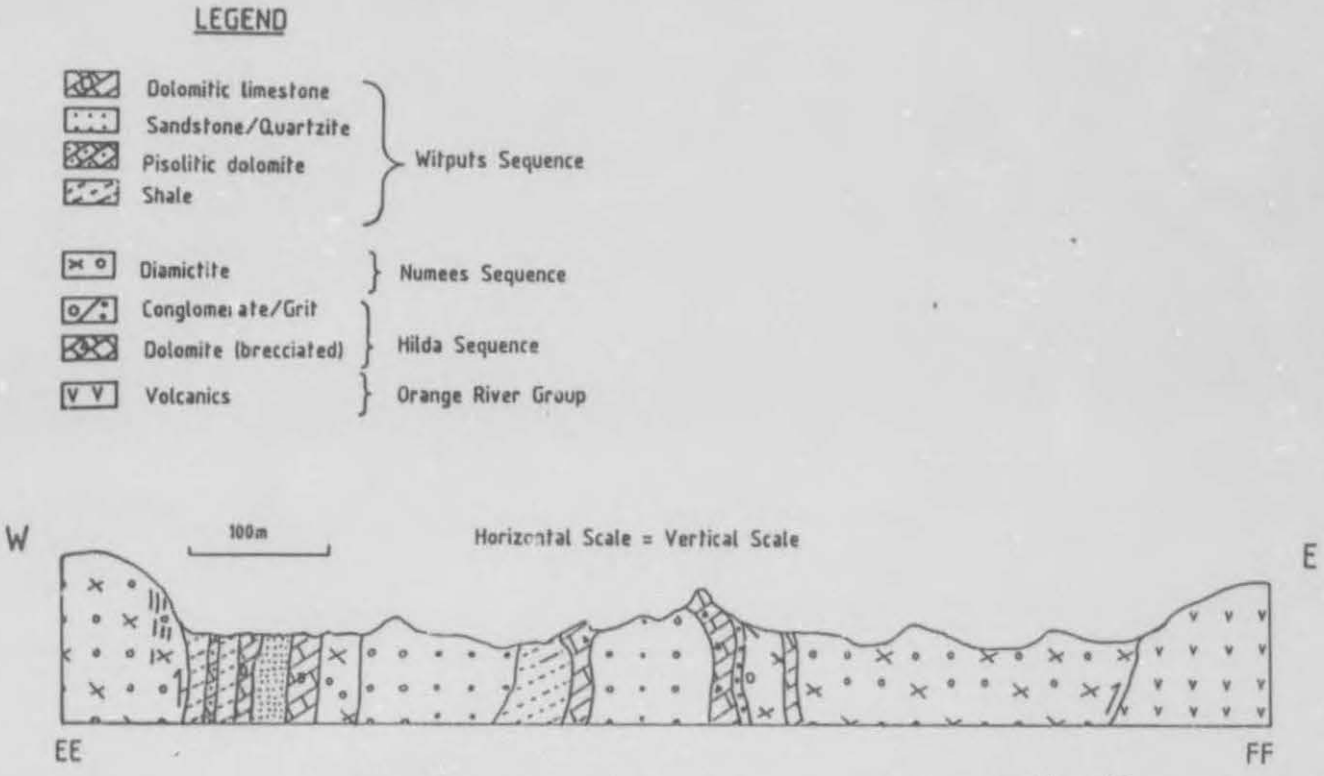

Fig. 14 Synoptic cross-sectional sketch to illustrate the tectono-stratigraphic sequence near the Orange River (EE-FF,R/16, Annexure 1).

In the sketch (Fig. 14) it can be seen that certain lithologic units are duplicated several times in varying sequence with other lithologies e.g. the blue-grey carbonates. The sandstone unit contains angular granodiorite lonestones, probably representing dropped-in clasts. In thin section (N 16) the grit zones, which are intercalated in the diamictites consist of clasts of quartz, microcline and dolomitic carbonate within a muscovite, biotite and chlorite rich matrix. The rocks are also slightly calcareous. The sheet silicates form a prominent cleavage, while the streaks of dark opaque minerals (heavy minerals) might indicate the bedding or cross-bedding trace.

A light-grey quartzite of the Hilda Sequence forms a thrust contact with the Numees diamictite in the east (R/16, Annexure 1). The unit is about 10m metres thick, and contains numerous stretched and folded quartz veins. All the veins dip steeply towards the west but the isoclinal fold axes plunge steeply north at angles greater than 50°.

6.4 The Numees Sequence

6.4.1 Distribution and stratigraphy

It is suggested here that the Numees Sequence has been duplicated in the Dreigratberg and the Sendelingsdrif synclinorium as a result of thrusting (Annexure 2). It forms a thrust contact with the Hilda and Witputs strata in the Namuskluft synclinorium (Fig. 2).

6.4.2 Lithology and petrography

The Numees Formation is composed essentially of massive, dark rudaceous rocks with a distinct glaciogenic appearance on surface outcrops, and contains various intra- and extrabasinal clasts. Some ripple-laminated shale interbeds become prominent on the farm Namuskluft and grade into clast-bearing beds both on the upper as well as lower contacts.

The diamictite is largely matrix supported with polymodal clasts of basement granodiorite, leucogranite, gneiss and pegmatite. Intrabasinal quartzite, schist, and carbonate clasts are subordinate, although locally carbonate clast concentrations are evident e.g. on the southwestern slope of the Dreigratberg. Granitic rocks of the Vioolsdrif Suite dominate, and the typical blue-grey Pickelhaube limestones are noticeably absent.

The clasts are distributed throughout the rock and may constitute from 10% to over 50% of the rock mass, with sizes varying from as little as 2mm to over 10m. They are usually subrounded but well-rounded clasts were observed near the Orange River. Most clasts are tectonically elongated with the long axes of the pebbles and boulders all plunging in a NW direction, generally at angles of between 30 and 40

degrees. The matrix of the rock can vary from dark argillaceous material to light or grey-brown quartzitic material, and is made up of muscovite, quartz, feldspar, biotite, and iron oxides.

Primary sedimentary structures within the diamictites are poorly preserved, being generally obliterated by a penetrative S_1/S_2 cleavage. Several turbiditic features however, are present in the Dreigratberg and Namuskluft areas e.g. normal grading, rip-up clasts, load and flute casts and sinuous ripple marks.

Locally some interdigitated blue-grey grits, arkoses or feldspathic quartzites form well-bedded sequences. Thin grit and sandstone units contain local heavy mineral zones outlining bedding as well as rare cross-bedding features.

In thin section (sample N 14) bedding is indicated by banded quartz and granular magnetite domains in a succession, which could be described as a poorly developed iron formation. Chlorite increases towards the base of the Numees as the matrix becomes argillitic to form a mudstone. Prominent dropstones within the chloritic schists confirm that the stratigraphy is facing upwards.

In samples N 11 and N 13 large hexagonal to tetrahedral grains of magnetite, some of which are oxidized to hematite, are placed within a fine-grained chloritic matrix with accessory biotite and muscovite. Minor dolomite and quartz is also present within the matrix. Biotite porphyroblasts have formed during the culmination stages of D_1 and are aligned oblique to the S_1 cleavage formed by the other sheet silicates.

Positive evidence for the reworked nature of the diamictite is the presence of a large composite boulder containing several smaller clasts (N/11, annexure 1). The clasts consist of subrounded to angular pebbles and boulders mostly of granodiorite and Orange River Group volcanics.

West of Dreigratberg two prominent bands of magnetite-quartzite form intermittent outcrops (O/18, Annexure 1).

They trend in a north-south direction and continue along strike south of the Orange River. On surface the rocks consist of finely laminated wind polished black silica and magnetite-rich bands. A petrographic examination (NT 136) indicates the presence of alternating quartz and magnetite bands with minor grunerite. Oxidation is present along grain boundaries. These rocks are typical Rapitan-type iron formations.

Outcrop widths vary between 1-15m and dips are steeply towards the west or often slightly overturned towards the east. These bands are always located within the dark chloritic diamictite. The iron formations were not completely solidified at the time of diamictite deposition as they contain numerous dropped in clasts.

These rocks bear similarities to the iron-rich, usually magnetic, quartzitic rocks occurring within the Chuos Formation diamictites (Henry et al., 1986). Although the banded magnetite quartzites of the Chuos Formation are not as continuous as those within the Numees diamictite the two formations could possibly be correlated.

Carbonates occur either as clasts or as distinct lenticular boudined pods within the Numees diamictites. They are dolomitic, varying from 2m to several tens of metres thick and pods may extend for up to a kilometre along strike (P/17, Annexure 1). Kröner (1974) interprets these clasts as disintegrations of dolomite layers or algal reefs by wave action or gravitational slumping. This seems to be the best interpretation.

In the north (P/10, Annexure 1) the Numees diamictites form a gradational contact with an underlying phyllitic unit. Clast-bearing beds near the contact grade into sandstones at the base. Similar lithologies are present in the Lorelei Mine area (S/15, Annexure 1) which suggest a correlation between these diamictites as belonging to the Numees. The varved arenites at the base consist essentially of quartz and plagioclase with accessory biotite and chlorite. The feldspars are extensively sericitized and talc may also be present. They contain several dropped-in pebbles, some of

which could be either felsite or weathered Orange River Group volcanics.

In the Sendelingsdrif synclinorium (Q/23, Annexure 1) only the light-grey Numees diamictites are present. A prominent fault is indicated by extensive quartz veins, brecciation and some pronounced gossans on the western limb of the syncline. This fault has been mapped by McMillan (1968) as the Namuskluft Fault and he extends it along strike past Rosh Pinah (Fig. 2). The fault runs along the edge of the Schakalsberg and has been mapped as the Jakkalsberg Fault by Von Veh (1988). This name is also used here for its continuation north of the Orange River. Small outcrops of blue-grey schists and blue dolomite (possibly Hilda lithologies) are exposed on the upthrown western block of this major interpreted thrust fault.

6.5 The Witputs Sequence

6.5.1 Distribution and stratigraphy

A sequence of clastic and carbonate rocks are exposed along the escarpment trending from due east of the Namuskluft farmstead southwards up to P/11 (Annexure 1) in the Namuskluft synclinorium and from P/16 southwards in the Dreigratberg syncline almost up to the Orange River.

6.5.2 Lithology and petrography

Within the Witputs Sequence four units (some possibly of tectonic origin), can be recognized which a[illegible] grouped in the Namuskluft Formation. Each unit begi[illegible] clastic sequence and is terminated by limestone or [illegible] rocks.

The stratigraphic relationships in the central Namuskluft synclinorium (O/9, Annexure 1) are outlined in a composite field sketch (Fig. 15).

The cream-coloured massive streaky dolomite (light-grey in fresh specimen) is a fine-grained rock (NT 3, NT 9, NT 51)

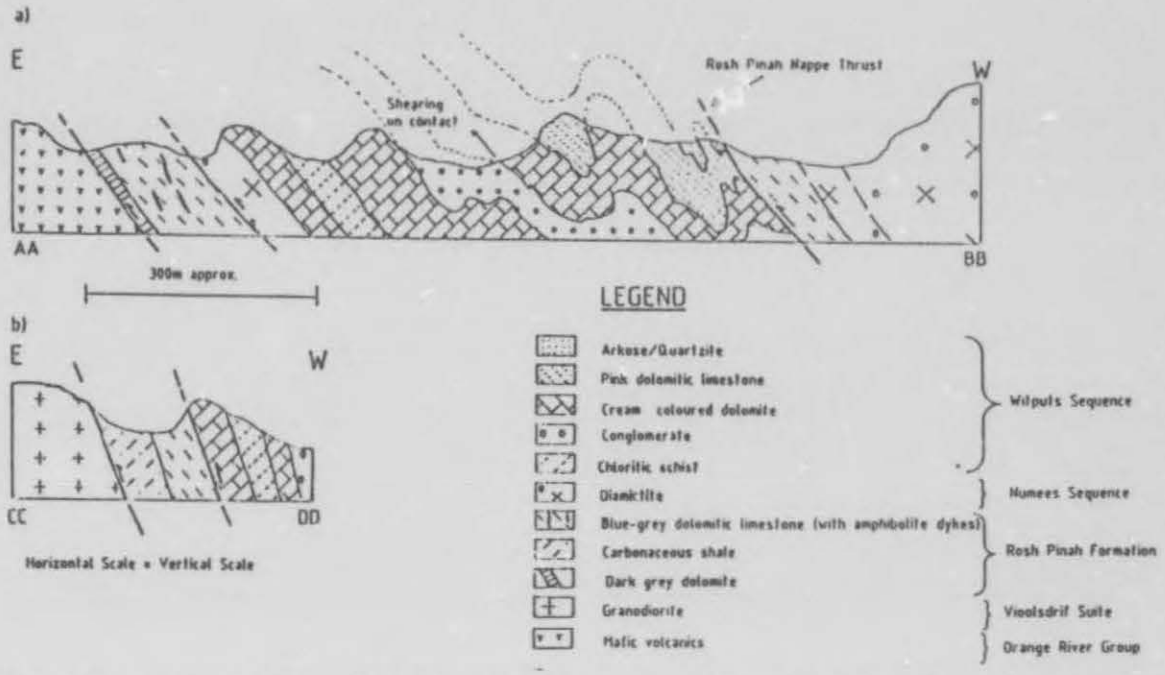

Fig. 15 Composite field sketch to illustrate the tectono-stratigraphic sequence in the:

a) central parts of the Namuskluft syncline
b) along the basement contact further north (looking south).

(See Annexure 1 for section localities AA-BB and CC-DD)

with vague grain boundaries, consisting largely of dolomite with minor quartz and calcite, accessory albite, chlorite and muscovite.

The muscovite-chlorite schists are similar to the Wallekraal schists and are characterized by the presence of small sheared grit bands. Near the thrust exposure on Namuskluft (M/4, Annexure 1) the rock consists of quartz and muscovite with accessory chlorite (NT 2). Magnetite occurs in specific bands as euhedral octahedra, and are sometimes oxidized to euhedral hematite. Grains have vague boundaries and are in a state of alteration, while quartz grains are aligned along the S_1 cleavage.

Near the Namuskluft fold closure the schists grade into feldspathic sandstones (NT 44) consisting of quartz and

feldspar (plagioclase and microperthite) within a muscovite, biotite and chlorite rich matrix. The schist is interpreted as a fine-grained sediment, which has been deposited within moderately deep water.

The overlying cream-coloured dolomite has intercalated thin (3-5cm) schist lenses at the base and contains elongated rip-up fragments of argillite as well as clasts of other dolomitic rocks. The pink-coloured dolomitic limestone (the upper Dolomite unit of the Numees, McMillan, 1968) is a meso-laminated rock, which consists essentially of medium-grained dolomite (sample NT 52) with minor quartz clusters, while chlorite replaces opaque mineral grains. Here and there some large quartz grains are embedded within a coarse- to fine-grained dolomitic matrix. Minor muscovite and biotite are also present. This unit is correlated with the Holgat Sequence as it is absent from the general stratigraphic sequence of the Obib hills north of the Orange River and east of the Rosh Pinah valley.

Small lenses of a steel-grey arkose overlie the pink dolomitic limestone intermittently. The arkose (samples NT 17, NT 53) is mainly coarse-grained with large serrated grains of quartz, sericitised anorthoclase and microcline. Original boundaries of quartz are no longer discernable. The matrix of this rock is made up of fine-grained quartz, with minor interstitial muscovite or may occasionally be dolomitic (NT 17). Some graphite and detrital tourmaline are also present.

The cream-coloured dolomite contains a conglomerate zone with 99% of the clasts composed of mainly cream-coloured dolomite and some pink limestone (Fig. 16). Subrounded to angular sandstone and grit clasts occasionally drift in the dolomitic matrix.

North of the area outlined on Fig. 14 a sharp thrust contact zone is present between a pisolitic dolomite and the Numees diamictite. The dolomite (NT 39a) is dark-grey to black with elliptical pisoliths. Banding in the pisoliths is revealed by alternating fine-grained light and dark-grey zones.

Fig. 16 *Conglomerate with carbonate clasts which occurs as a marker within the Witputs Sequence in the central Namuskluft syncline (P/10, Annexure 1). Note the well developed elongation of clasts along* S_2

Accessory quartz, chlorite and muscovite are also present in the matrix.

From P/8 to Q/11 and between the Namuskluft Thrust and the RPNT (Annexure 1) the synclinally infolded Witputs strata rest via the dark carbonate on volcanics of the ORG on the eastern limb of the syncline but on diamictites of the Numees Sequence along the western limb.

Still further south at R/15, R/16-Annexure 1, a blue-grey diamictite unconformably overlies the Orange River Group volcanics and the dark dolomite is absent. All this evidence is regarded as a good indication for a thrust contact between basement and cover rocks, (viz. the Namuskluft Thrust). The thrust planes are deformed into open asymmetrical folds affecting both basement and Gariep cover strata.

The dolomitic sequence of the Dreigratberg (Fig. 17) is located within a prominent F_2 syncline, striking

approximately NNW -SSE (Q-R/ 16-20, Annexure 1). Two well defined massive cream-coloured dolomite beds some tens of metres thick form the three sharp peaks. The contact between the Dreigratberg succession (Annexure 1) and the Numees diamictite in the east is marked by a 1-2m thick black massive dolomite (see 1, Fig. 17) which is similar to the one present along the basement in Namuskluft (N/5, Annexure 1).

A thick (100m) sequence consisting of various shales, phyllites, chloritic and calcareous schists (pelites) with a single quartzite bed conformably overlies the black dolomite (see 2, Fig. 17 and Fig. 18). Numerous sheath folds

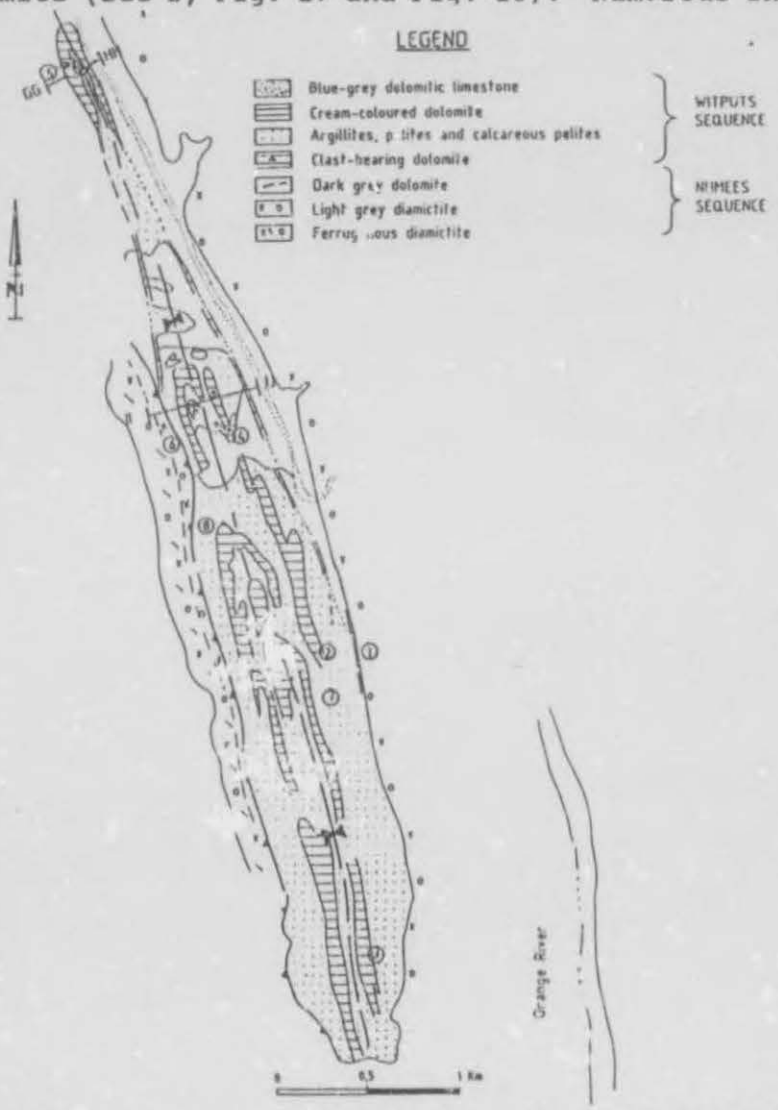

Fig. 17 Photogeological map of Dreigratberg syncline. See text for description of reference poin's and geology.

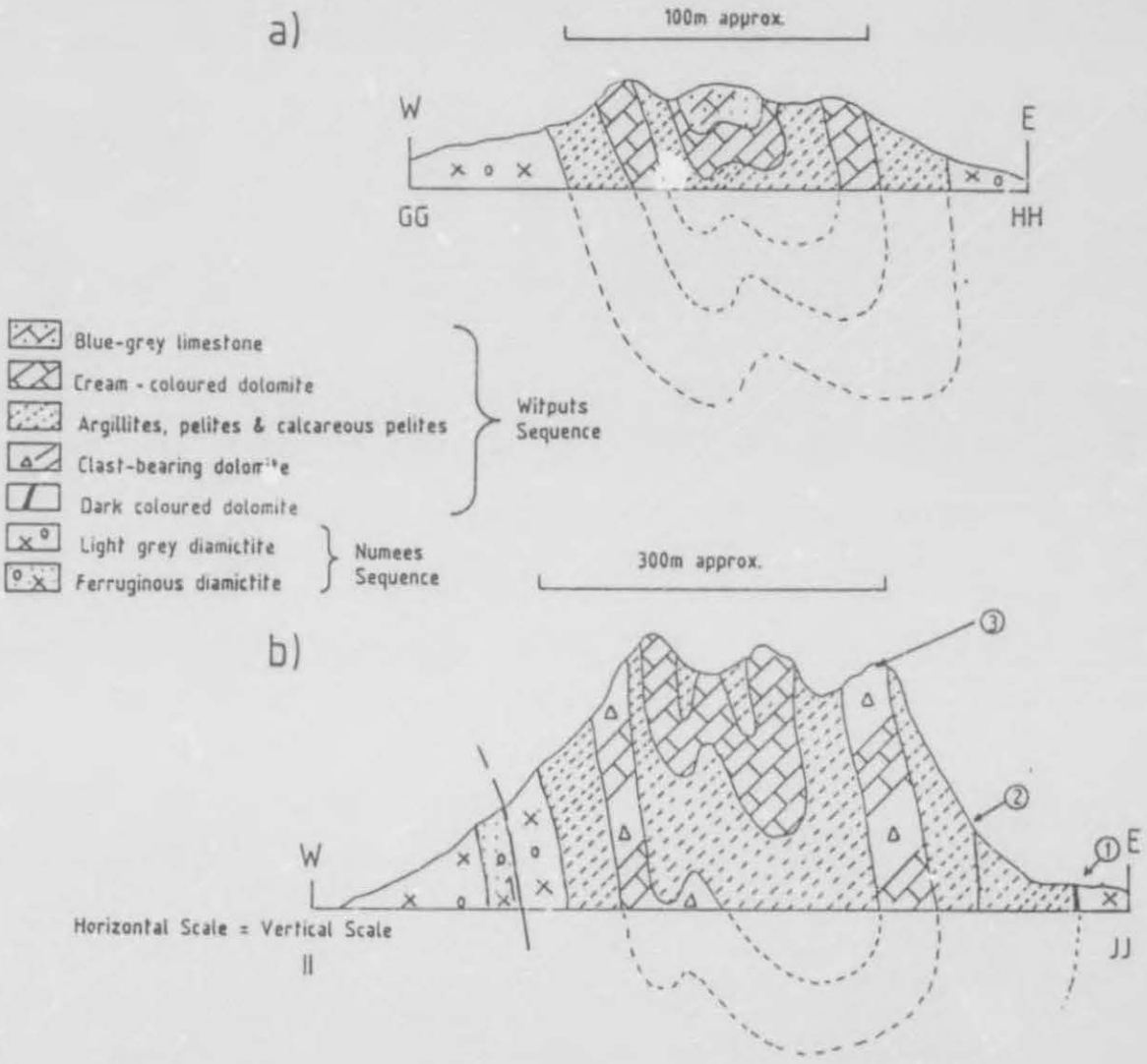

Fig. 18 Schematic sketches to illustrate the stratigraphic sequence and structure of Dreigratberg (sections looking north).

(See Annexure 1 and Fig. 17)

1. *Black dolomite*
2. *Thin quartz band*
3. *Synsedimentary breccia*

and quartz veins along the contact of the shale with the overlying cream-coloured dolomite outlines prominent shearing.

The dolomite sequence contains a lenticular 1m thick arenite with carbonate shards at the base, which is overlain by a 5m thick syn-sedimentary dolomite breccia, (See 3, Fig. 17).

The original bedding has been broken into tabular clasts, probably by sliding and rotation. These now float in a fine-grained sandstone matrix (Fig. 19).

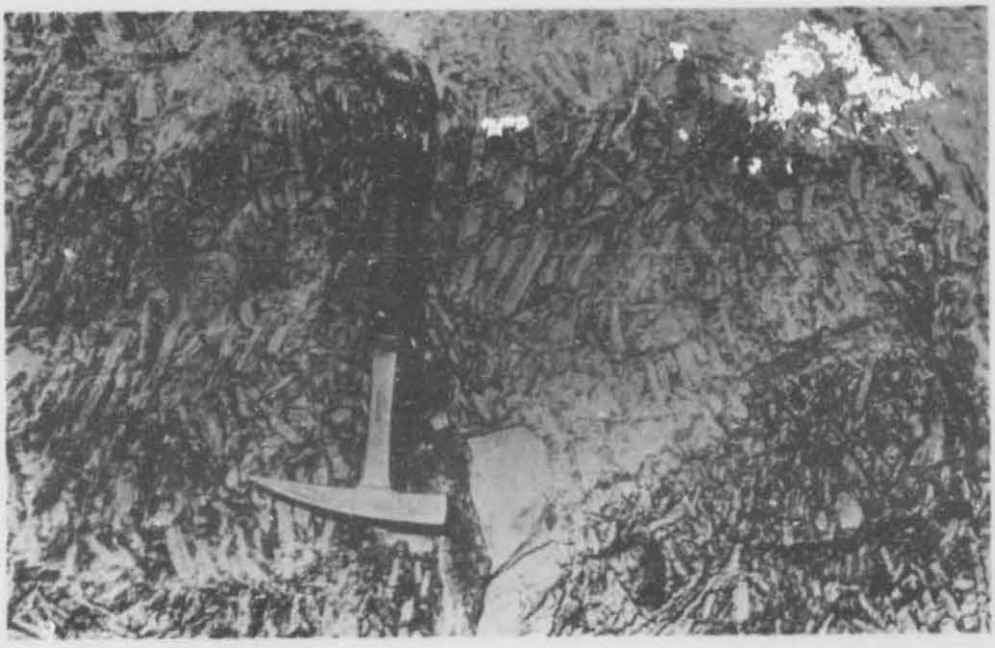

Fig 19 Synsedimentary breccia of dolomite with tabular clasts floating in a sandstone matrix. Eastern limb of Dreigratberg (P/11, Annexure 1 and Fig. 17).

Petrographically (specimen NT 39) the slumped bed consists mainly of dolomite laths surrounded by large quartz grains with minor microcline. The matrix is fine-grained quartz and even finer-grained dolomite. Minor muscovite, microcline, biotite and opaque minerals are present in the matrix.

The quartz was originally well-rounded, but now has sutured boundaries. The overlying cream-coloured dolomite is

extensively brecciated and contains sandstone clasts over a metre in diameter.

The upper dolomitic unit forming the eastern peak (Q/19, Annexure 1, and Fig. 18b) contains angular, matrix supported, unsorted clasts dominated by sandstones with less abundant dolomites and rare granites of variable sizes (see 4, Fig. 17). The rock may grade northwards to the fold closure from conglomerate to calcareous arenite and eventually to dolomite.

The stratigraphic top at locality 5 (Fig. 17) consists of an alternating sequence of various blue-grey finely laminated limestones with fine-grained brown mesobands of limestone, buff-brown weathering limestones, and an upper zone of intercalated blue-grey to cream-coloured carbonates with light-yellow bands.

The laminations are formed by thin calcite bands, which are extensively crinkled and folded and may be interpreted as of algal origin. The dolomitic rock (specimens NT 61, NT 62) consists mainly of medium-grained interlocking grains of dolomite with minor muscovite and biotite orientated along a poorly developed cleavage.

Along the western limb of the Dreigratberg syncline a sharp contact is present between the dark-green, ferruginous and chloritic Numees diamictites and the Dreigratberg succession, (see 6, Fig. 17 and Fig. 10). Quartz veins and ferruginization indicate the faulted nature of the contact.

The chloritic schist is approximately 75m thick here and contains single small cobbles of subrounded carbonate and granodiorite, together with a boudined dark dolomite lens, which could be a remnant of the undisturbed dark dolomite bed on the eastern limb. Orthogonal quartz filled joints trend in all directions and seem to define chocolate-tablet boudins.

Towards the west and south of Dreigratberg Peak the stratigraphy changes to a sequence of brown weathering dolomite bands, which are intercalated with grey chloritic

schist units (20-40cm) thick (see 7, Fig. 17). These intercalated units consist primarily of fine-grained chlorite, with minor quartz blebs prominently aligned along the west-dipping S_1 cleavage. A later S_2 crenulation cleavage dipping steeply east deforms the latter and intersects it at approximately right angles (NT 41).

The intensity of banding increases until the rock forms a sharp contact (see 8, Fig. 17) with a black argillite unit. The latter is interpreted as a fault zone because it contains stretched quartz veins and is extensively ferruginized. In turn the light-grey diamictite forms a sharp contact with a ferruginous dark-green chloritic diamictite, which is taken as the base of the Numees. This unit is absent from the eastern limb.

6.6 Structure

Fabric elements of the various deformation phases are outlined below and then described for each separate area.

6.6.1 Fabric elements of the Gariep Cover rocks

a) The first deformation phase

The polyphase sequence of structures are interpreted as being related to a single progressive Pan-African deformational phase in which structures were differentiated on the lines of fold style and orientation.

i) F_1 folds

The F_1 phase of folding is manifested by the earliest recognizable near cylindrical and tight structures in S_0 with axial planes parallel to the regional penetrative S_1 foliation. The latter is outlined by the growth and preferred orientation of metamorphic minerals. Their average trend is NW to NNW. The fold style ranges from class 1c through 2 to 3 (Ramsay, 1967), which is indicative of a ductile shear mechanism.

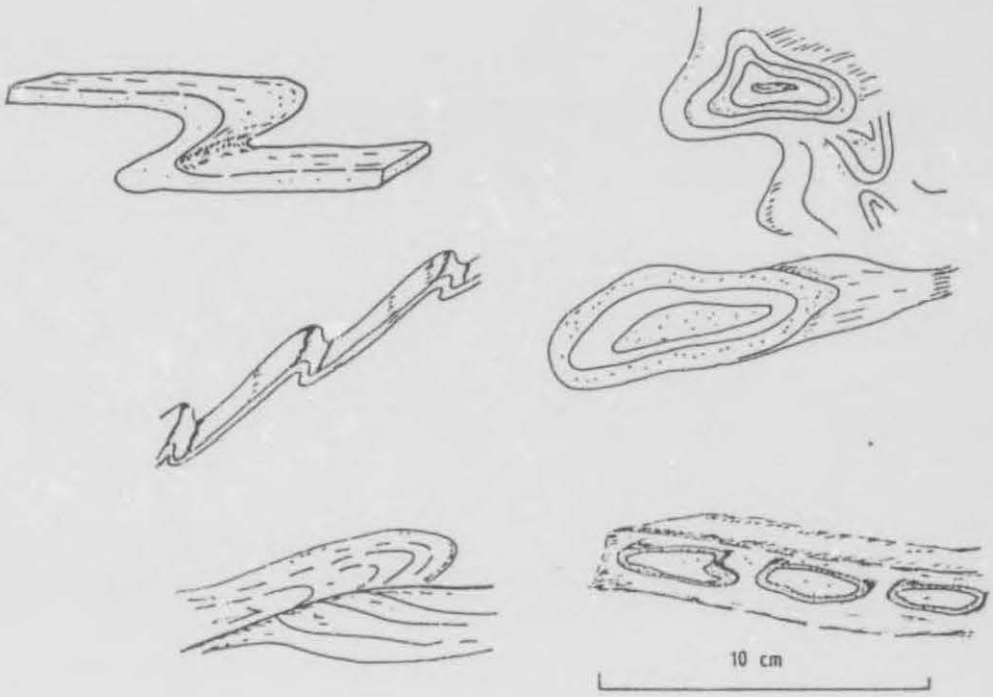

Fig. 20 *Field sketches (looking north) of various east- verging F_1 meso-folds (left column) or F_1 sheath folds (right column) located in the Witputs Sequence and along the Orange River Group contact (P/7, Annexure 1).*

Fig. 20 shows field sketches of various mesoscopic F_1 folds. During progressive deformation many of these meso-folds have become detached and redeformed to now appear as sheath folds and rootless structures. Other F_1 structures are manifested as tight isoclinal to recumbent folds, which are overturned towards the east or northeast. The short limbs have often acted as shear (thrust) planes along which bedding parallel slip has occurred. The folds display both "S" and "Z" shapes with strongly asymmetric forms, ranging from class 1b (parallel), via 1c to 2 (similar) according to Ramsay's (1967) classification.

The type of folds which form in a sequence depend to a large extent on competency contrast and the thickness of successive layers of varying rock types. Conditions seem to benefit the preferential development of these folds in the less competent Pickelhaube limestones and dolomites. Curvilinear and sheath

fold axes trend NW-SE to NNW-SSE and are conspicuous in areas of intense shearing, e.g. near the cover-basement contact.

The F_1 folds have formed during the first intense phase of contractional deformation, which is also characterised by NNW to NW orientated thrust faults. An intense bedding parallel fabric has developed near large scale thrusts, which destroyed most folds in the shear zone. Minor F_1 folds were only preserved during the culmination of this episode and occur in greater numbers in areas distal to intense shear zones.

ii) **S_1 cleavage**

A penetrative axial planar cleavage is related to the first phase of folding. This cleavage strikes in a NNW direction and follows bedding planes or cuts across the latter at low angles. Dips range from shallow to very steep towards the west, with the steepening controlled by imbricate zones and the attitude of the basement contact.

In rocks rich in sheet silicates a slaty cleavage develops e.g. the Wallekraal schists, but as grain sizes increase the cleavage becomes disjunctive and spaced. In arenites and rudites, boulders, pebbles and grains may be aligned to help define S_1.

The strongly developed bedding parallel planar fabric within the dolomitic Pickelhaube limestones are taken as evidence of a penetrative S_1 shear cleavage, because intrafolial shear folds and rootless folds are commonly seen in this rock.

iii) **L_1 lineation**

A prominent mineral growth lineation (L_1) in the form of elongated mica flakes, hornblende, feldspar and microscopically aligned quartz grains along the S_1 cleavage planes, is associated with the first deformation phase. Elongated deformed pebbles and boulders within the Numees diamictite and Wallekraal conglomerates also define the L_1 lineation, as does the maximum of the B_1 fold axes.

Slip directions on mylonitic zones and quartz veins are present as fine striations with biotite coatings or parallel corrugations plunging NW.

Pure shear (irrotational strain) was responsible for the flattening of F_1 folds, and conjugate shearing symmetric to the cleavage of some of the larger clasts in the Numees diamictite. Progressive simple shear rotated the axes of sheath folds into the shear direction (Ramsay, 1967). F_1 and F_2 folds are commonly coaxial although the F_2 folds may also have shallower plunges.

iv) **Faults and planar discontinuities**

NW to NNW trending reverse faults and/or folded thrusts record major displacements during the D_1 deformational event. These faults follow the arcuate shape of the Gariep Belt and have been folded by subsequent D_2 and D_3 deformational events.

Thrust planes steepen towards the granitic foreland and/or as a result of the development of the Pickelhaube Duplex Structure (Annexure 2). They are identified by schist zones with quartz melange in outcrop and extensive flattening fabrics, which are especially conspicuous in conglomeratic horizons. Tectonically intercalated basement granite slivers also often demarcate these zones (Annexures 1 and 2).

Although thrusts often obliquely truncate F_1 folds (Fig. 8, and along tectonically defined boundaries of the Namuskluft synclinorium, Annexure 1), they are interpreted to be related to a single deformational episode more or less co-eval with the final stages of D_1.

b) <u>The second phase of deformation</u>

i) **F_2 folds**

Folds of the second generation are recognized by their open, slightly asymmetric forms and slight overturning towards the west. They also form minor to major mildly plunging structures, ranging from open rounded buckle folds within the more competent units to sharp hinged kink folds in less

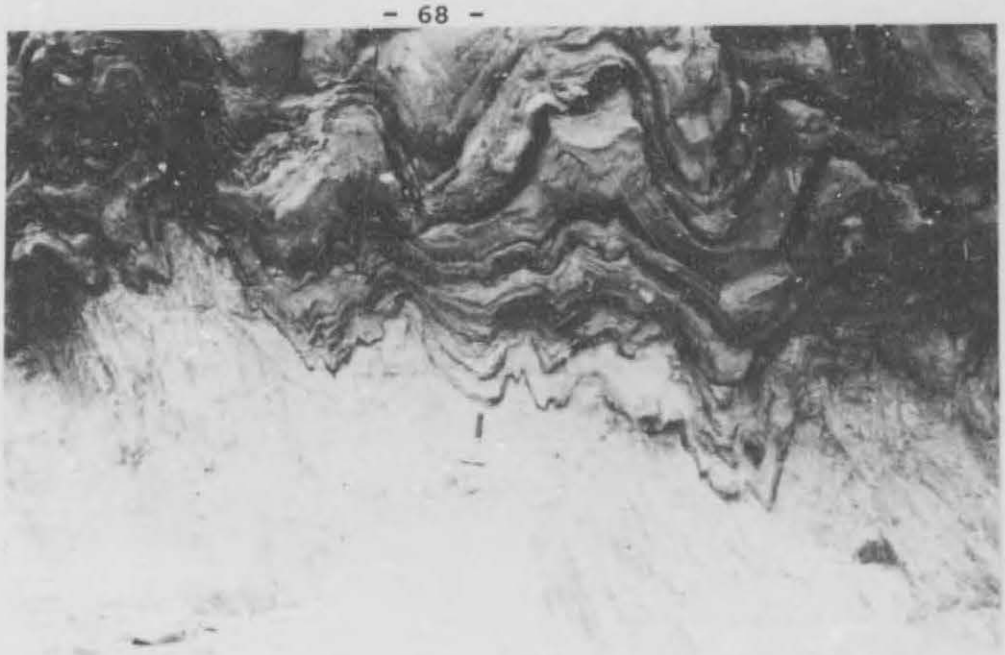

Fig. 21 *The contact zone of the overlying Pickelhaube carbonate with the Wallekraal schists with F_2 kink folds. Hammer handle indicates contact. An east-dipping S_2 axial planar cleavage is prominent in the schists below. The locality is approximately 1 km to the northeast of Pickelhaube Peak.*

competent units at or near lithological boundaries with high ductility contrast (Fig. 21). Several major backfolded F_2 structures occur in the Pickelhaube Peak area (Fig. 22).

The fold mechanism varies from flexural slip in competent units to ductile flow in the incompetent units. Often two interbedded lithologies seem to have been folded alternatively according to classes 1c and class 3, thus propagating through relatively great thicknesses of beds. These structures are often conical and plunge northwest as well as southeast (Fig. 23, 24).

The fold mechanism responsible for the second phase of deformation is mainly due to simple shear acting directly on F_1-fabric where this is planar.

The most common interference patterns noted between F_1 and F_2 structures (Fig. 25) are type 3 patterns (Ramsay, 1967) which are produced by coaxial refolding where the second folds have axial planes making a large angle with those of the first

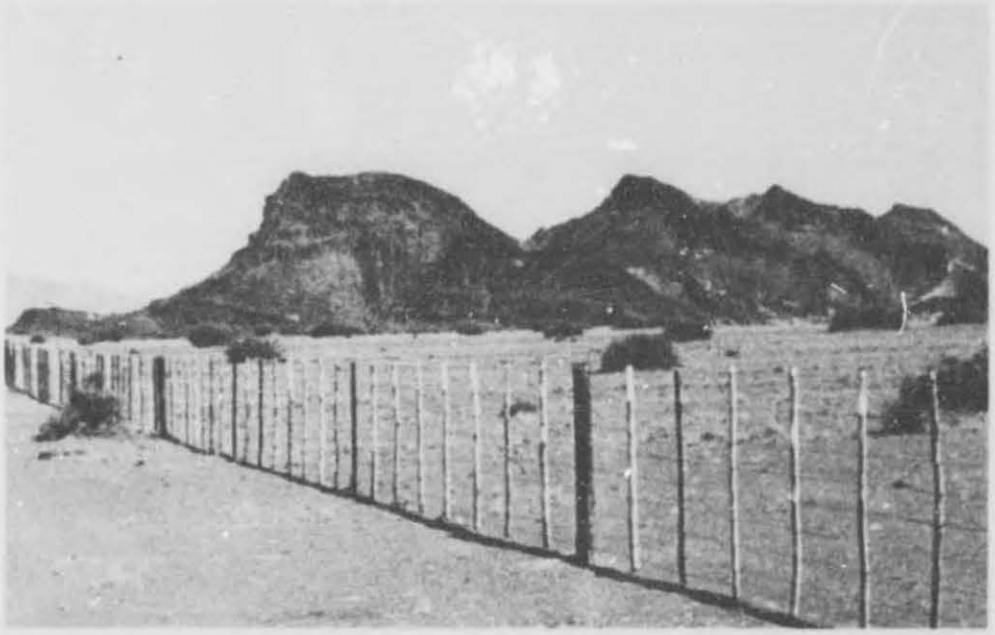

Fig. 22 *Macro- F_2 backfold just overturned towards the west (right) in Wallekraal conglomerates and grits. The locality is approximately 3 km to the northeast of Pickelhaube Peak.*

Fig. 23 *Near symmetrical F_2 folds in Wallekraal schists. S_1, prominent S_2 axial planar cleavage and S_2/S_1 intersection lineations are also recognized. The locality is approximately 1 km to the southeast of Pickelhaube Peak.*

generation. Where the folds are non-coaxial the less common typical mushroom type folds occur (Type 2 interference

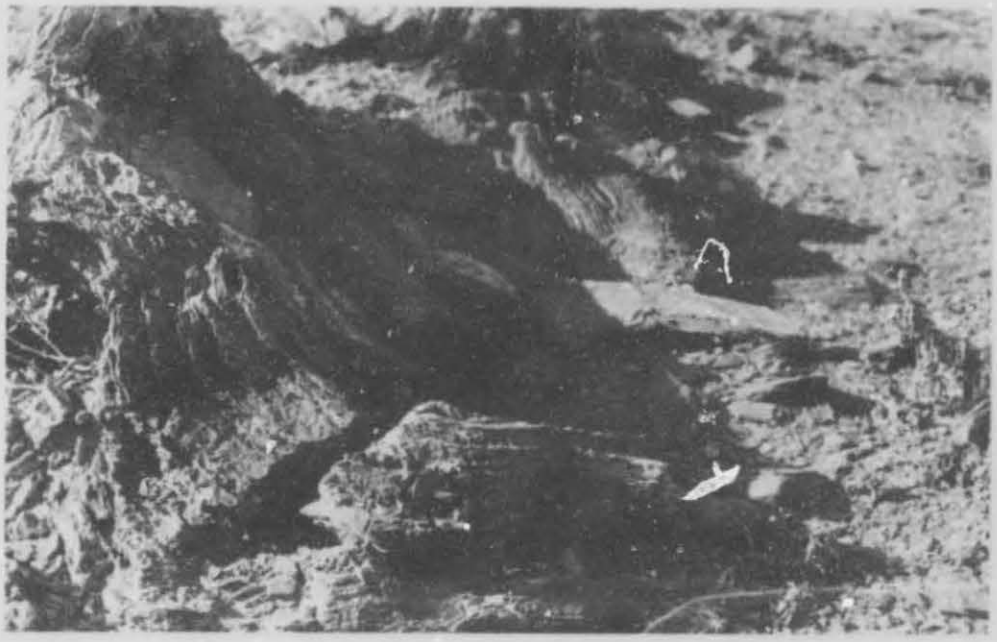

Fig. 24 *Open F_2 fold with east-dipping (left) S_2 axial planar cleavage. The locality is approximately 1 km east of Pickelhaube Peak. Camera lens cap for scale.*

patterns). A possible reason for the presence of two styles of interference may be due to differential movement within the thrust nappe, causing F_1 folds to be rotated into the plane of transport to variable degrees.

ii) **S_2 cleavage**

The second most prominent cleavage is a NW-SE trending crenulation cleavage, which dips towards the northeast, mostly at steep angles.

This structure is axial planar to the second phase of folding and commonly cuts the slaty S_1 cleavage in the Wallekraal schists at high angles. In the Numees diamictite outcrops S_2 appears to have developed mainly parallel to S_1 or it has largely obliterated bedding and S_1. Locally, however, a spaced S_2 shear cleavage displaces varve laminae in Numees diamictites (Fig. 26), and S_0 in Wallekraal schists.

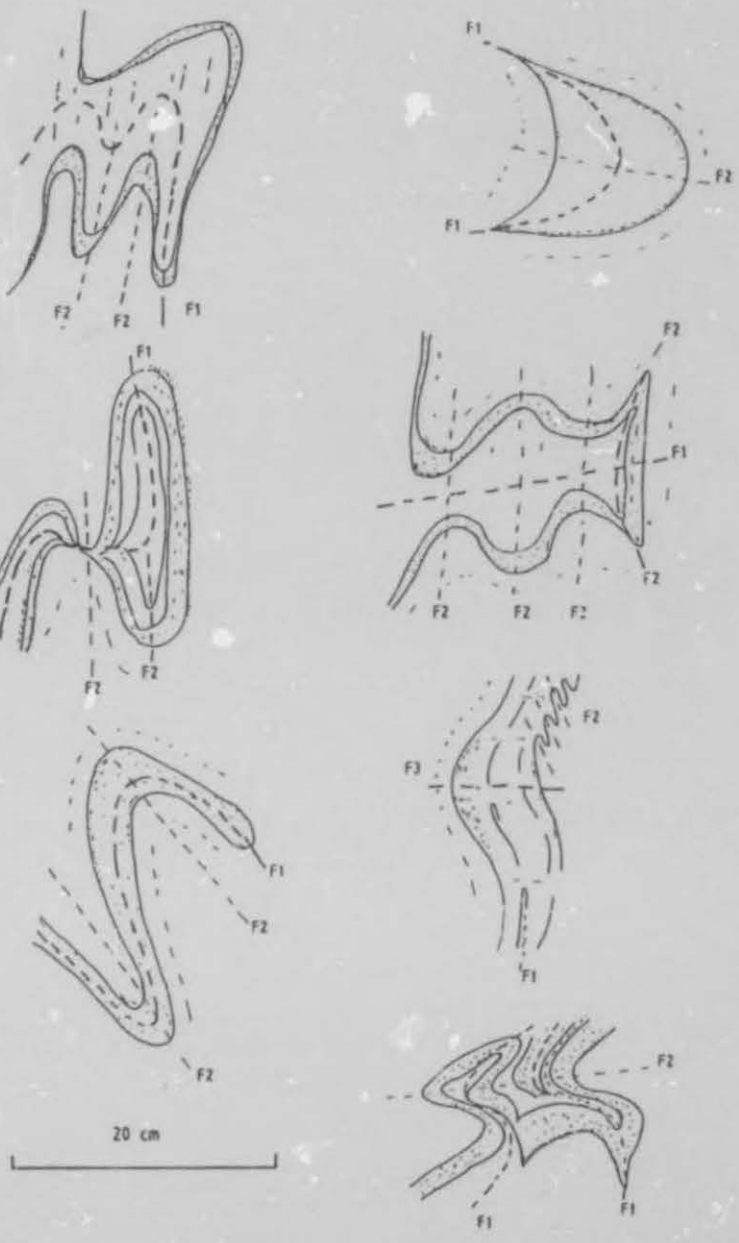

Fig. 25 Field sketches of meso-$F_1/F_2/F_3$ interference folds in the study area as seen in profile looking north.

iii) L_2 lineation

The L_2 lineation is a crenulation lineation, which is formed by the B_2 axis of small crenulation folds, which deform the earlier S_1 cleavage. These lineations are very prominent in the valley at the southern foot of Pickelhaube Peak.

Fig. 26 *Varved shales within the Numees Sequence (looking north) with steeply east dipping S_2 spaced cleavage. The locality is 500m north of Namuskluft farmstead.*

A pencil cleavage lineation structure is also formed locally where the S_2 cleavage intersects laminated bedding planes and/or S_1 (Fig. 23). Lineations plunge at shallow angles towards the NNW as well as SSE, and are similar to patterns described by Von Veh (1988).

iv) **Faults and planar discontinuities**

Quartz and calcite-filled brittle faults occur approximately 1 km to the west of Rosh Pinah near the Rosh Pinah Nappe Thrust (Annexure 3), to the east of Pickelhaube Peak and on the eastern limb of the Rosh Pinah anticlinorium. The fault breccias range from less than one to several metres thick.

Minor displacements seen along markers in carbonates of the Pickelhaube Formation suggest that these are normal faults. They are interpreted as listric extensional structures, which have formed during gravity gliding of sediments into the Sendelingsdrif synclinorium off the bordering Annisfontein

anticlinorium. This happened because of amplification of the latter during thrust stacking in its core.

Displacements of F_2-backfolds of the Rosh Pinah orezone on the eastern limb of the Rosh Pinah anticlinorium indicate that these faults mark the termination of D_2 in the Rosh Pinah Nappe.

Fig. 27 *Open, near symmetric F_3 fold with plunge towards the west. The locality is 1 km to the southwest of basement granites along Gumchavib Thrust (domain 8, Annexure 2).*

c) The third phase of deformation.

i) **F_3 folds**

The third deformation phase is characterized by open, symmetric (Fig. 27) or asymmetric to slightly overturned WSW trending folds, which verge towards the south or southeast. Plunges are westerly or south-westerly, and the folds are non-cylindrical, concentric structures.

F_3 kink folds are prominent in Numees outcrops (Fig. 28). and they may verge either SE or NW in conjugate fashion.

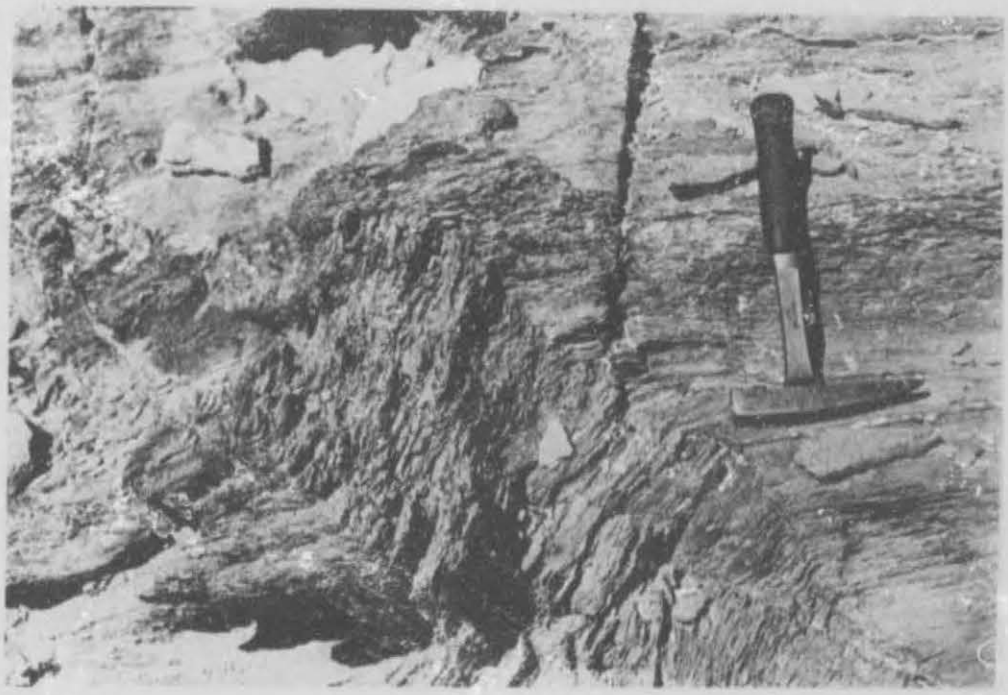

Fig. 28 Asymmetric F_3 kink fold with NW-dipping axial planes (kink planes) in diamictites of the Sendelingsdrif Formation. The locality is domain 10, Annexure 2.

F_3 megafolds are responsible for the undulation of the strata as seen in a N-S section, e.g. when looking towards the west from Rosh Pinah. Their fold axes are nearly normal to those of F_1 and F_2 folds.

ii) S_3 cleavage

A southeast or northwest-dipping axial planar cleavage is related to the F_3 phase of folding. This cleavage is a crenulation feature, which may be sinuous or anastomosing and locally contains calcite veins.

iii) L_3 lineation

The L_3 lineations are mainly defined by the B_3 fold axes, which plunge dominantly towards the southwest, but also to the east or north-east. Below Obib Peak (Annexure 2), an L_3 mineral lineation was observed, which overprints the older L_1 mineral lineation.

iv) **Faults and planar discontinuities**

A NNE-SSW trending set of faults can be recognized and field evidences e.g. displacement of F_3 folds indicates that they are related to the third phase of deformation (Annexure 4).

d) The fourth phase of deformation

The final phase of deformation (D_4) may be related to the emplacement of the Kuboos pluton. This phase seems to be only poorly expressed in the study area north of the Orange River due to the distance from the pluton.

The ubiquitous east-west and SE-striking often quartz-filled near-vertical fractures and joints are accompanied by small crenulations and kink folds within the Numees diamictites.

6.7 Structural domains

The study area has been divided into several structural domains, which are bounded by either structural and/or lithological discontinuities to obtain statistically homogeneous domains, which are defined by: constant orientation of a specific generation of foliation planes, lineations, fold axes or of axial planes e.g. fold vergences.

6.8 The Structure of the Namuskluft-Dreigratberg area

The structural style along the dissected escarpment in the Namuskluft-Dreigratberg area is largely that of a fold-thrust imbricate that steepens up against the foreland ramp. The Sendelingsdrif synclinorium is described as a graben by several authors, (De Villiers & Söhnge 1959, Martin, 1965), but is here interpreted as a thrust-fold slice (imbricate) (Annexure 2 b).

The Namuskluft synclinorium generally has open folds with a varying shallow plunge north or south. However, tight folds appear on the eastern limb close to the Rosh Pinah Nappe Thrust. A steep east-dipping S_1/S_2 axial planar cleavage obliterates most of the bedding traces within the Numees Sequence. Where bedding is visible e.g. within varved shales

or as thick units, they dip west at approximately 55°. Within the Numees diamictites extensive shearing is indicated by pinching and swelling of disrupted quartz veins. The cleavage steepens towards the east.

F_3 folds deform the S_1/S_2 axial planar cleavage (Annexure 1, domains 3 & 5) with F_3 (S_2) axes plunging steeply east to northeast. F_2 folds deform isoclinal quartz veins (Fig. 29). along the basement contact (N/4, Annexure 1) into open folds with north to north-east dipping axial planes often marked by a calcite-filled spaced cleavage that dips at angles of 10-25° towards the NE.

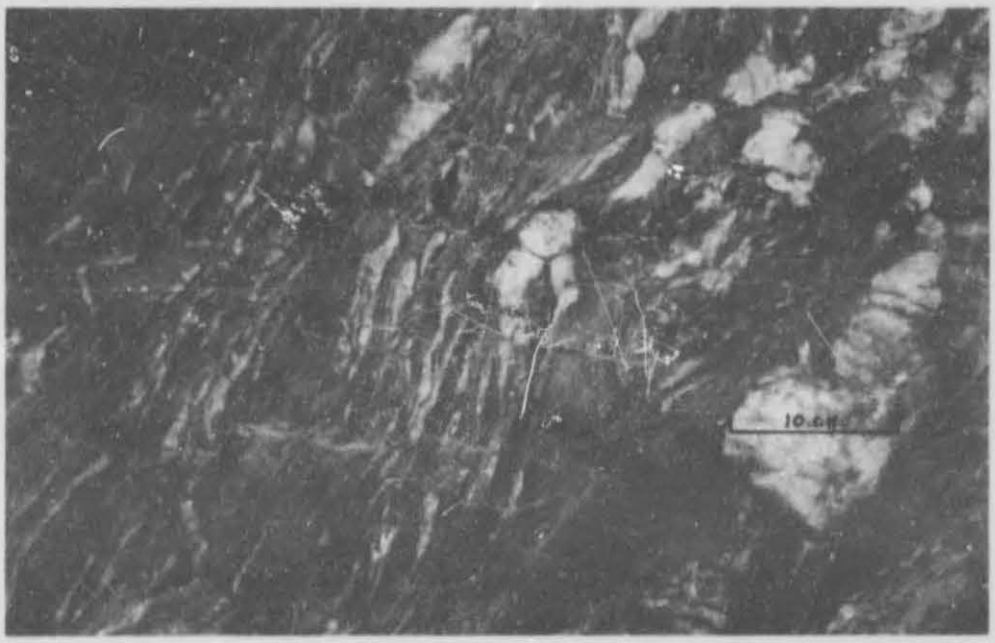

Fig. 29 *Part of a zone of shearing and cataclasis of quartz veins along the thrust contact of the basement and cover sequence (N/4, Annexure 1). Isoclinal F_1 shear folds with axial planes dipping steeply west are seen. They are refolded by open F_2 folds with calcite filled S_2 cleavages dipping east at low angles. The locality is 2 km north of Namuskluft farmstead.*

A conspicuous northwest-dipping L_1 mineral lineation (domains 3, 5, Annexure 1) is defined by black streaks of biotite on S_1/S_2 cleavage planes in pelites. It parallels the long axes of clasts within the diamictite that lie within the foliation

and plunge towards the north at varying angles. This defines the L_1/L_2 lineation and D_1/D_2 transport direction (Fig. 30a, b).

These rocks have been subject to intense deformation as indicated by the undulose extinction of quartz grains and the presence of shear related en-echelon quartz veins. Several NNW-SSE trending quartz veins dip steeply towards the ENE, while less prominent veins trend NE-SW and dip towards the NW.

A local north-trending lineation (not shown) is formed by the intersection of a local shallow dipping fracture cleavage with the steep easterly-dipping S_2 cleavage. This lineation plunges at shallow angles towards the north.

Later fractures and faults with an east-west trend and occasional small scale kink folding of the same orientation as found in the Numees Formation can be ascribed to the final phase of Gariep deformation (D_4) as outlined by Kröner, (1974).

The structural importance of the Sendelingsdrif synclinorium is indicated by the emplacement of one of the largest post-tectonic, post-Nama intrusions, the Kuboos pluton near its centre and a 80km Gannakouriep dyke following the strike of the synclinorium in the Richtersveld.

6.9 Results of Strain Analysis

The methods and assumptions are outlined in the appendix and will not be repeated here. Strain estimates of orientated clasts in the Numees diamictites should be regarded as minimum values as the assumptions outlined in the index are not applicable throughout. Care was taken to take measurements in areas where the matrix of the rock is largely quartzitic or gritty, with present competencies often similar to those of the dominantly granitic clasts. Mudstone matrix was avoided. The results of the strain measurements are summarized in Table 2.

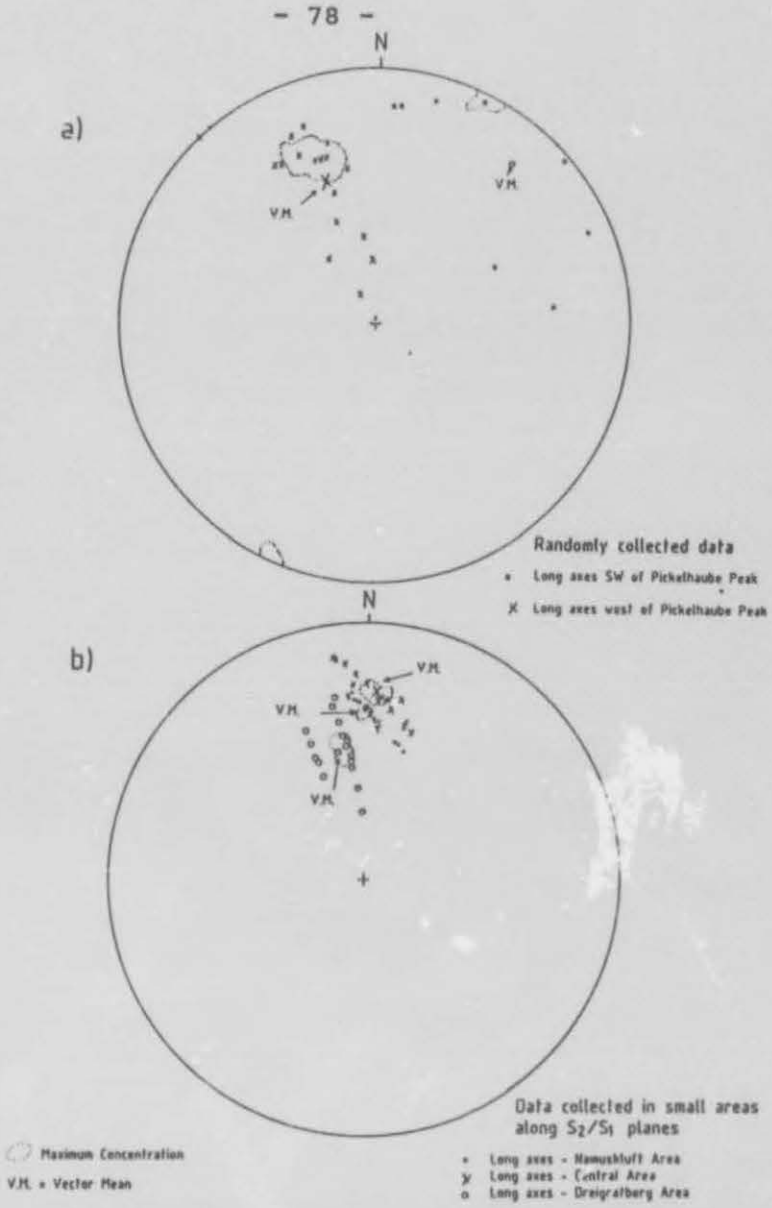

LOCALITY OF LONGAXES DATA	VECTOR MEAN
SW of Pickelhaube Peak	339°/41°
W of Pickelhaube Peak	40°/18°
Namuskluft Area	001°/35°
Central Area	003°/27°
Dreigratberg Area	347°/48°

Fig. 30 The orientation of long axes of clasts in the:

a) the Wallekraal conglomerates
b) Numees diamictites in study area (see Annexure 1).

Table 2 STRAIN DATA GATHERED ALONG XY PLANES OF THE STRAIN ELLIPSOID

AREA	N	ARITHMETIC MEAN	GEOMETRIC MEAN	HARMONIC MEAN	ϕ VALUE	I_{sym}	MEAN LONG AXIS	STRAIN RATIO
1. Namuskluft Farmstead	48	2,71	2,91	2,70	0,70	0,80	001°/35°	5,91: 2,19: 1
2. Central Area	47	2,14	2,36	2,23	2,10	0,86	003°/27°	4,59: 2,06: 1
3. Dreigratberg	75	2,62	2,68	2,51	2,55	0,84	347°/48°	5,12: 2,04: 1

STRAIN DATA GATHERED ALONG XZ PLANES OF THE STRAIN ELLIPSOID

AREA	N	ARITHMETIC MEAN	GEOMETRIC MEAN	HARMONIC MEAN	ϕ VALUE	I_{sym}	MEAN LONG AXIS	STRAIN RATIO
1. Namuskluft Farmstead	52	2,33	2,19	2,10	-	-	-	-
2. Central Area	52	2,17	2,06	1,90	-	-	-	-
3. Dreigratberg	51	2,19	2,04	2,00	-	-	-	-

Because there could be a positive relationship between size and shape of clasts as a result of crystal plastic deformation, the markers in the Dreigratberg area were grouped into clasts smaller and greater than 4cm and values recalculated along S_2/S_1 cleavage planes (XY planes).

The results are as follows;

Harmonic mean for pebbles < 4cm = 2,38
Harmonic mean for pebbles > 4cm = 2,26

There is a fair correspondence, which indicates that values given for the three areas are reasonable minimum estimates of the strain.

The following results are indicated by these measurements;

i) The flattening of clasts across the S_1/S_2 cleavage planes (the XY plane of the strain ellipsoid) confirms significant contractional deformation of lithologies against the basement as also shown by tight folding of the Sendelingsdrif synclinorium and by the steep attitude of thrust planes.

ii) As F_1 and F_2 folds are approximately co-axial and S_1 and S_2 cleavages follow the same trends e.g. in the Sendelingsdrif synclinorium it is not always possible to differentiate between the latter in the steepened imbricate zone. Here we therefore study the combined effect.

iii) The exact reason for the change in the axial ratios of the strain ellipsoid as well as the orientation of the long axes (X) can possibly be related to:

a) the change in direction of the original floor unconformity as well as its composition. This in turn influences the attitude and dip of the ramps along which cover rocks are imbricated. Depending on the angle between the ramp and the tectonic transport direction the dip and strike

slip components will change from place to place.

b) The effect of the third phase of deformation, which can clearly be seen in the deformation of the S_1/S_2 fabric of domain 3.

The combination of Von Veh's (1988) data together with results of this study (Fig. 31a and b) indicate the following:

i) the relationship of X/Z to X indicates that clasts with steeper plunging long axes are normally more deformed than shallower plunging ones

ii) this indicates that flattening of clasts increases towards Namuskluft, which implies higher strain in this area

iii) the near parallelism of fold axes to X, north and south of the Orange River, as well as sheath fold axes which plunge to the NNW indicate transformation of fold axes into the transport direction

iv) a NW to SE to WNW-ESE transport direction is indicated by all analyses of deformed markers near the basement contact. The reduction in the vertical component southwards may indicate that the basement contact may dip considerably flatter towards the west, or that its orientation changes from NNW in the north to NW in the south.

From the structural analysis of the Dreigratberg-Namuskluft areas it is evident that;

i) transpressional shear dominated the area

ii) the XY plane is parallel to the fold axial planes, the S_1/S_2 cleavage planes and is slightly oblique to major dislocations

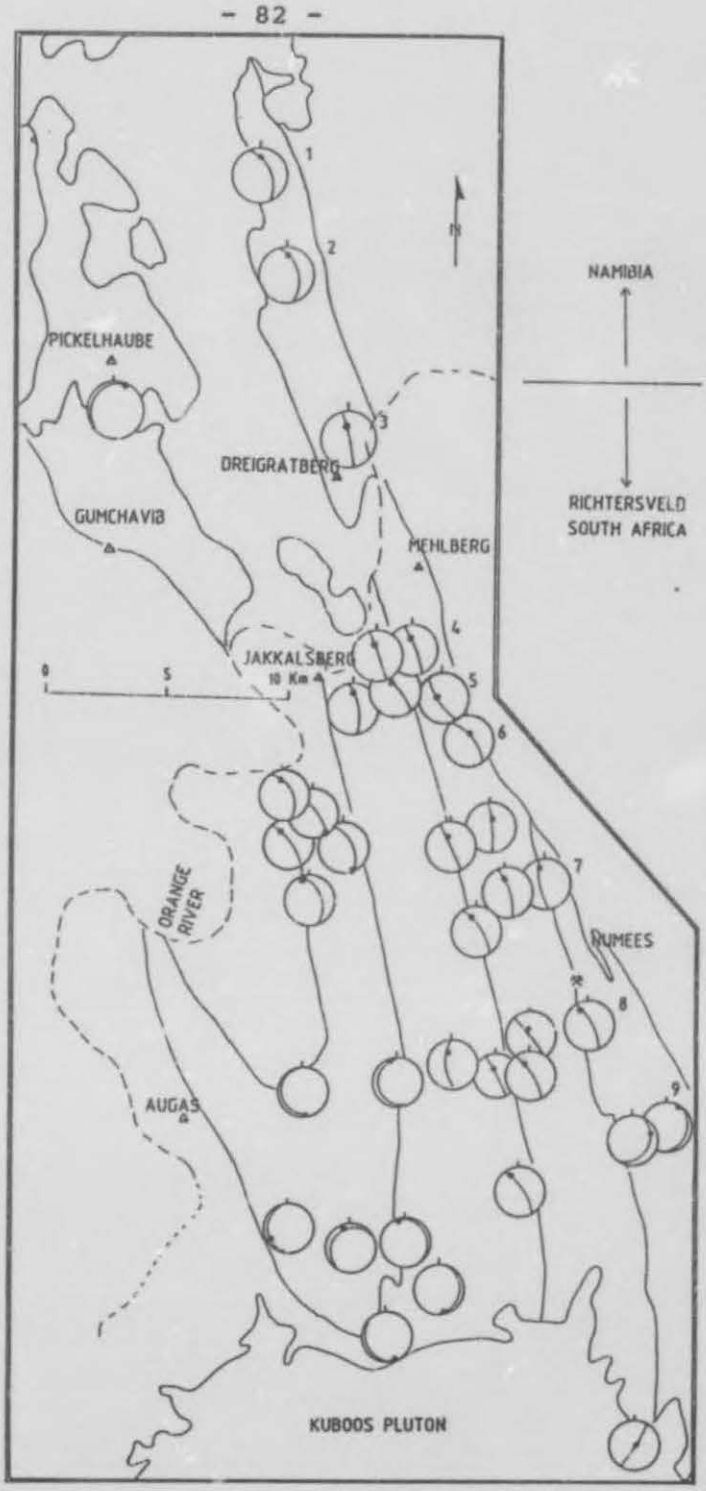

Fig. 31a Map of the northwestern Richtersveld and southwestern Namibia showing the variation in orientation of the X-axis of the strain ellipsoid. Richtersveld data after Von Veh (1988).

Subdivisions on the map is based on main lithological boundaries.

iii) $X_{1/2}$ (axis of elongation in the S_1/S_2 plane) is therefore the transport direction and is moderately inclined to the NNW, as shown by analysis of strain markers.

iv) minor sheath folds are parallel to $X_{1/2}$

v) the tectonite is explained as an imbricate zone of oblique F_1/F_2 ramps formed in a transpressional regime which transformed and translated F_1 folds and thrusts.

Where S_0 is absent (as in diamictites) an S_1/S_2 cleavage is the dominant structural element. All folds and dislocations have been steepened as the south-easterly directed transport vector develops a vertical and a horizontal component during multiple oblique ramping.

The next step is to investigate the structural nature of the Gariep tectonite further away from and west of the imbrication zone to be able to tell how this imbricate zone was formed. This was done by studying the structure along two E-W traverses.

7. THE GEOLOGY AND STRUCTURE OF AN EAST-WEST TRAVERSE IN THE PICKELHAUBE PEAK AREA

7.1 The Basement Complex

7.1.1 Distribution and Stratigraphy

Basement granites and gneisses are exposed along the Gumchavib Thrust in the western part of the traverse northwest of Gumchavib Peak (Annexure 2a). These rocks have been the subject of much controversy and were originally interpreted to have formed through a process of granitization (McMillan, 1968).

The controversy was only resolved after Rb/Sr dating carried out by Welke et al. (1979) confirmed a metamorphic Namaqua age of 1100 Ma for these rocks. Hence they must be correlated with the older Vioolsdrif Granitoid Suite and form a basement inlier.

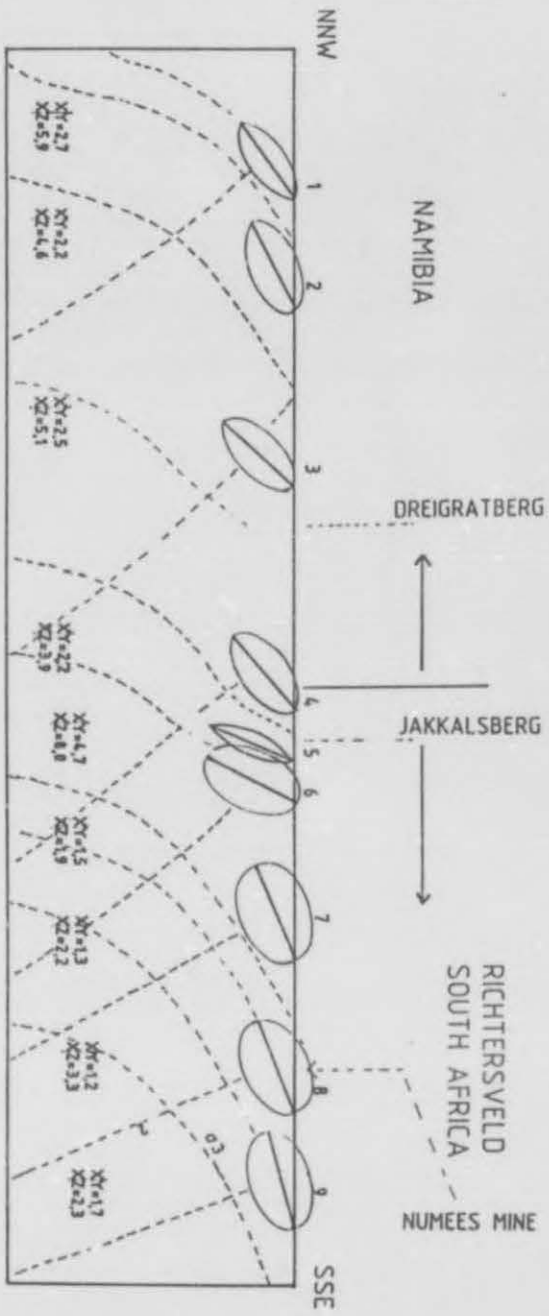

Fig. 31b Projection of the attitude of the X/Y strain ellipsoid onto a NNW to NNE near vertical plane along the eastern contact to the basement. X/Z strain ratios as well as possible changing σ3/σ2 stress trajectories are also shown.

7.1.2 Lithology and petrography

The granitic sequence consists largely of thick zones of elongated leucogranite bodies orientated parallel to the regional SW-dipping S_1 cleavage (Domain 8). Thinner lenses

of extensively sheared blue-grey augen-gneiss are intercalated locally.

The augen-gneisses contain large feldspar and quartz porphyroblasts, often > 1cm in diameter. Along the eastern boundary the granites form a thrust contact with sediments (the Gumchavib Thrust) and are accompanied by pervasive ferruginization and epidotization. The granite is also enriched in biotite and chlorite here.

A petrographic study of the granites (NT 154, NT 155, and NT 156) indicates that they consist essentially of quartz and feldspar (plagioclase) and hornblendes as major constituents, while chlorite, muscovite and epidote form minor components. Accessory zircon is present in all the samples. The sheet silicates are aligned along the penetrative cleavage, and feldspars have been extensively altered and sericitized.

7.2 The Stinkfontein Sequence

7.2.1 Distribution and stratigraphy

Quartzitic lithologies of the Stinkfontein Sequence unconformably overlie the upthrust basement lithologies in the west. The Sequence has been duplicated by the Gumchavib Thrust. Lithologies grouped within the Rosh Pinah Formation underlie the granites, while quartzitic lithologies of the Gumchavib Formation unconformably overlie the basement granites. The presence of an intensified cleavage however, suggests some shearing along the upper granite contact.

7.2.2 Lithology and petrography

Lithologies directly overlying the basement inlier consist of fine-grained Gumchavib Formation quartzites commonly alternating with thin pelites with parallel laminations apparently representing shear planes. Several thin (3-5m) light or medium-grey dolomitic bands are intercalated in the stratigraphically higher parts of the succession and at the top form a thrust contact (the Valley Thrust) with the Rosh Pinah Formation. The contact zone displays numerous bedding parallel quartz veins over a width of several metres.

Similar dolomite bands occur in the same stratigraphic position along the Obib Peak traverse (Fig. 47).

In the hanging wall of the Valley Thrust a sequence of light-brown, medium-grained quartzites with intercalated blue-grey, fine- to medium-grained and laminated limestones occurs. A thin, black dolomite band is also found locally in these rocks, which are grouped within the Rosh Pinah Formation.

The Stinkfontein lithologies, which tectonically overlie the Numees diamictite along the Obib Waterhole Thrust (Domain 11, Annexure 2) are coarse-grained, blue-grey or light-grey dolomites with minor intercalated light-brown quartzite beds, which are also grouped within the Rosh Pinah Formation. The dolomitic marble, (NT 149), of this thrust sheet consists entirely of a matrix of small interlocking dolomite grains with clusters of large calcite grains drifting in it. Towards the west these rocks disappear under the dune cover.

7.3 The Hilda sequence

7.3.1 Distribution and stratigraphy

The Pickelhaube carbonates are duplicated in the Pickelhaube Duplex Structure and are well developed below Pickelhaube Peak (Fig. 2). The Hilda Sequence is represented by a thin slice of Pickelhaube carbonate rocks followed by a thin zone of Wallekraal Formation grits and conglomerates ir the southwestern part of domain 10, Annexure 2. The latter is conformably overlain by a 50m thick diamictite unit, which is thought to belong to the Numees Sequence.

In the central parts of the Annisfontein anticlinorium the Pickelhaube carbonates have been eroded away. Along the eastern limb of the Annisfontein anticlinorium the Wallekraal Formation is prominently developed.

East of Pickelhaube Peak (Domain 6, Annexure 2), the Wallekraal schists locally abut against an east-dipping thrust, the RPNT. Above this sole thrust and to the east the sequence of conglomerates and arenites is repeated at least

three times by hinterland-dipping duplexes steepening up from E to W.

The Wallekraal Formation lies unconformably above the Pickelhaube Formation in the Richtersveld (Von Veh, 1988). In the study area this situation is reversed and can only be explained by thrusting of the Pickelhaube Formation over the latter along the RPNT, or by major recumbent folding.

The presence of the RPNT is physically evident in the field as a slightly east-dipping, silicified contact zone between overlying Pickelhaube carbonates and the underlying Wallekraal lithologies.

7.3.2 Lithology and petrography

The lithologies of the Pickelhaube dolomitic limestones have been described previously. However, the central Pickelhaube unit within the duplex zone contains a zone of angular often pisolitic dolomite clasts within a dolomitic matrix, which seems to represent a sedimentary breccia. In places this zone consists of several clearly distinguishable units with upwards fining clasts (Fig. 32). Subrounded to rounded quartzite clasts similar to those of the Wallekraal Formation are also present.

This unit may have originated as a gravitationally triggered debris or mudflow deposit, derived largely from carbonate reefs in higher, marginal parts of the basin. Stratigraphic thinning seems to occur westwards which points to an easterly source.

In the steeply west-dipping imbricate zone (Domain 6, Annexure 2) intercalated grits of the Wallekraal Formation often have a reddish colour, locally grading into arkoses with prominent feldspar clasts. The sequence is upward fining. Small quartz pebble conglomerate lenses contain up to 50% rounded, subrounded or angular feldspar clasts with diameters up to 1cm.

These grits are similar to lithologies found at Obib Peak (Annexure 3) and indicate very rapid transport and burial,

Fig. 32 Carbonate breccia zone with mudflow characteristics. The locality is approximately 2 km to the NE of Pickelhaube Peak.

probably at low average annual temperatures and a semi-arid climate.

Huge isolated dolomite boulders, blocks or lenses drift in the grits and schists and their frequency increases towards the base of the Wallekraal Formation. They may measure up to 8m x 8m across. These features have been interpreted as bioherms (Kröner, 1980), but they may even represent extremely boudined carbonate bands or deformed, slumped carbonate blocks. The Wallekraal Formation schists form a sharp apparently conformable but prominently sheared contact with the overlying Picklehaube dolomite at the top of each thrust slice.

In domain 7 Wallekraal lithologies underlie most of the Annisfontein anticlinorium southeast of the Rosh Pinah Nappe Thrust along which they have been transported over the Rosh Pinah Formation because the RPNT is cutting stratigraphically downwards (see section, Annexure 2). Micaceous conglomerate

and grit lenses abound, with biotite porphyroblasts aligned oblique to the S_1 cleavage.

Generally conglomerate lenses increase towards the top of the formation concurrently with an increase in the percentage of Wallekraal schist fragments in them. The intercalated quartzites contain several thin quartz pebble conglomerate layers with feldspar clasts. These quartzites may grade upwards into blue-grey arkose.

Alternating normal as well as inverse grading sequences confirm local duplication of units because of isoclinal folding. Considerable thinning of beds has occurred along the limbs.

Near the base of the lower Wallekraal schists below Pickelhaube Peak, disorientated fragments of quartz veins occur in a cataclasite. This is interpreted as a sole thrust to the exposed sequence. The contact of this schist zone with the overlying conglomerate is knife sharp.

A petrographic examination of some of the gritty rocks (specimen NT 83) outline a mineralogy consisting mainly of rounded to subrounded quartz grains with a polygonal-granoblastic texture. Large brown porphyroblastic biotite flakes as well as brown ferruginous fillings of cracks are present. The matrix is made up of chlorite and biotite. The medium-grained pebble conglomerates (NT 84) have a similar mineralogy except that feldspar becomes a major phase. Most feldspar grains are sericitized.

7.4 The Numees Sequence

7.4.1 Distribution and stratigraphy

A 50m thick lens of blue-grey diamictite unconformably overlies the Wallekraal conglomerates and grits in the southwestern part of domain 10. Similar outcrops are found along strike intermittently north of the study strip of Annexure 2. The stratigraphic position of these rocks indicate that they belong to the Numees Formation. They have

also been mapped as such south of the Orange River by Von Veh (1988).

A dolomitic limestone-quartzite unit (here correlated with the Rosh Pinah Formation) overlies these rocks along a thrust contact (the OWT).

7.4.2 Lithology

The Numees diamictite is a severely deformed grey-green rock with unsorted clasts of dolomite, Wallekraal grit, leucogranite, granodiorite and quartzite within a green chloritic matrix. McMillan (1968) also noted some red granite clasts probably of basement granite derivation in similar diamictites outcropping along strike towards the north.

The rest of the lithology and stratigraphy of the strip map east of the Rosh Pinah valley (the Dreigratberg-Namuskluft area) has been described on pages 47-56.

7.5 The Structure of an east-west traverse in the Pickelhaube Peak area

The stratigraphy, major structures and subdomains with fabric analyses are shown on Annexure 2(a). The main structural features of this traverse are indicative of southeasterly directed thrusting, thrust stacking, thrust steepening and backfolding against anticlinoria, and basement ramps.

Towards the east the Pickelhaube and Wallekraal Formations have been duplicated in the Pickelhaube Duplex Structure, which lies within the Rosh Pinah Nappe. Several macro west-verging F_2 backfolds can be outlined here (Annexure 4).

These and the younger Numees rocks in the Sendelingsdrif synclinorium have probably been duplicated as a result of gravity gliding along the Rosh Pinah Nappe Thrust, which was a consequence of late rising of the Annisfontein anticlinorium because of an antiformal thrust stack developing in its core (Von Veh, 1988). A normal stratigraphic sequence is present along the escarpment where

the Witputs lithologies unconformably overlie the Numees diamictites. However, thrusts are well exposed along and west of the basement contact where several thin slivers of granite crop out.

The latter are remnants of basement granite in the roof of the Rosh Pinah Nappe Thrust and appear wedged in between the upper limestone and diamictite unit of younger formations, possibly the Namuskluft Formation (N/4, N/5, Annexure 1).

Domains along this traverse are numbered 1 to 11 from E to W. Contoured fabric diagrams are given in Annexures 1, 2 and 3 and point distribution diagrams in the text. Only the most prominent structural features are outlined on fabric diagrams on Annexures 1, 2, and 3.

The east-west section in the Pickelhaube Peak area is discussed first because it is closest to the profiles drawn south of the Orange River by Von Veh, (1988).

i) Domain 1

Domain 1 includes the older basement rocks, which are separated from the Gariep cover rocks over long distances by a major thrust zone. Just north of the Orange River however, (R/5,14,15, Annexure 1) an unconformable contact has been preserved.

Lithologies include the mafic Orange River Group volcanics with less felsic volcanics, intruded on a large scale by the co-genetic Vioolsdrif Granitoid Suite (See chapter 2.1.2).

South of Lorelei Mine (14/R +S, Annexure 1) the volcanics have been thrust over the Vioolsdrif granite, and deformed together with the cover rocks. These rocks have been affected by the following tectonic events:

a) D_1b (After Von Veh, 1988)

The first recognized tectonic event is the (>1900 Ma) Orange River Orogeny outlined by Bertrand (1976) and Ritter (1978, 1980). This event is only indicated by local remnants of a

folded schistosity. In the Orange River Group two prominent cleavages have been measured, with the west-dipping discontinuity interpreted as S_1, possible remnants of an earlier basement cleavage.

The S_1 basement cleavage poles (Fig. 33a), however, follow a partially developed great circle girdle distribution, with a π-axis at 292°/66°. They are obviously deformed (curviplanar refracted cleavage) and probably had an original orientation dipping steeply to the SW or W.

Fold axes with a north-westerly orientation are characteristic of the F_2 phase of folding in the cover sequence. The vague delineation of a wide S_1 π-girdle may be due to the effect of the still younger F_3 folding in the cover rocks.

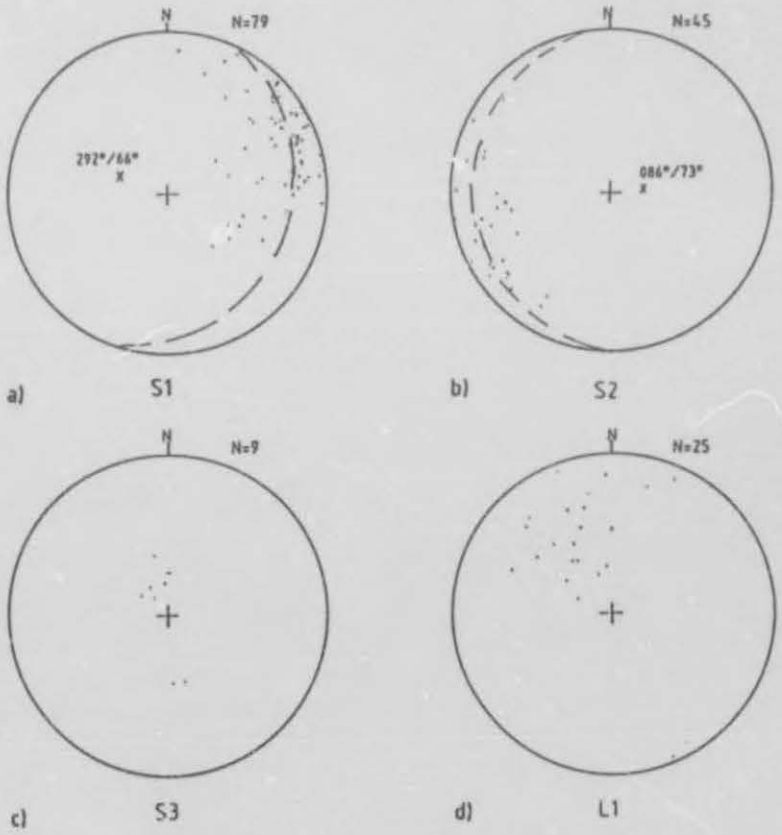

Fig. 33 Fabric data from domain 1

The second cleavage is an east-dipping crenulation cleavage (Fig. 33b). It seems related to the S_2 cover cleavage overprinting the S_1 cleavage of the basement. S_2-basement cleavages define a π-axis trending 086°/73° possibly related to a younger deformation producing NE-SW trending F_3-folds in the cover rocks. S_2 is also deformed or fanning and seems to have had an original orientation dipping steeply to the E or ENE. This agrees with attitudes of similar S_1 and S_2 cleavages in domain 2 and 5 (Annexure 1).

A poorly developed S_3 cleavage is only found sporadically and generally dips at low to moderate angles to the SSE (Fig. 33c). Locally a set of prominent NNW plunging asymmetric kinks, which verge towards the east (F_4 of the cover rocks) deform the older basement S_1 cleavage to define an L_1 lineation (Fig. 33d) in the chloritic mafic rocks near the cover/basement contact. Shearing along cleavage planes is common here.

b) D_1n (After Von Veh, 1988)

A major shearing episode along the northeastern and southern margins of the Richtersveld Subprovince can be related to the ≈1200 Ma Namaqua Orogeny (D_1n) (Blignault, 1974, 1977; Bertrand 1976; Theart, 1980; Booth 1987).

The granodioritic rocks commonly contain pre-Gariep shear zones several metres in width with limited strike length, which commonly abut against the younger Gariep rocks. The dominant trend of these features is towards the NW and NNW, but dips may be either steeply towards the SW or shallow towards the NE. Some of them are possibly reactivated structures, which were formed during a backthrusting event (Von Veh, 1988) of the Namaqua tectogenesis.

ii) **Domain 2**

Domain 2 includes lithologies of the Witputs, and underlying Numees and Hilda Sequences (Fig. 2). These rocks form thrust-fold slices embracing several mega-F_1 anticline-syncline pairs in the Namuskluft synclinorium.

This domain is demarcated by the Rosh Pinah Nappe Thrust in the west along which upthrust slivers of granite are found (N/4, N/5, Annexure 1), and the Namuskluft Thrust in the east along the contact to basement. A conspicuous quartz vein melange zone is present along this contact north of Namuskluft farmstead (N/4, Annexure 1).

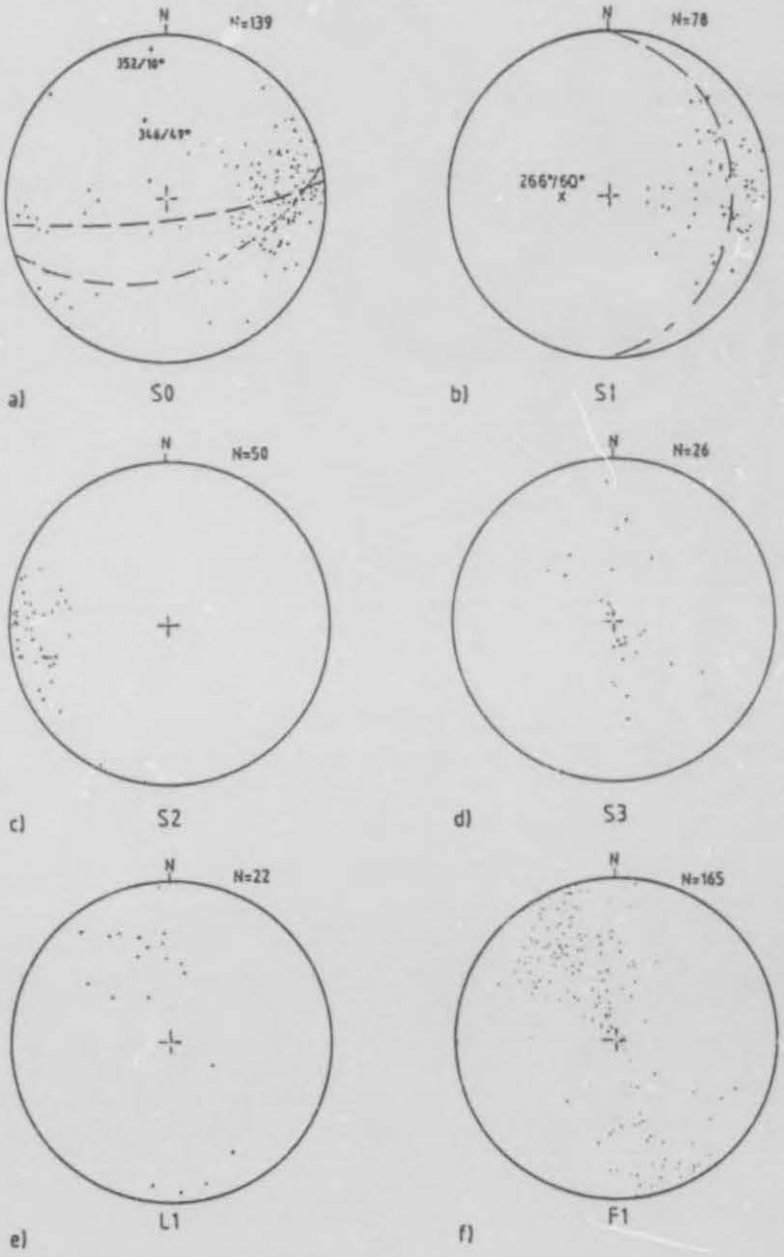

Fig. 34 Fabric data from domain 2

Poles to S_0 define a somewhat vague π-axis plunging at low to moderately high angles into the NE-quadrant (Fig. 34a), and parallel to the F_1 fold axis maximum (Fig. 34f)

West-dipping fold limbs are more prominent than steeper east-dipping limbs and indicate an easterly vergence, which is related to the first deformation phase. No obvious F_2 backfolding has been observed in this domain, but the fact that the S_0 distribution is so dispersed means that some later deformation has affected bedding.

This is also confirmed by the diffuse maxima of S_1 and S_2 as well as the bipolar distribution of L_1 and F_1, which confirms F_3 crossfolding. The S_1 cleavage is an almost bedding parallel feature that either mimics bedding or cuts slightly across it. It distributes on a great circle girdle with a π-axis at 266°/60°, which approximates the F_3 fold trend, and is on average slightly shallower than bedding (Fig. 34b).

A well defined S_2 crenulation cleavage dips steeply towards the east (60° - 80°, Fig. 34c) and is especially prevalent within the diamictite unit, while S_3 cleavages either dip shallowly towards the NW or SE (Fig. 34d).

L_1 (Fig. 34e) is an intersection lineation formed by S_1 and S_0, which is paralleled by F_1 fold axes (Fig. 34f). F_1 folds outline a NNW trending girdle with submaxima, which indicates the influence of D_3 deformation. The steeper cluster of NNW plunging F_1 axes were measured in the southern part of the Namuskluft synclinorium towards the Orange River (Annexure 1).

Open F_2 folds have a vector mean on 331° with a plunge of 33° towards the northwest, which is similar to that of possible S_0,π-pole positions and L_1 as well as F_1 fold axis maxima. Shear planes follow the NNW trending axial planes of prevalent folds and dip either steeply to the SW or NE. Sheath folds are preferentially developed within zones of shearing along the basement contact e.g (P/8, Annexure 1), and their axes have attitudes near the attitudes of F_1 fold-axis maximum (Fig. 34f).

Due east of the Namuskluft farmstead (N/6, Annexure 1) some prominent foliation-dominated shear indicators (the S-C fabrics) which are controlled by the relative slip rate along surfaces (Bjornerud, 1989) are located in pink limestones of

the Witputs Sequence. They indicate a sense of contractional shearing across a west-dipping S-plane. Several examples of minor thrust imbricates are present along the basement contact (Fig. 35).

Fig. 35 Thrust imbrication (overstep thrust sequence) along cover/basement contact on Namuskluft (P/8, Annexure 1). Looking south. Hammer on lowest imbricate for scale.

At this locality there are two distinct lineations in the rock with the older NNW trending lineation (L_1) (Fig. 34e) truncated by the younger lineation trending 317° (L_2). An asymmetric mega-F_2 fold indicates a sinistral sense of movement in a SSE direction along the basement contact (O/8, Annexure 1).

The structural analysis of this domain allows a clear distinction between three deformation phases, the first two of which are very nearly co-axial and almost co-planar, but their vergences differ and F_1 deformation intensities are generally much higher.

L_1 and F_1 and sheath folds plunge to the NW at angles very comparable to those of $X_{1/2}$-axes derived in chapter 7.9 for

domain 3 and 4 (Annexure 1 and 2). This indicates that stretching and re-orientation occurred along fold axes F_1 and F_2, and where shear was concentrated. Some F_1 (and F_2?) folds, which were oblique to the shear direction, developed into sheath folds, which eventually trend almost parallel to the re-oriented ones.

iii) **Domain 3**

This domain includes a thick sequence of monotonous Numees diamictites with minor varved shales and grits. These lithologies form a prominent anticlinal ridge trending from due north of the Namuskluft farmstead southwards, to the Orange River (Annexure 1). The structure is interpreted as an F_1 ramp anticline steepened by imbrication and backfolded during F_2 (see Annexure 1, profile A-B).

A major dolerite dyke apparently forming two branches has intruded the eastern limb along the entire length of the exposure. Bedding features are scarce but are recognizable in the banded iron formations or as large scale structures within the diamictites (Fig. 7). As S_1 cleavages (Fig. 36a) seem to be subparallel to S_2 very few of these planes were recognized.

The most prominent structural feature is a penetrative east-dipping S_1/S_2 cleavage with attitude 337°/68°E (Fig. 36b). The cleavage poles distribute along a great circle girdle with a π-axis on 062°/72°, which defines the F_3 fold axis direction. Occasionally the cleavage (S_1/S_2) may also dip towards the west. Locally in the central parts of the Sendelingsdrif synclinorium the S_1 cleavage is subparallel to S_2 and deformation of this cleavage indicates shallow single NNW or SSE plunging F_2 folds.

Conspicuous E-W striking master joints dip either steeply north or south and often form erosion gullies. Meso-F_2 folds are scarce and have an azimuth of 160° with either shallow or steep plunges towards the southeast. Shears and faults generally strike parallel to the axial planes of the NNW trending folds, although a single NE-SW (F_3) trending shear was also measured (Fig. 36d).

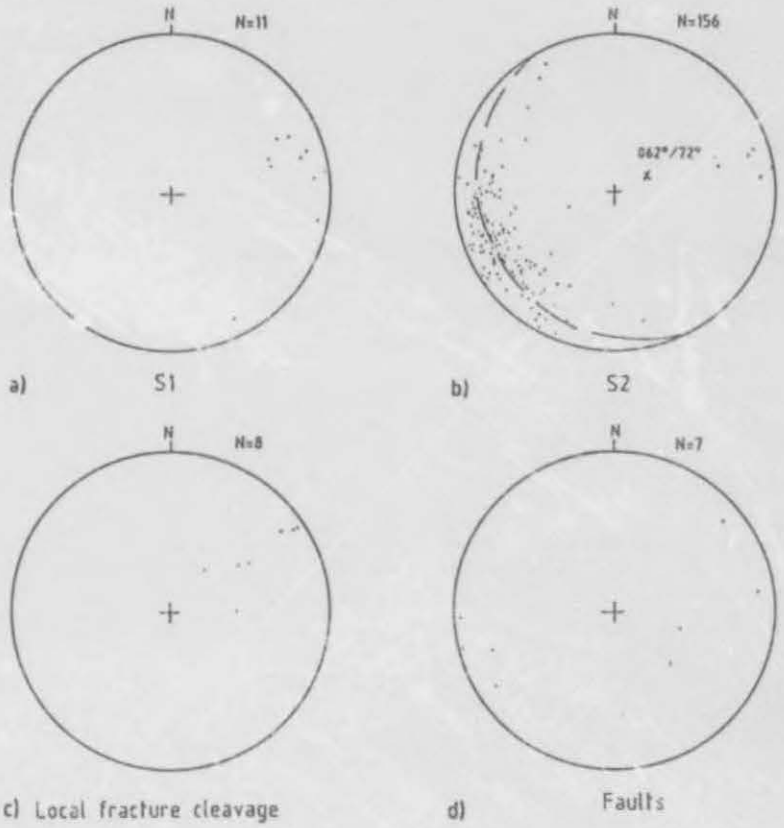

Fig. 36 Fabric data from domain 3

iv) **Domain 4**

Domain 4 includes the Dreigratberg syncline (Fig. 2) containing lithologies of the Witputs Sequence and underlying diamictites of the Numees Sequence. The syncline is fault bounded on the western limb (Fig. 10).

This domain was singled out as it contains dolomitic and schist lithologies within a thick sequence of diamictites. S_0 fabric data define the steep limbs of a major syncline with near horizontal axis (Fig. 37a). The S_1 cleavage can be seen as a deformed slaty cleavage within the intercalated schist units (Fig. 37b).

The pronounced steeply east-dipping axial planar (S_2) cleavage (Fig. 37c). confirms that this is a mega-F_2 fold (See Sections GG-HH and II-JJ, Figure 18). The cleavage has a mean attitude of 343°/67° N. A poorly developed shallow

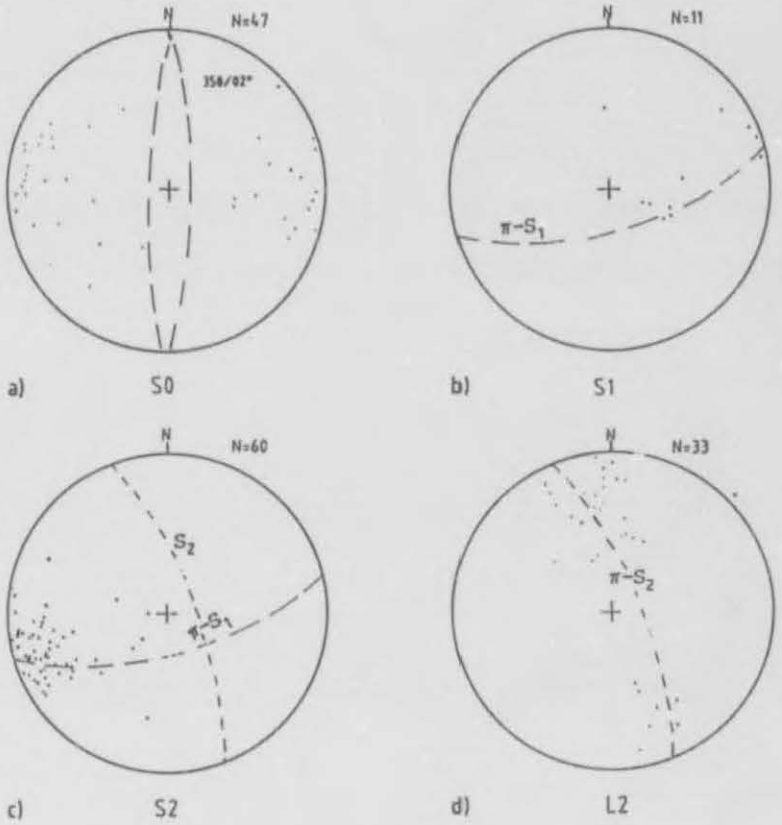

Fig. 37 Fabric data from domain 4

north-west dipping cleavage can be related to the third phase of deformation.

The L_2 intersection lineations define the F_2 fold axes (Fig. 37d), plunging at low to intermediate angles to the NNW as well as SSE probably because of some F_3 cross-folding.

v) Domain 5 (see Annexure 1 and 2)

Domain 5 consist exclusively of diamictite rocks of the Sendelingsdrif synclinorium and lithologies towards the west of Dreigratberg and should therefore be compared with domain 3.

A few available S_0 measurements seem to indicate a SSW-NNE trending F_1 fold axes within a sequence of massive, unbedded diamictites (Fig. 38a). However, lineaments on aerial

photographs seem to outline the fold closure of a synclinorium (Annexure 1) with a NNW trend.

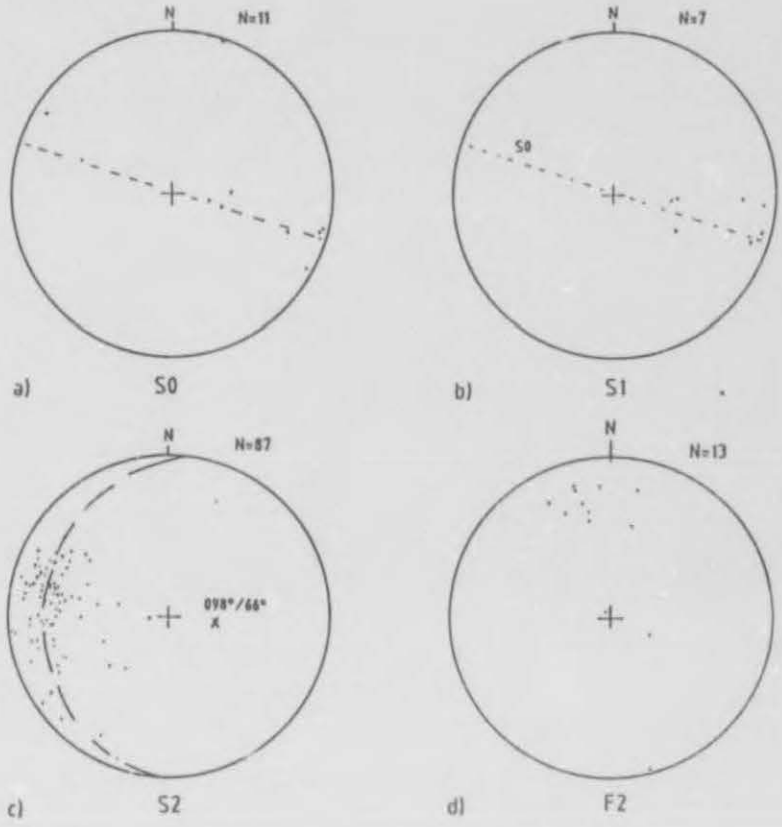

Fig. 38 Fabric data from domain 5

Remnants of S_1 cleavages with varying dips towards the west are rare and approximately follow S_0 (Fig. 38b). S_0 and S_1 data however, are too few to be of significance in determining the orientation of F_1.

Abundantly available S_2 data lie on a great circle girdle, indicating that it has been modified by a later folding episode (F_3), trending almost E-W (Fig. 38c). This could also have affected the S_0 and S_1 planes. The dominant steeply east-dipping S_2 cleavage has a mean trend of 006° with a dip of 64° to the east. Relative to domains 2 and 3, it seems to have been rotated towards the NNE. F_2 folds plunge towards the NNW.

In the field it is apparent that master Q-joints (cross joints or a-c joints) as well as L-joints (longitudinal joints) follow the clockwise rotation of about 20° of S_2 cleavages towards the NNE in this domain.

This change in the general strike direction of the Sendelingsdrif synclinorium could be F_3 related (See Fig 2 for a similar deformation of the axial plane of the Annisfontein anticlinorium). The Jakkalsberg fault splay forms the roof thrust of the Pickelhaube Duplex Structure.

vi) **Domain 6** (See Annexure 2)

Domain 6 is underlain entirely by conglomerates, grits, schists and carbonate rocks of the Hilda Sequence. A zone of obtrusive imbrication duplicates Wallekraal and Pickelhaube lithologies several times along the eastern limb of the Annisfontein anticlinorium forming the Pickelhaube Duplex Structure within the Rosh Pinah Nappe.

The S_0 data are widely scattered but define two possible great circle girdles, with π-axes trending 340°/07° and 302°/44° respectively (Fig. 39a). The S_1 slaty cleavage mimics bedding and strikes 166° with an average dip of 49° SW (Fig. 39b) subparallel to west-dipping strata. S_1 is overprinted by a prominent S_2 spaced crenulation cleavage with a strike of 166° and dip of 68° NE (Fig. 39c). Bedding transposition occurs locally along S_2 cleavage planes.

Sporadic westward dip reversals of the east-dipping S_2 cleavage can be observed below Pickelhaube lithologies in the zone between folds of opposing vergence (see also section CC-DD, Annexure 4), and is related to the open, near symmetrical F_2 folds below Pickelhaube beacon, which are occasionally slightly overturned towards the west. The overturning is coupled with back-folding possibly induced by gravity gliding of sediments into the Sendelingsdrif synclinorium.

Few S_3 cleavages were observed and indicate that F_3 folds could plunge into the NE-quadrant in agreement with their measured trends from elsewhere (Fig. 39d). L_1 intersection lineations (Fig. 39e) and L_2 intersection lineations (Fig.

39f) are subparallel and have shallow plunges towards the SSE and NNW respectively.

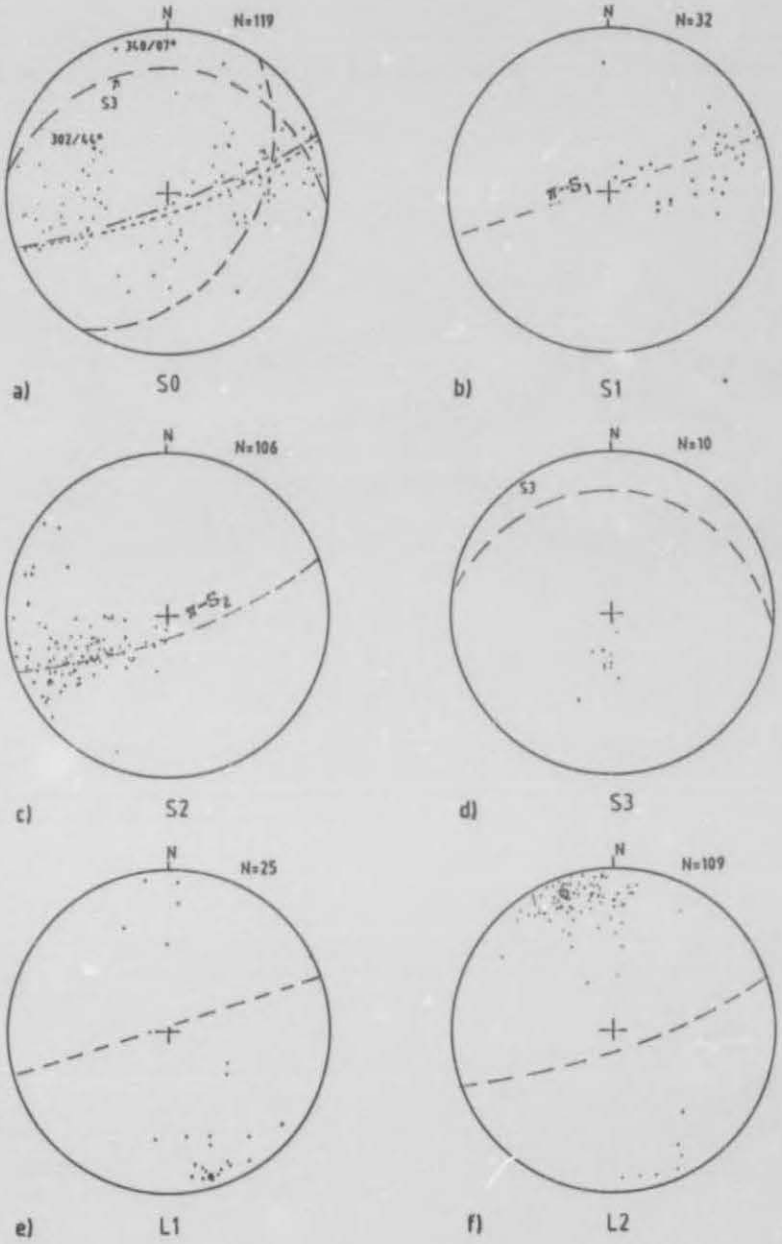

Fig. 39 Fabric data from domain 6

The L_1 maximum indicates that it is possible to draw a S_0/S_1 great circle girdle (see Fig. 39b) which could explain the east-verging F_1 folds in the western part of the Rosh Pinah Nappe. Similarly the π-axis on 340°/07° can be explained by

the distribution of the L_2 maximum and S_0 great circle girdle, which fall on the maximum S_2 distribution.

The partial great circle distributions of S_1 and S_0 indicate the increased complexity of deformation in the area. The synclinal parts of F_1 folds are often truncated by thrust planes (see eastern part of CC-DD, Annexure 1).

Several major backfolds can be observed in lithologies at the edge of the Rosh Pinah valley (Fig. 2), with open F_2 folds having prominent S_1/S_2 intersection lineations (L_2) (Fig. 23). The intersecting planes often form pencil structures below Pickelhaube Peak (EE-FF, Annexure 4). These F_2 folds have a plunge of $343^\circ/27^\circ$, which approximates NNW plunging π-axes on the S_0 diagram.

Up to 1m thick quartz veins in the Wallekraal schists are abruptly terminated along the contact with the overlying Pickelhaube carbonates suggesting structural discordance. Major brittle faults can be followed on aerial photographs and trend in a NW to NNW direction, although a less prominent SW-trending direction is also present. These faults are interpreted as listric extensional faults, which are related to the gravity gliding effect (see Annexure 2) along the RPNT.

Quartz veins show wide diverging trends, but a conspicuous NW trend with steep dips can be related to shearing along the axial planes and limbs of F_2 folds. Boudin long axes measured in quartz veins mainly along the Wallekraal schist-Pickelhaube carbonate contact trend 246°, which might indicate stretching normal to the F_1/F_2 tectonic transport towards the SE. Minor intraformational backthrusts are scarce but have been recognized within the Pickelhaube carbonates.

vii) **Domain 7**

Domain 7 covers the central dome of the Annisfontein anticlinorium and includes lithologies of the Wallekraal and Pickelhaube Formations. It is bounded by the Gumchavib Thrust (GT) in the west.

A shallow dipping S_0 (Fig. 40a) defines the domal structure of the Rosh Pinah Formation of the central anticline. S_1 is semiparallel to the latter in these rocks but only a few readings were gathered.

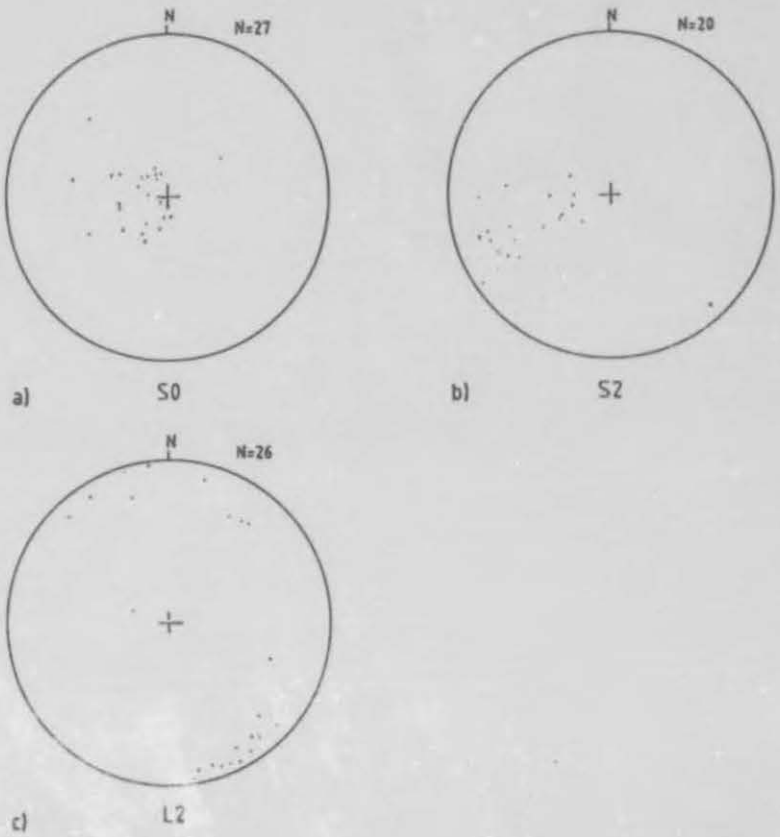

Fig. 40 Fabric data from domain 7

The S_2 crenulation cleavage is prominent in Wallekraal schists and usually intersects the S_1 cleavage at a large angle (Fig. 40b).

The L_2 lineations plunge at shallow [illegible]wards the NNW or SSE (Fig. 40c), but only very few [illegible]ng F_2 fold axes could be measured. Some minor westwar[illegible]verturned F_3 folds are also occasionally seen.

viii) **Domain 8**

Domain 8 consists entirely of upthrust granites and gneisses within the Gumchavib fault block. Bedding features are

absent and the most prevalent fabric is a pervasive shear cleavage (S_1) which has developed parallel to the thrust plane. The S_1 cleavage on average strikes 136° with a dip of 29° towards the southwest (Fig. 41a).

The cleavage dip reversals only noted towards the east in the region of the aplitic granites indicate dragfolding against the Gumchavib Thrust plane (Fig. 41b), where the rock becomes a quartz-sericite schist.

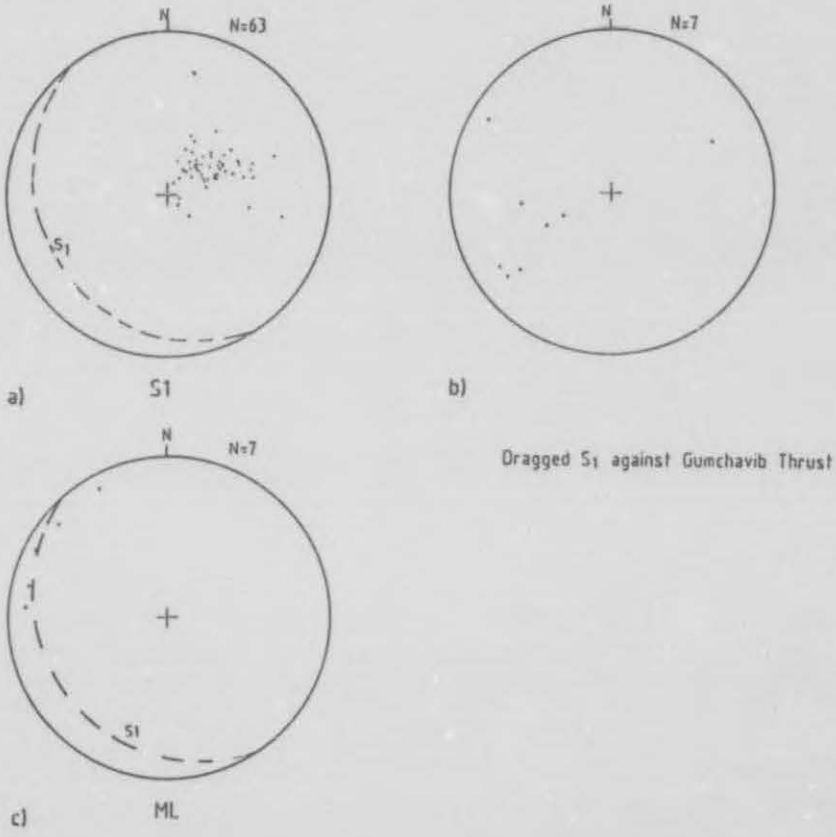

Fig. 41 Fabric data from domain 8

An L_1 mineral lineation (Fig. 41c) is formed by biotite streaks on S_1 cleavage planes near the eastern boundary and lies in the D_1 thrust planes. A NW-SE slip or transport direction is indicated.

This is subparallel to all lineations and fold axes of the first two generations in domains 6,7 and 8.

ix) **Domain 9**

Domain 9 includes lithologies of the Gumchavib Formation (Stinkfontein Sequence) which are bounded by the basement granites in the hanging wall of the Gumchavib Thrust in the east and the Valley Thrust in the west. Although distinct thrust criteria are scarce along the latter, a definite change in stratigraphy across this boundary is evident.

Bedding dips somewhat shallow towards the west with a mean strike of 140° and dip of 39° towards the SW (Fig. 42a). Small scale ramping and shearing occurs above the granite contact.

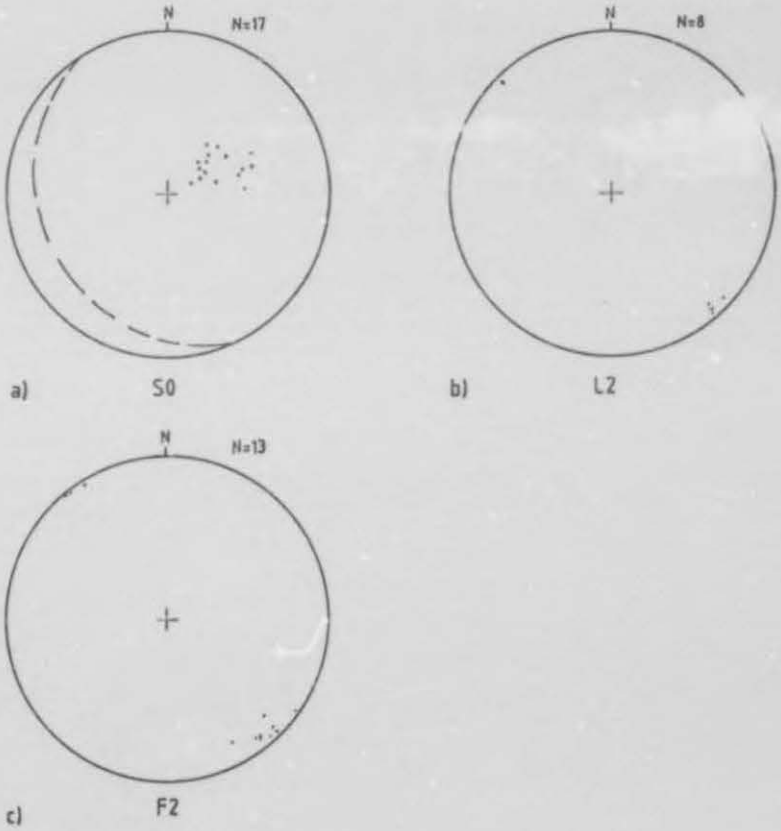

Fig. 42 Fabric data from domain 9

Slickenside striations on bedding-parallel quartz veins indicate two directions of movement, one trending in a NW-SE direction and the other from the SW to NE. These are comparable to regional transport directions.

L_2 intersection lineations of S_1/S_0 and S_2 (Fig. 42b) follow the axes of prominant SW-ward overturned F_2 folds, which plunge 6° in a direction 139° (Fig. 42c).

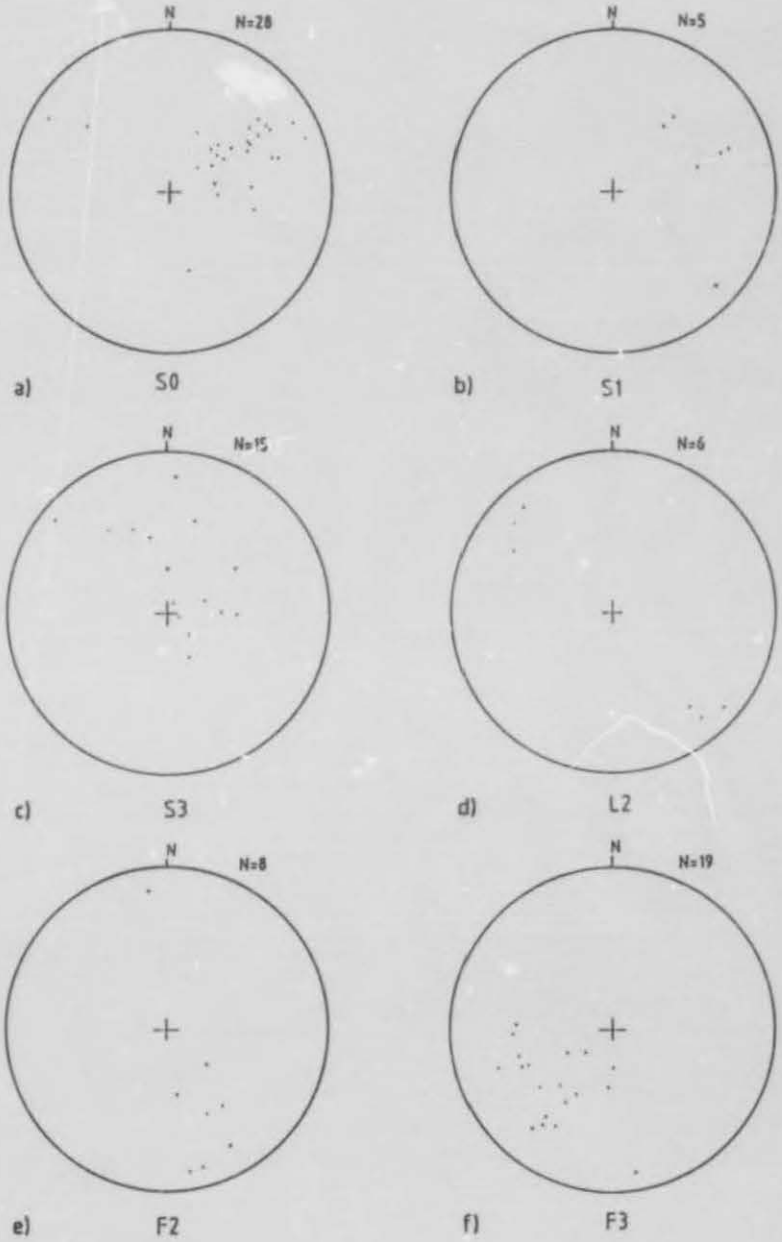

Fig. 43 Fabric data from domain 10

x) **Domain 10**

Domain 10 is bounded by the Obib Waterhole Thrust in the west and the Valley Thrust in the east. It is underlain by a stratigraphic succession consisting of the Rosh Pinah Formation at the base overlain by a thin band of Pickelhaube carbonate.

Grits and conglomerates of the Wallekraal Formation overlie the carbonates, which in turn are unconformably overlain by an approximate 50m thick diamictite succession, which is here considered to be the Sendelingsdrif Formation.

Bedding planes strike 148° and dip moderately west at 49° (Fig. 43a) and are mimicked by the S_1 cleavage. Trends for S_1, S_3 and L_2 intersection lineations are outlined on Fig. 43b, c and d respectively. An S_2 cleavage is poorly developed in the quartzites overlying the upthrust basement granites (Domain 10, Annexure 2). Minor SSE plunging F_2 folds (Fig. 43e) are present.

The most prominent folds are asymmetric to slightly overturned towards the south or south-east. They are related to the third phase of deformation and have a mean azimuth of 261° with a plunge at 46° towards the SW (Fig. 43f). These folds have modified the plunge of the earlier F_2 fold as well as the L_2 lineations and are themselves not following a very constant direction.

xi) **Domain 11**

Domain 11 covers lithologies of the Rosh Pinah Formation west of the Obib Waterhole Thrust to the dune cover. They consist of a thick sequence of blue-grey limestone with intercalated red-brown arkoses and quartzites with minor basic intrusions.

These rocks overlie the Numees diamictites along the west-dipping Obib Waterhole Thrust. The flat dipping Obib Peak succession and thrust (Annexure 3) have been removed by erosion.

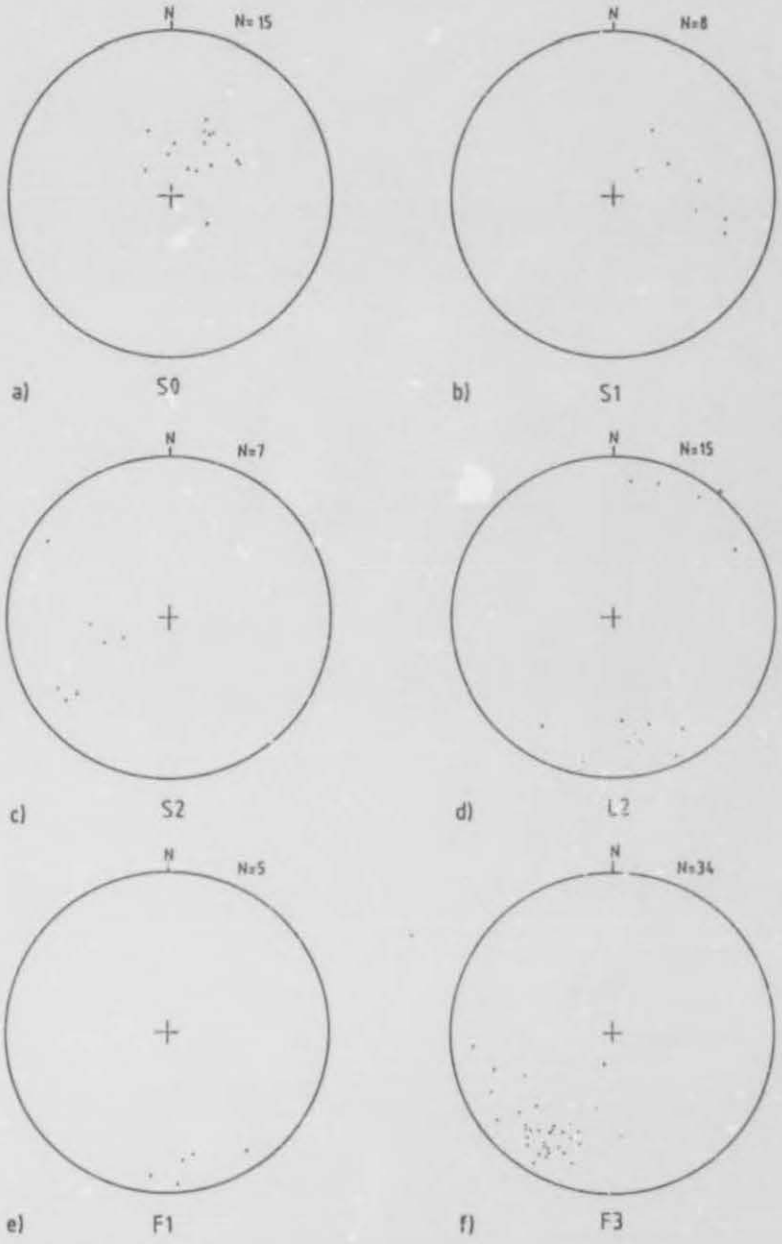

Fig. 44 Fabric data from domain 11

The S_0 data confirm a moderately SW-dipping succession with a near bedding parallel S_1 cleavage (Fig. 44a, b). S_2 cleavages (Fig. 44c) follow trends similar to other areas. L_2 lineations (Fig. 44d) have been deformed by F_3 folds. F_1 folds plunge dominantly towards the southeast (Fig. 44e).

The most prominent feature here, however, are numerous SW plunging F_3 folds (Fig. 44f), but very few S_3 cleavages (not shown) have been measured with dips towards the NW. Numerous steep or minor fault zones trend in a NNW direction.

7.6 The Pickelhaube Duplex Structure

The Pickelhaube Formation in the Richtersveld is interpreted as the oldest unit within the Hilda Sequence (Von Veh, 1988) and is overlain by the Wallekraal Formation (see legend, Annexure 1). In the study area both formations underlie large parts of the mountainous area west of the Rosh Pinah valley (Fig. 2). In the Pickelhaube Duplex Structure the Pickelhaube and the Wallekraal Formations or parts thereof are structurally duplicated several times.

The general fabric and interrelationships of lithologies to each other were given special attention in an effort to explain the structural peculiarities in the duplex. Results are outlined on detailed field sketches of profiles in Annexure 4. The position of the profiles AA-BB, CC-DD and EE-FF are given on Fig. 2. They occur in the vicinity of the strip map of Annexure 2.

At least six thrust planes, some of which truncate local isoclinal F_1 macro-folds have been mapped within the frontal imbricate zone, but several more minor imbricates may be present. Lithological units can be observed to wedge out or abut along thrust planes, and fold detachments are present on various scales (Annexure 4a).

Four west-verging mega-backfolds can be defined which terminate in the west near Pickelhaube Peak in Pickelhaube carbonates where fold vergences apparently change to easterly (Annexure 4c). This may be a remnant of the earlier D_1 deformation.

The backfolding is tight and S_2 cleavages dip steeply towards the east at approximately 70°. Evidence for inversion on

thrusts occurs in some places to form small antithetic thrusts to the east of Pickelhaube Peak (Annexure 4c).

The structural setting changes to the east of Pickelhaube Peak (Annexure 4b) where S_2 cleavage dips become shallower towards the east and folds are more open. However, S_2 cleavages in the imbricate zone continue to dip steeply towards the east.

The sole thrust to the Rosh Pinah Nappe is interpreted as the contact of the Pickelhaube carbonate with the underlying Rosh Pinah Formation (Fig. 2). Thrust stacking of Stinkfontein lithologies took place over the structural high possibly caused by fault-bend folding (ramping) during the development of the Annisfontein anticlinorium (Annexure 2).

Continued pressure from the SW or W eventually resulted in tightening of the Sendelingsdrif synclinorium above the sole and basement. As the ramps steepen towards the hinterland they eventually become backfolded and cascade towards the southwest.

Structures in the upper Pickelhaube unit and the underlying Wallekraal Formation i.e. above and below the F_2 deformed upper duplex ramp (1 in Annexure 4b and c), just east of Pickelhaube Peak are compared below (Fig. 45a, b).

a) Bedding dips at shallow angles in all directions, and forms ill defined basin and dome structures as a result of F_2 and F_3 fold interference.

b) A pervasive spaced cleavage (S_2) is well developed in Wallekraal schists but is less obvious in the less competent Pickelhaube carbonates.

c) Minor F_2 folds plunge primarily towards the SSE, with L_2 intersection lineations (b-lineations) plunging in this direction as well as towards the NNW or NW because of F_3 fold interference.

d) Joints trend semi-parallel to major faults.

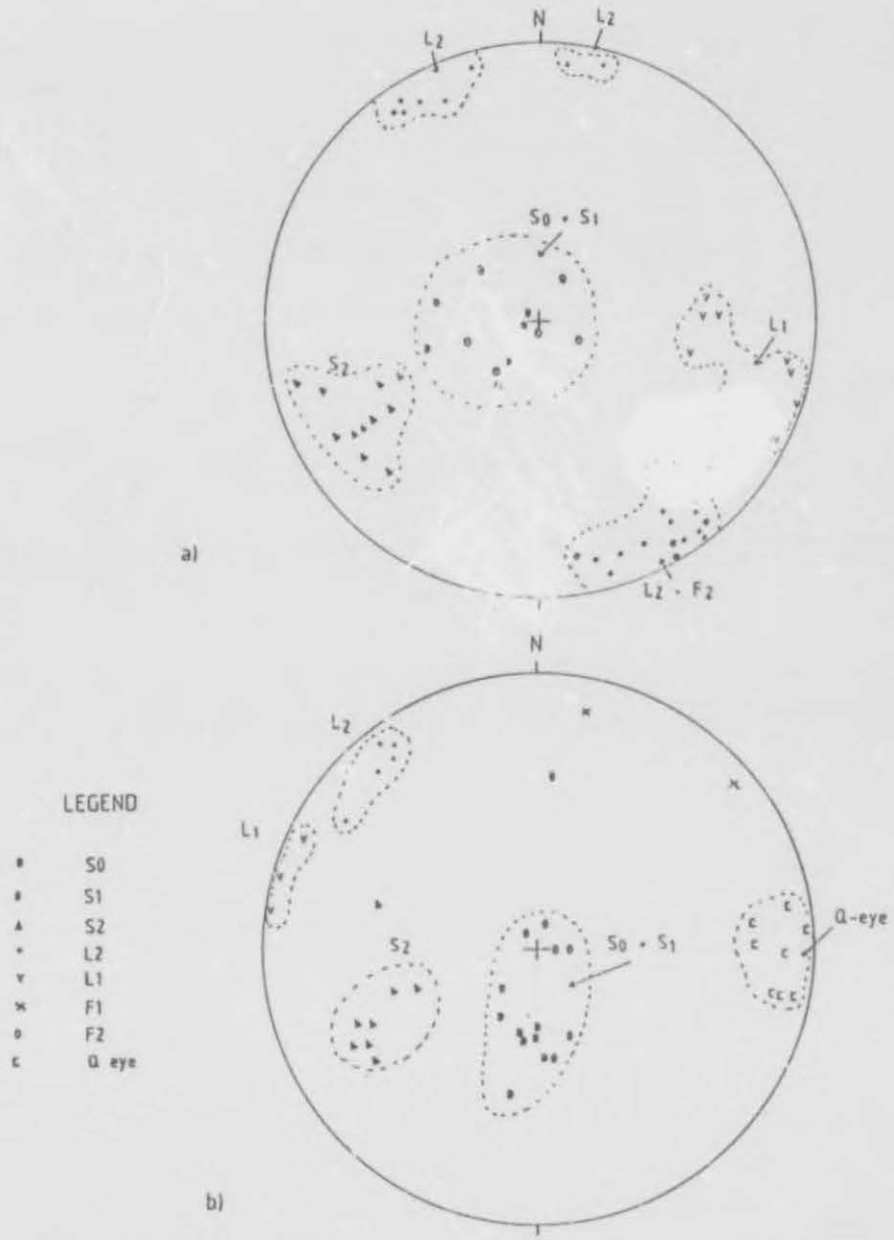

Fig. 45 Fabric data from: (a) the Wallekraal schists, and (b) the overlying Pickelhaube carbonates to illustrate discordance in structures.

e) The S_1 cleavage is a bedding parallel shear fabric related to the D_1 phase of deformation. Recumbent, isoclinal F_1 fold closures are only occasionally found as intrafolial structures on a decimeter and metre scale.

f) An important feature of the Pickelhaube limestones is the presence, especially against the basal thrust of

each ramp, of extremely attenuated and sheared quartz veins and lenses. The long axes of lenses plunge towards the east.

g) In cross-section the internal structure and shape of lenses may reveal righthanded as well as lefthanded rotation, indicating that they probably originated by reorientation of earlier quartz vein folds into the slip direction of the slip plane.

h) L_2 lineations in the Pickelhaube Formation trend somewhat more SSE than in the Wallekraal lithologies.

From this it may be concluded that slip occurred along S_0/S_1 in an ESE-WNW direction with some flow across this direction during D_1. Ductile conditions prevailed as wide shear zones developed.

7.7 Strain analysis

Strain data were also gathered in clast-supported Wallekraal conglomerates on the eastern limb of the Annisfontein anticlinorium. In this area (about 2-3 km south of Pickelhaube Peak - Fig. 2 and Annexure 2) the clasts consist mainly of quartz vein and quartzite clasts with less granite.

Area	Arithmetic mean	Geometric mean	Harmonic mean	θ - Value
1. South of Pickelhaube Peak (N=54)	2,40	2,37	2,32	2,20
2. South of Pickelhaube Peak (N=17)	3,15	2,83	2,72	2,85

The first data sets were measured along bedding planes (the S_1 cleavage is semiparallel to the S_0 plane), which very nearly represents the X_1Y_1 plane. Results using the R_f/θ

method are outlined above (see 1. above). No data were collected along crossjoints.

These results are comparable to those obtained for the Numees along the same X_1Y_1 plane of the strain ellipsoid in the Namuskluft-Dreigratberg area, where the X_1Y_1 plane is near vertical.

One of the problems of this locality has been to ascertain the competencies of the quartzitic rock matrix relative to the constituents. For this purpose deformation of granite clasts are compared with shale clasts. The ratio for shale clasts in the same area and with the same matrix is outlined under 2. above.

The values for the θ- Distribution Test is 2,85 and these results confirm that values found here are a minimum for granite pebbles but shale pebbles probably give X_1Y_1 ratios that are close to that of the matrix even if the latter is more sandy.

The centre to centre method was also used for some conglomerates that are matrix supported. Several sine curves of varying amplitudes and wave lengths were found, which might either indicate incorrect sampling, or inhomogeneous strain on the scale of observation. The maximum amplitude gives a strain ratio of 2,76 (N=31) which is very close to the harmonic mean of the shale clasts, and shows that within the assumptions that apply to both these techniques, the ratio of about 2,7 for X_1/Y_1 is a fair estimate.

The average orientation of long axes for the Numees varied from 001° to 347°, with L_3 lineations and calcite and quartz eyes lying transverse on this direction on an E-W trend. The latter indicates transpressive movement oblique to major basement faults.

The fairly constant X_1/Y_1 ratios, whether derived for the matrix in the horizontal Pickelhaube Nappe zone or for the $X_{1/2}/Y_{1/2}$ in the steeply upturned escarpment zones, seem to indicate that F_2 backfolding had little if any homogenous strain effect.

All internal strains seem to have occurred during F_1, whereas F_2 was only responsible for upturning and backfolding the strata. In the near horizontal nappe sequence around Pickelhaube Peak transport directions were mainly ESE as indicated by L_1 mineral lineations (Fig. 45a,b)

8. THE GEOLOGY AND STRUCTURE OF A TRAVERSE FROM OBIB PEAK TO EAST OF ROSH PINAH

8.1 The Stinkfontein Sequence

8.1.1 Distribution and stratigraphy

The Gumchavib Formation forms a distinct lithological sequence, which has been thrust over the Rosh Pinah Formation along the Gumchavib Thrust. East of this thrust a unit (Domain 15, Annexure 3) which consists of gradational or interfingering blue-grey limestones, dolomites, light to reddish-brown quartzites and arkoses crops out between the Gumchavib Formation in the west and the Pickelhaube Formation in the east.

These rocks somewhat resemble those of the Pickelhaube Formation as defined by Von Veh (1988). However, amphibolite dykes and sills (which are absent from the Pickelhaube Formation in the type area) suggest that these rocks belong to the older formations and should therefore be placed in the Stinkfontein and correlated with the Rosh Pinah Formation. Similar volumes of carbonates occur in the Rosh Pinah Formation type area (around Rosh Pinah mine).

8.1.2 Lithology and petrography

The Gumchavib Formation consists of a monotonous sequence of light-brown quartzites, arkoses, with minor grits and conglomerate lenses. Thin dolomite bands occur towards the top of the sequence. Some weathered felsites crop out in the sandy plain east of Obib Peak.

Small lenticular zones of biotite and quartz-sericite schists and thin carbonaceous shale bands are intercalated locally.

The sericite schist zones seem to be related to shear zones rather than representing felsic volcanic rocks. The sediments are graded and planar cross-bedded sequences (Fig. 46) indicate major sediment transport towards the W.

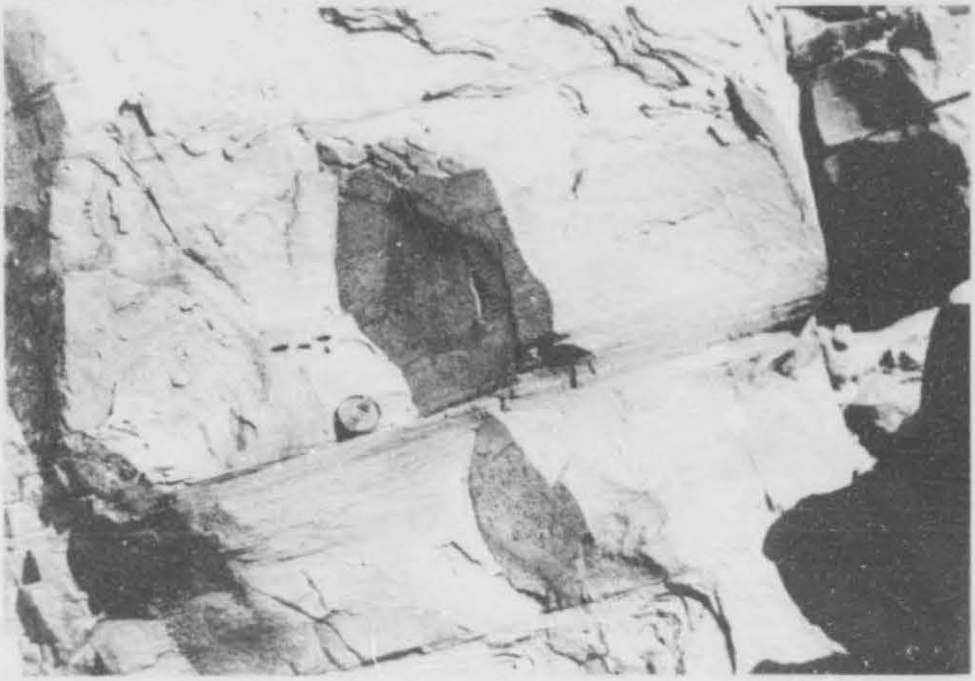

Fig. 46 Planar crossbedded sequence in Gumchavib quartzites approximately 3 km to the north of Obib Peak.

The unit may be duplicated, by internal folding and/or thrusting because a blue-grey carbonate marker band recurs in the local stratigraphy due east of Obib Peak (Annexure 3) as well as a phyllitic biotite schist zone.

The tectono-stratigraphic relationships along an east-west traverse from Obib Peak to the Valley Thrust are shown in Fig. 47. The lithologies, which directly overlie the Valley Thrust (Domain 12, Annexure 3) are here correlated with the upper parts of the Rosh Pinah Formation. Those below the thrust belong to the Gumchavib Formation.

The carbonate beds above and below the Valley Thrust are Pickelhaube-type blue-grey limestones. Just above the thrust a carbonate unit contains a sulphide-bearing zone with

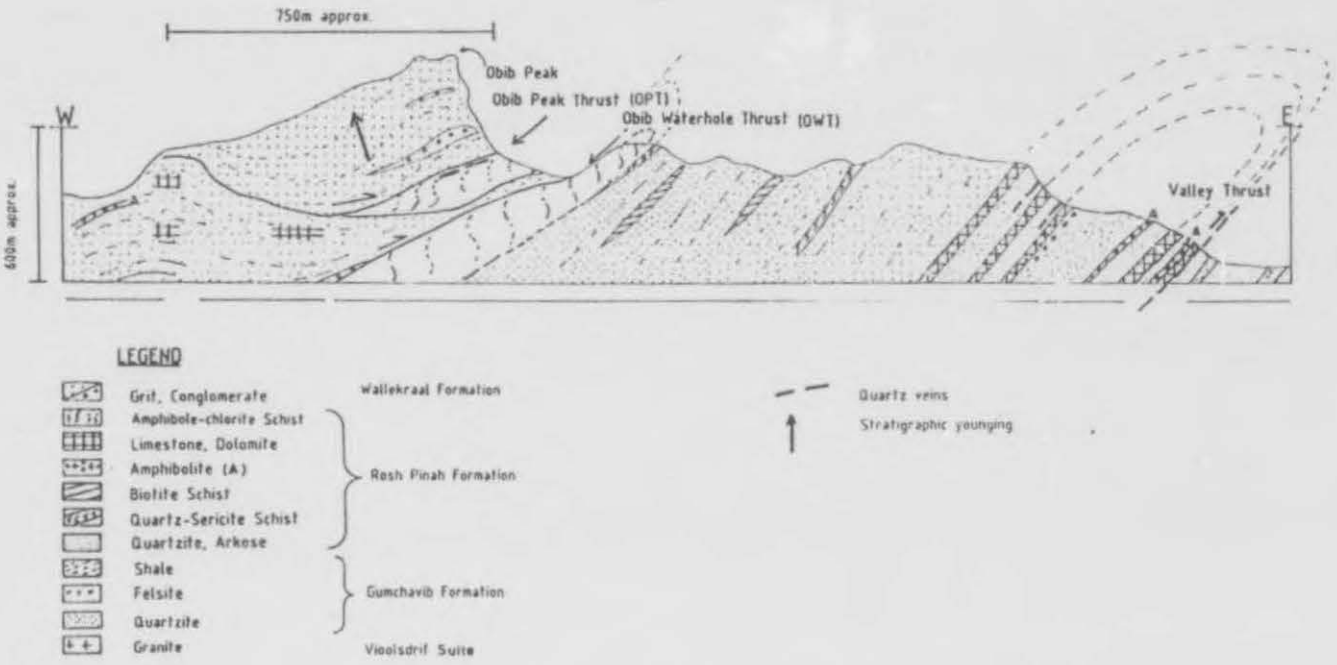

Fig. 47 Cross-sectional sketch to illustrate the tectono-stratigraphic sequence in the vicinity of Obib Peak.

disseminations of pyrite and galena in a boxwork gossan. These rocks seem similar to those surrounding the Rosh Pinah ore beds.

Dipping beneath the first dolomite band above the Valley Thrust (Fig. 47) there is a thin matrix supported polymict conglomerate with a light-brown quartzitic matrix that contains unsorted and rounded quartz boulders and tectonically stretched dolomite boulders. The matrix is a light-brown quartzite.

The next higher dolomite unit contains thick bedding parallel quartz veins dipping west at 27° (Fig. 48). It has acted as a thrust zone, (the Valley Thrust) as indicated by strong silicification, ferruginization and brecciation of the unit and underlying arkoses. The thrust zone has a thickness of at least 50 m. Prominent northwest plunging slickenside striations on movement planes in the quartz veins indicate south-easterly directed slip (see Fig. 66).

Fig. 48 *Quartz veined zone typical of the 50m wide thrust fault exposure approximately 2km to the east of Obib Peak. (Valley Thrust). The vein zone is 1,5-2m thick.*

Intercalated gritty and thin carbonaceous sandstone layers prove the clastic origin for these dolomitic rocks. In thin section (NT 143) the rock consists of fine-grained dolomitic marble with epidote and muscovite platelets subparallel to bedding. Accessory quartz is also present.

The intercalated "biotite schist" lenses consist of subparallel biotite, chlorite and quartz alternating with bands of quartz and biotite. Quartz displays a well developed preferred shape orientation (specimen NT 102, NT 105, NT 111). The quartz sericite schists (specimen NT 100, NT 101), microscopically consist almost entirely of flattened quartz grains within a sericitic matrix that bends around the quartz grains. The rock is mesoscopically strongly lineated mainly because of the preferred orientation of the quartz grains.

A later crenulation cleavage (S_2) is evident in specimen NT 91 of the same schists. Occasionally quartz grains with perfectly hexagonal shapes may be present.

A rare purplish isotropic mineral has been microscopically identified as fluorite, which possibly together with post-metamorphic (post-F_1) crosscutting quartz veins may point to local hydrothermal activity. The fluorite may, however, also precipitate at low temperatures in groundwater. A pre-metamorphic and pre-tectonic hydrothermal silicification event (relative to gravity gliding and F_2 backfolding) accompanies the Rosh Pinah ores. A similar and possibly contemporaneous history of mineralization may be inferred.

The fine- to medium-grained quartzites commonly have tabular crossbeds and are intercalated with thin grit bands. A steel blue-grey arkose or feldspathic quartzite similar to the Rosh Pinah hanging wall rocks is usually present towards the base of the unit.

Some localized spotted quartzites (specimen NT 113) consist essentially of quartz, with accessory plagioclase, microperthite and anorthoclase, whereas minor muscovite, biotite and chlorite are present as interstitial material. Large porphyroblasts of unorientated biotite and chlorite represent the spots. The rocks can be classified as micaceous feldspathic quartzites (specimen NT 94) with minor calcareous quartzites (NT 116) and arkoses. Some quartzites bear traces of epidote (NT 95) and single detrital tourmaline grains are occasionally noted.

The most westerly unit of the Rosh Pinah Formation consists of micaceous light-brown quartzites with conglomerate lenses containing thin cream-coloured sericitic dolomite bands towards the top of the sequence. These rocks have a sheared contact with the overlying amphibole-chlorite schists.

A 50 cm thick blue-grey ruptured and sheared limestone bed found along the contact of the Wallekraal arenites underlying Obib Peak, with the amphibole schist, outlines the Obib Peak Thrust. Pinching and swelling of quartz veins confirm the sheared nature of this contact.

The amphibole-chlorite schists are fine-grained intensely cleaved rocks with prominent kinks, which are defined by trains of amphibole or biotite. A conspicuous mineral

elongation lineation (L_1), trending SSE, is defined along the schistosity by dark green amphibole needles. Needles may sometimes also be radially arranged during post-tectonic growth.

Specimen NT 139 reveals that the rock consists largely of bladed hornblende grains, with biotite and chlorite interspersed within quartz and albite. The typical mineral paragenesis here is green **hornblende + quartz + biotite + albite**. The rocks are interpreted as mafic meta-volcanics, dynamo-metamorphosed to the intermediate greenschist facies. Hornblende grains grow in the two cleavage planes, whereas isolated zircon grains are widely dispersed. Calcite may be prominent in clusters.

To the west of Obib Peak and below the Obib Peak Thrust (Domain 12, Annexure 3) the lithologies consists of bands of brown carbonatic sandstone, which vary from less than 1m to several metres thick, interspersed with thicker blue-grey laminated limestone beds. Biotite schist lenses and amphibolite sills are present and lithologies are similar to those previously described for the area east of Obib Peak.

The dolomitic limestone beds (NT 90) consist mainly of crystalline dolomite and calcite and have a mineral paragenesis of **dolomite + calcite + quartz + biotite**. This paragenesis remains only unaffected at very low grade metamorphism (Winkler, 1976). Some of the quartz crystals grow into perfect hexagons. Thin brown sandy beds, which are intercalated in the dolomitic sequence consist of quartz, minor plagioclase and anorthoclase with a biotite, chlorite and muscovite matrix. Alternatively the matrix may be dolomitic (NT 77, NT 82, NT 88, NT 92). The latter paragenesis indicates a lower greenschist metamorphic facies.

Where arkosic (sample NT 86), these rocks contain a fair amount of plagioclase and microperthite feldspar with quartz. Some post-kinematic biotite porhyroblasts can be seen to overgrow these minerals. Possible post-tectonic plagioclase blasts (specimen NT 92) are retrograded to sericite. Replacement of several opaque minerals by quartz is visible.

There is a general increase in sandstone beds towards the stratigraphic top of the dolomitic sandstone-limestone unit. These beds are extensively boudinaged, with boudin long axes plunging towards the southeast (F_1).

The lowest volcanoclastic unit of the Rosh Pinah Formation in the Rosh Pinah Mine area unconformably overlies the basement with a basal conglomerate on the farm Zebrafontein and consists of a thick accumulation of rhyolites, felsites and felsic agglomerates (McMillan, 1968).

The felsic lithologies within the allochthone surrounding the Rosh Pinah Mine have been described in detail by Watson (1980). He recognized several textures including porphyritic, glomeroporphyritic, spherulitic and hypidiomorphic types.

The massive felsites consist essentially of equigranular grains of feldspar and quartz with a felsitic texture. Porphyritic felsites are characterized by large single grains and composite phenocrysts consisting of quartz, perthite, orthoclase and albite drifting in the matrix. Clusters of quartz and feldspar grains define a glomeroporphyritic texture, while the spherulitic type contains small to large spherulites. The hypidiomorphic "felsites" have no typical felsitic texture, and in the felsitic tuff and agglomerate spherical to angular particles of felsite are set in a felsitic matrix. Despite shearing, textures are often well preserved. Sericite is common but biotite and chlorite have also developed. Petrochemically the analysis of these rocks agrees with that of felsites and rhyolites of various formations in South Africa (McMillan, 1968).

Numerous interbedded lenses of hematite appear within the felsitic sequence and are associated with impure, ferruginous dolomite. This association can be interpreted as of possible fumarolic vent origin.

The upper part of the Rosh Pinah Formation in the Rosh Pinah Mine area (domain 16) consists of a $\pm$ 900m thick succession of dirty-grey, well-bedded, but poorly sorted feldspathic quartzites or arkoses with numerous thin intercalated

argillite bands. The bands vary from less than a centimetre to several metres thick. Contorted fragments and rip-up argillite clasts occur intermittently near the base of coarser units.

Recrystallized quartzites have polygonal-granoblastic or foam textures and secondary overgrowths on feldspar clasts are common. The latter are usually orthoclase, microcline and perthite, with microcline dominating. Albite is only present in very subordinate quantities. Where quartzites become calcareous, dolomite occurs as interlocking grains between quartz and feldspar, and are very similar to the calcareous quartzites of the Gumchavib Formation.

Limestones and dolomitic limestones are fine-grained grey to dark-grey rocks, which usually occur together with carbonaceous, dolomitic quartzite. The sulphide-bearing carbonates of the ore zone are considered to have been primary dolomitic limestones (Watson, 1980), and are commonly overlain by barytic carbonates (Fig. 49).

Argillites are typically dark-coloured, well-laminated, carbonaceous rocks composed essentially of dispersed grains of quartz and feldspar, with accessory sericite, muscovite and chlorite. The microquartzite rocks represent silicified argillites. Small lenticular flows or sills of felsite are restricted to the hanging wall rocks, and intrusive bodies of quartz porphyry are present towards the base.

Angular and rounded dolomite clasts set within a dolomitic to sandy matrix are present in the upper parts of the Rosh Pinah Formation and would be interpreted as disintegrated near shore carbonate reefs (Kröner, 1974 p.7), or as local mudflow deposits. Thin lenticular quartz-clast bearing conglomerate horizons are exposed towards the top of the Rosh Pinah Formation.

Within the Rosh Pinah Mine the sulphide mineralization is hosted mainly in dolomitic carbonate rocks, or may also be present in silicified argillites, argillites or in zones of silicification (sugary quartzite). Lithologies of a typical ore zone profile for the Northern Orefield No 1 orebody are

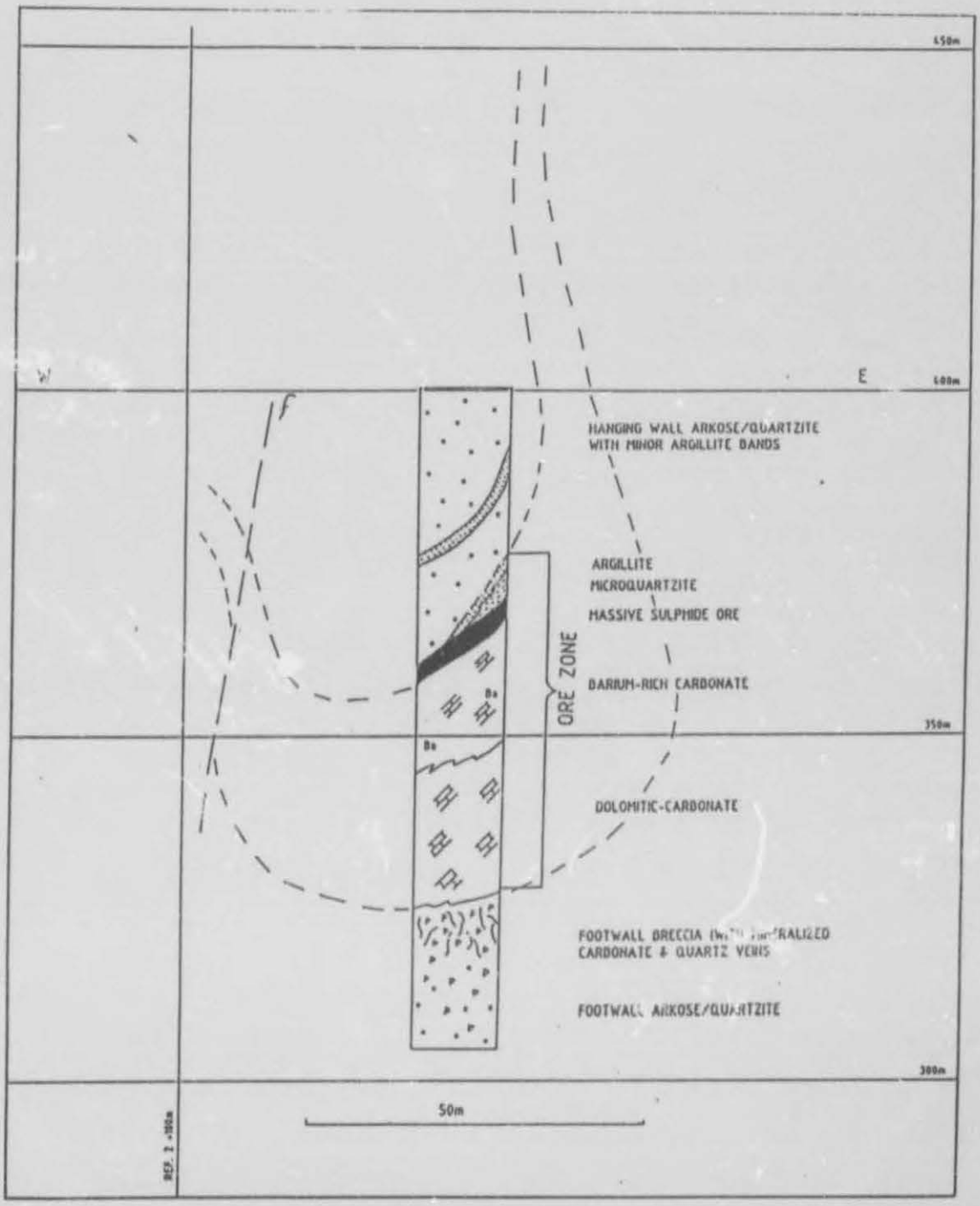

Fig. 49 Lithostratigraphic profile of the Northern Orefield No.1 orebody, Rosh Pinah Mine (domain 16, Annexure 3).

given in Fig. 49.

The arkosic to feldspathic quartzites underlying the orebodies are extensively fractured and brecciated and contain ubiquitous mineralised carbonate veins and veinlets.

Dark green amphibolite sills occur to the north and in the proximity of the mine workings as fine-grained lenticular bodies. These can either be interpreted as altered basic lavas or as dyke and/or sill intrusions, and bear resemblance to the numerous amphibolite dykes and sills within the Gumchavib Formation. They may point to a Stinkfontein correlation.

8.2 The Hilda Sequence

8.2.1 Distribution and stratigraphy

Von Veh (1988, p.36,) has found that the Pickelhaube beds rest conformably on and interfinger with the Gumchavib Formation arenites in the Richtersveld. In the study area the Pickelhaube Formation is thrust over the Gumchavib Formation along the Rosh Pinah Nappe Thrust (Annexure 3) in the Gumchavib hills. The gritty Obib Peak unit overlies the Rosh Pinah Formation along the shallow west-dipping Obib Peak Thrust. This unit is correlated with the Wallekraal Formation.

8.2.2 Lithology and petrography

The Pickelhaube Formation comprises essentially a thick sequence of clastic blue-grey, finely-laminated dolomitic limestones. Along this traverse they are well developed some kilometres SW of Rosh Pinah Mine as a range of low hills on the western side of the Rosh Pinah valley. Locally some light to dark-brown layers of chert have developed parallel to bedding.

A petrographic examination (sample NT 85) indicates that the rock is constituted dominantly of interlocking grains of dolomite. Occasionally quartz veins and minor amounts of slightly orientated muscovite flakes are present. A single, 10 m thick white limestone bed occurs towards the top of the sequence. It consists primarily of recrystallised calcite, minor biotite flakes, some opaque minerals and very subordinate quartz (sample NT 93). Some alignment of the biotite and muscovite flakes parallel to the S_1 cleavage is observed.

The Wallekraal Formation is a largely rudaceous unit with extensive areas of conglomerates on the eastern limb of the Annisfontein anticlinorium and crops out here in a small hill SE of Rosh Pinah town (Annexure 3).

The Obib Peak unit consists of feldspathic and arkosic arenites and grits (Fig. 50). Small (<1m) scour channels are occasionally developed and indicate stratigraphic younging towards the top of the hill. This is confirmed by graded bedding showing fining in the same direction. Fine laminations are present but no cross-bedding features were noted.

Fig. 50 Obib Peak with thrust contact in the east. Looking north.

These arenites also occur on an isolated outlier approximately 1 km towards the north of Annexure 3, as well as in the region of the Obib Waterhole (Fig. 2). A characteristic of the rocks are thin lenticular intercalated feldspar-rich grit and conglomerate beds containing quartz, granite as well as slightly deformed cream-coloured carbonate clasts. The rock is also characterized by a honey-comb weathering surface.

Both grits and conglomerates are usually clast supported, with well sorted subrounded to angular pebbles averaging 4-5mm in size. The pebbles are normally constituted mainly of quartz and anorthoclase with a matrix of accessory muscovite, calcite and epidote (Specimen NT 141).

Feldspar clasts (often pinkish) may constitute up to 80% of lithic fragments and have often been sericitized to the extent that only relict grain boundaries are still discernable. They are generally poorly orientated. Average pebble sizes at the Obib Waterhole commonly exceed 1cm in diameter. In contrast dolomite clasts have been tectonically stretched and have developed a preferred long axis orientation trending northwest. Locally the arenites are also calcareous with a dolomitic and calcitic matrix.

On close inspection the rocks reveal small tightly folded east-verging isoclines within finer-grained zones. Bedding-parallel shears near the base are intersected by a set of younger near vertical quartz veins. Specimen NT 103 indicates a strong alignment of sheeted muscovite to form a pervasive S_1 cleavage anastomosing around sericitized plagioclase and quartz grains with secondary overgrowths.

8.3 The Structure along a profile from Obib Peak to east of Rosh Pinah

This northern structural profile covers a traverse from Obib Peak to east of Rosh Pinah Mine and includes domains 12 to 17.

i) Domain 12

Domain 12 incorporates all lithologies of the Rosh Pinah Formation west of the Obib Waterhole Thrust (Annexure 3 and Fig. 2) up to the dune cover. The Obib Peak unit of Wallekraal affinity overlies these lithologies as a klippe along the shallow dipping Obib Peak Thrust and is included here. Granites are exposed north of this traverse along the steeper Obib Waterhole Thrust and are surrounded by an biotite schist horizon.

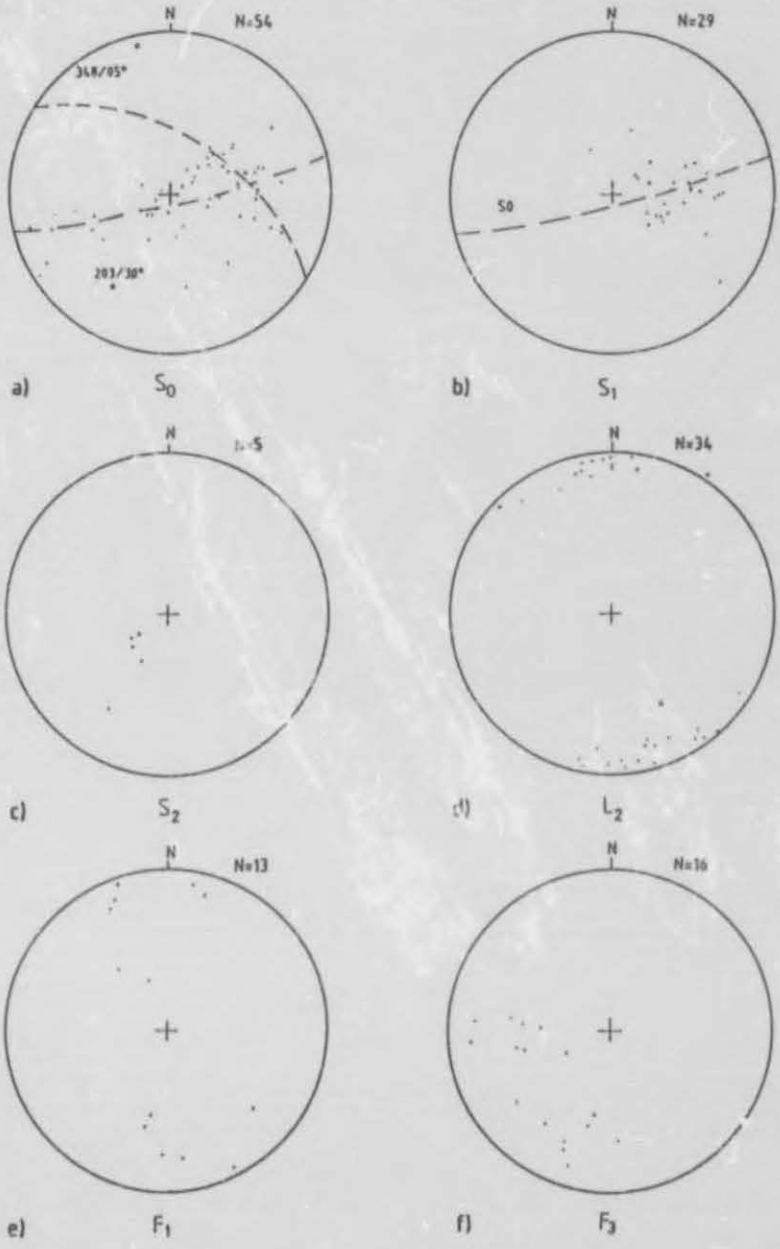

Fig. 51 Fabric data from domain 12

The bedding data define two partial great circle girdles, one with a π-axis attitude of 348°/05° (Fig. 51a), the other with south-west plunging π-axis at 203/30° (F_3). Structural data for S_1, S_2, L_2, F_1 and F_3 are given on Fig. 51b, c, d, e, f and indicate patterns similar to other domains, with the F_1 and F_3 fold directions being confirmed by the S_0 diagram.

Two mineral elongation lineations (not shown in Fig. 51) are prominent in amphibole schists below the Obib Peak Thrust. The oldest and most prominent lineation (possibly L_1) is near horizontal with a trend of 165°, while the later ill-defined lineation (Possibly L_3) trends 192° and plunges at moderate angles to the SW. Both lineations decrease in prominence away from the thrust contact.

The long axis of quartz eyes follow the F_3 trend (Fig. 51f), while shears trend dominantly towards the NNW but a distinct NE-SW direction is also present.

Fig. 52 East-verging macro-F_1 fold in the proximity of the Valley Thrust. The locality is 3 km northeast of Obib Peak, looking west (domain 13, Annexure 3).

ii) Domain 13

Domain 13 incorporates all lithologies between the Obib Waterhole Thrust and the Valley Thrust (Annexure 3) and are correlated with the Rosh Pinah Formation.

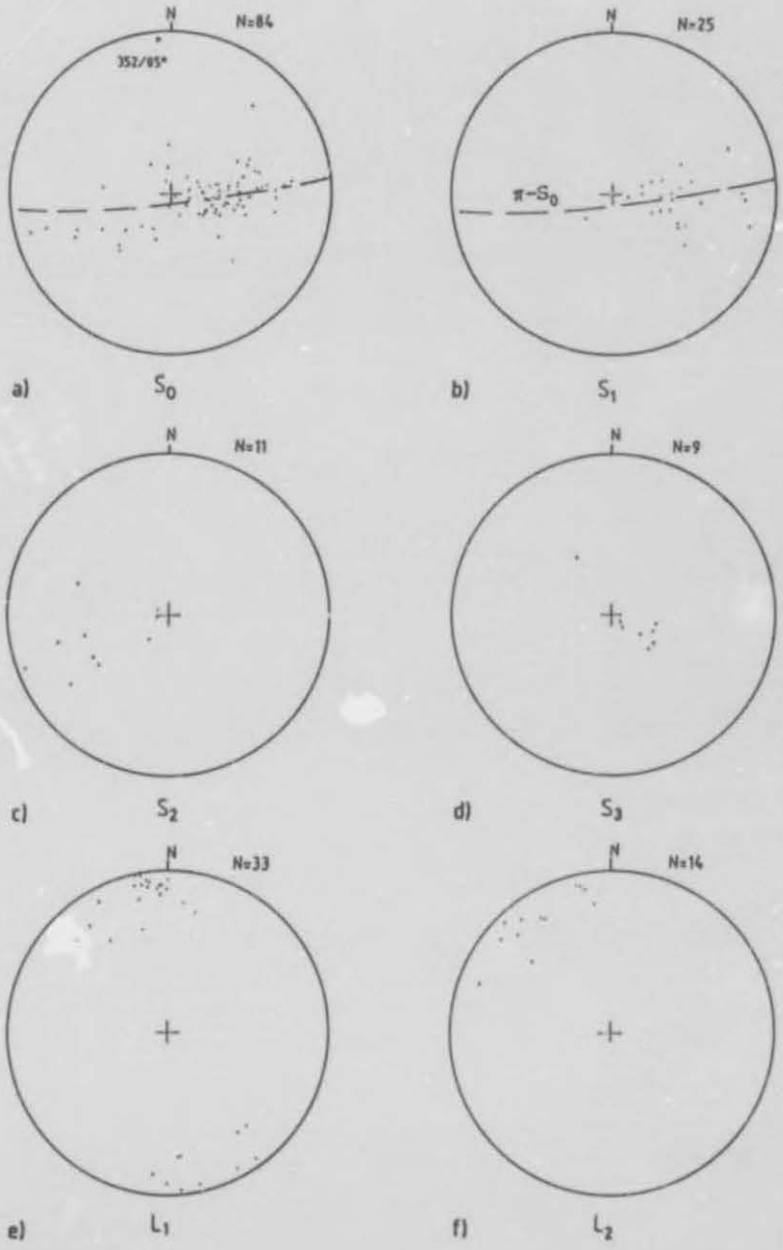

Fig. 53 Fabric data from domain 13

Other than the prominent Valley Thrust exposure there are also macro-F_1 folds (Fig. 52), accompanied by prominent meso-sheath folds in zones of shearing. Both indicate the degree of structural disturbance here.

These closed to isoclinal and eastward overturned F_1 structures dominate the S_0 distribution (Fig. 53a) and are

prominently developed just above the Valley Thrust plane. Axial planar S_1 cleavages (Fig. 53b) fall on the S_0 great circle and dip west at moderate angles. S_2 (Fig. 53c) and S_3 cleavages (Fig. 53d) are only seen occasionally.

L_1 (Fig. 53e) and L_2 follow F_1 and F_2 trends. F_2 folds are generally symmetric open structures which gently refold F_1 structures and plunge dominantly to the NW (Fig. 53f). The two structures are almost co-axial which is also evident from the single π-girdle in Fig. 59a. Occasional F_3 folds plunge towards the south-west.

iii) **Domain 14**

A thick sequence of quartzites, calcareous quartzites and arkosic rocks underlie domain 14 between the Valley and Gumchavib Thrusts. These rocks are correlated with the Gumchavib Formation.

Poles to S_0 indicate a mainly westward-dipping sequence (Fig. 54a) having a partial great circle girdle with a π-pole trending 349°/05° (F_1).

Poles to S_1 are subparallel to bedding with a mean cleavage strike of 356° and dip of 35° towards the west, slightly steeper than bedding (Fig. 54b), but nearly parallel to the west-dipping limb of F_1 folds, and probably subparallel to the Gumchavib Thrust.

Open F_2 meso-folds contain a prominent S_2 cleavage, which on average strikes 335° and dips 64° towards the NE (Fig. 54c). Rare north-dipping cleavages are related to the third phase of folding. Quartz vein boudins (LAB, Fig. 54d) lie parallel to the F_3 fold direction (being related to extension accross F_1/F_2), but also to the F_1, F_2 fold direction and indicate extension in two directions (chocolate tablet boudinage).

Isoclinal recumbent F_1 folds are seen in less competent dolomite beds, or sometimes as intrafolial folds within the planar fabric in the quartzites (Fig. 55). They plunge

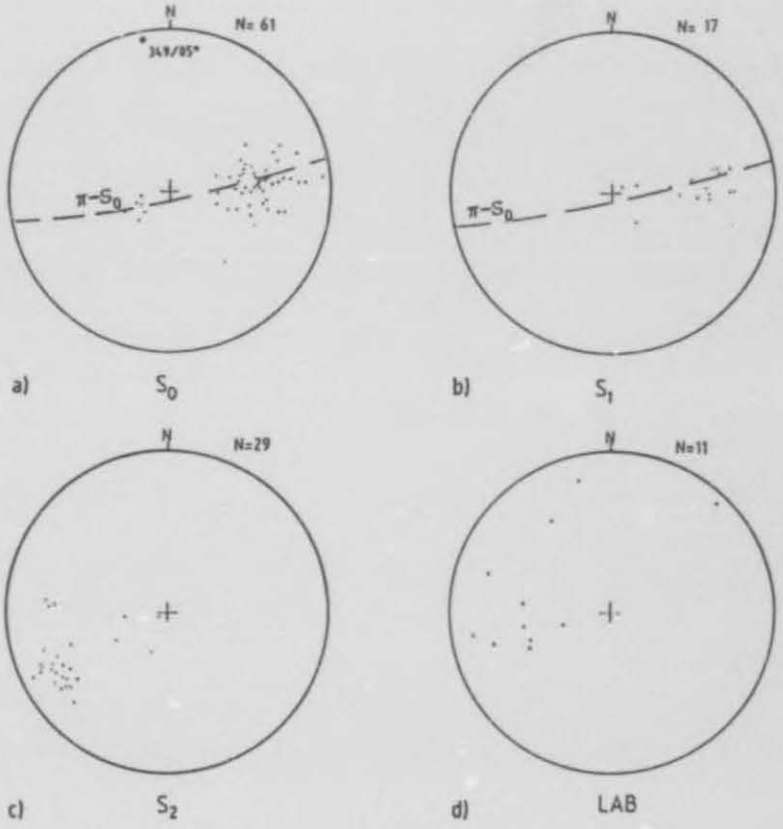

Fig. 54 Fabric data from domain 14

towards the SE and NW at low to moderate angles, and although difficult to recognize in the thick quartzitic sequence might represent the dominant phase of folding.

Most of the joints can be described as quartz-filled dilatational, mainly NE-SW trending a-c joints of the first and second deformation phase (D_1/D_2) but b-c joints are also present.

iv) **Domain 15**

A sequence of intercalated arenaceous and carbonate lithologies of the Rosh Pinah Formation with minor basic sills underlies this area.

Fig. 55 *Intrafolial F_1 fold in quartzite, truncated by a D_1 thrust at the base. The locality is 2 km NE of Obib Peak.*

The S_0 data form a broad E-W girdle and reflect some doming and basining because of F_1/F_2 and F_3 interference (Fig. 56a). Tight east-verging meso-F_1 isoclinal folds with steeply dipping S_1 cleavages are still present within the lithological units, but have been reorientated on the limbs of near symmetric F_2 macro-folds. S_1 cleavages have also been affected but still generally dip west (Fig. 56b). S_2 cleavages mainly vary from steeply to shallow east-dipping but are occasionally also rotated to dip west (Fig. 56c).

This is related to the backfolding of units just above the Rosh Pinah Nappe Thrust and may indicate that backfolds formed by gravitational sliding or some other triggering mechanism possibly rotated the early formed S_2 cleavage in these folds.

The latest structures are north to north-westerly dipping cleavages, which may be related to the third phase of deformation (Fig. 56d). F_1 (Fig. 56e) and F_2 (Fig. 56f) structures are approximately co-axial and near horizontal.

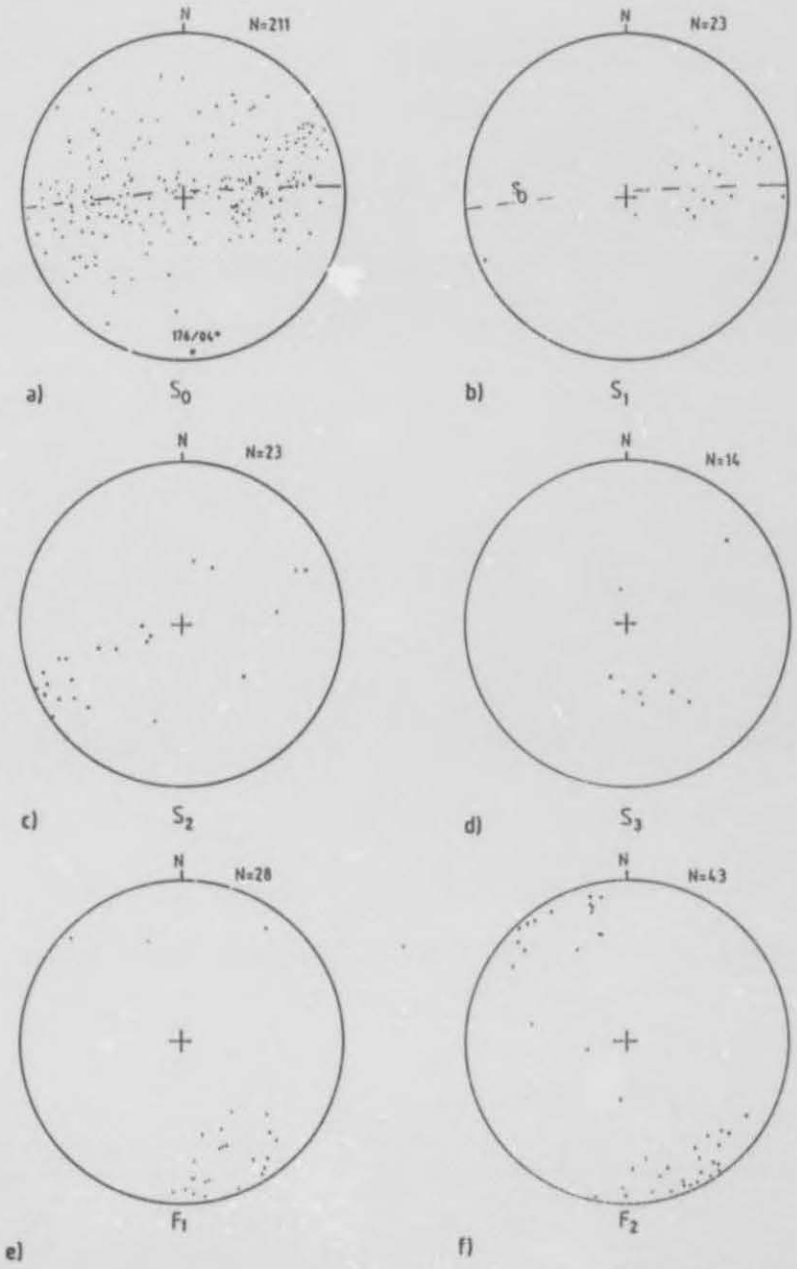

Fig. 56 Fabric data from domain 15

Prominent joint sets trend towards the ENE-WSW, (extensional a-c joints for F_1 and F_2 folds) while less common sets lie parallel to these fold axes. Quartz veins follow all directions of joint sets. Major faults are conspicuous in the field along the eastern-most outcrops in this domain. Faults dip steeply towards the west or east which may be related to the attitudes of thrust imbricates within the Pickelhaube Duplex Structure.

v) **Domain 16**

This domain includes all the backfolded lithologies of the Rosh Pinah, Pickelhaube, as well as Wallekraal Formations, which lie above the Rosh Pinah Nappe Thrust. The structure differs considerably from that of domain 15 (Annexure 3).

Structural readings from the Pickelhaube Formation indicate a wide range of bedding dips (Fig. 57a). π-Poles on 334°/15° and 212°/40° could represent the F_2 and F_3 fold axes respectively. A few doubtful S_1 readings were recorded (Fig. 57b).

S_2 data indicate that F_2 folds may be overturned towards the west (Fig. 57c). A fanning S_3 fracture cleavages is widely spaced (Fig. 57d). L_2 and F_2 data are outlined on Fig. 57e and Fig. 57f respectively. The F_2 fold axes have been refolded by NE-SW trending F_3 folds (Fig. 57f).

Other structural data were mostly collected by students from the University of Cape Town (I'ons and Light, 1971; Hodgson et al., 1972) and the University of Stellenbosch (Hälbich, 1971, 1972, 1973) on the western limb of the Rosh Pinah anticlinorium. Their results are here partly re-interpreted in the light of the current study.

Bedding data of I'ons and Light (1971) of the University of Cape Town for an area south-east of the Rosh Pinah Mine outline a great circle girdle with a well-defined π-pole at 121°/45° (Fig. 58a). The structure is defined as an F_2 anticlinal fold with a prominent north-easterly dipping cleavage subparallel to the axial plane (S_2).

Faults are parallel to S_2 cleavage (Fig. 58b) with displacement of the eastern block described as upwards relative to the western block. These are therefore backthrusts that originate during the D_2 phase but have not been confirmed during current mining operations.

Data for two areas north-west of the mine (Hälbich, 1972) are given to illustrate the structural resemblance of different areas here. S_0 data are given in Fig. 59a+b. Fig. 59a

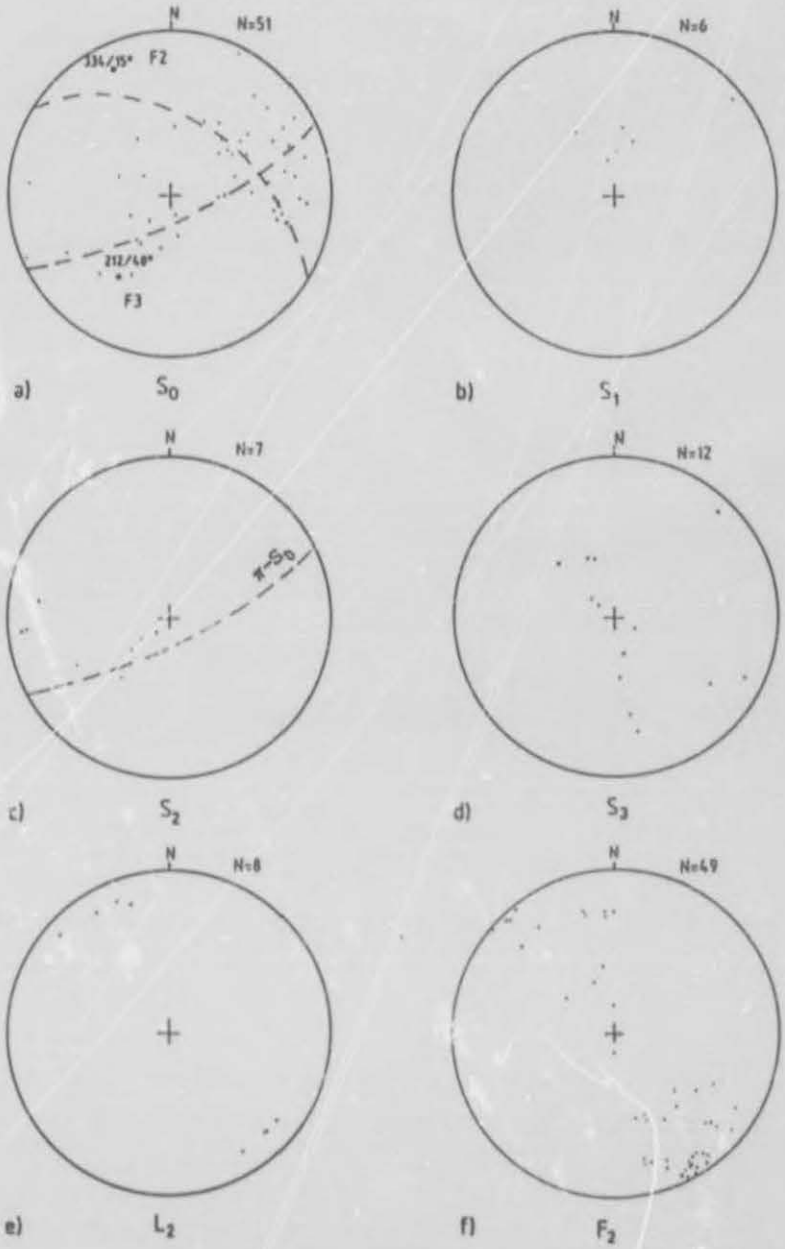

Fig. 57 Fabric data from domain 16

defines an F_2 fold axis with an azimuth of 157°/35°. On Fig. 59b only a single straight limb or parallel limbs of an isoclinal fold is defined. This is not incompatible with Fig. 59a but depends on the size of domain chosen.

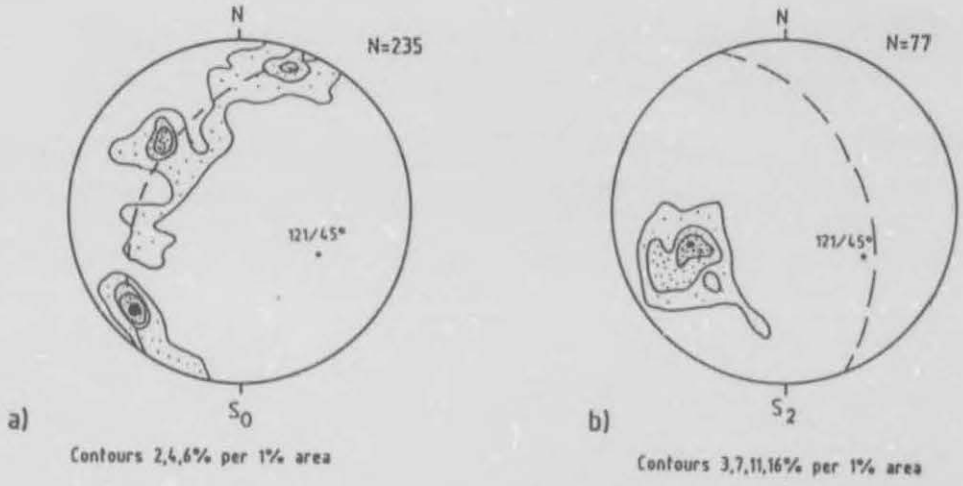

Fig. 58 Fabric data from domain 16 (After I'ons and Light, 1971)

The prominent cleavage (S_2) trends 350° and dips 62° towards the northeast (Fig. 59c) but differs slightly in Fig. 59d.

The L_2 lineations (Fig. 59e+f) follow a great circle through F_2 with maxima at or near F_2 and are therefore deformed by NE-SW trending younger F_3 fold axis. This F_3 effect is also seen in Fig 59a where some bedding poles spread out across the π-girdle.

Another set of S_0, S_2 and L_2 data (Annexure 3a) from a small area in proximity to those from Fig. 59, also reveals the reorienting effect of a D_3 deformation. The westerly vergence of these F_2 folds confirm a phase of backfolding.

The general plunge of Rosh Pinah orebodies is towards the south-eastand therefore in the general direction of F_2 fold axes here. The interference effect of the third phase of deformation is clearly seen as undulating rolls across this south-easterly trend.

The present study relates local thickening of orebodies to interference between F_2 open and F_3 crossfolds (Fig. 60). The F_3 folds are actually exposed by the attitude of the footwall breccia in the B-mine open pit area.

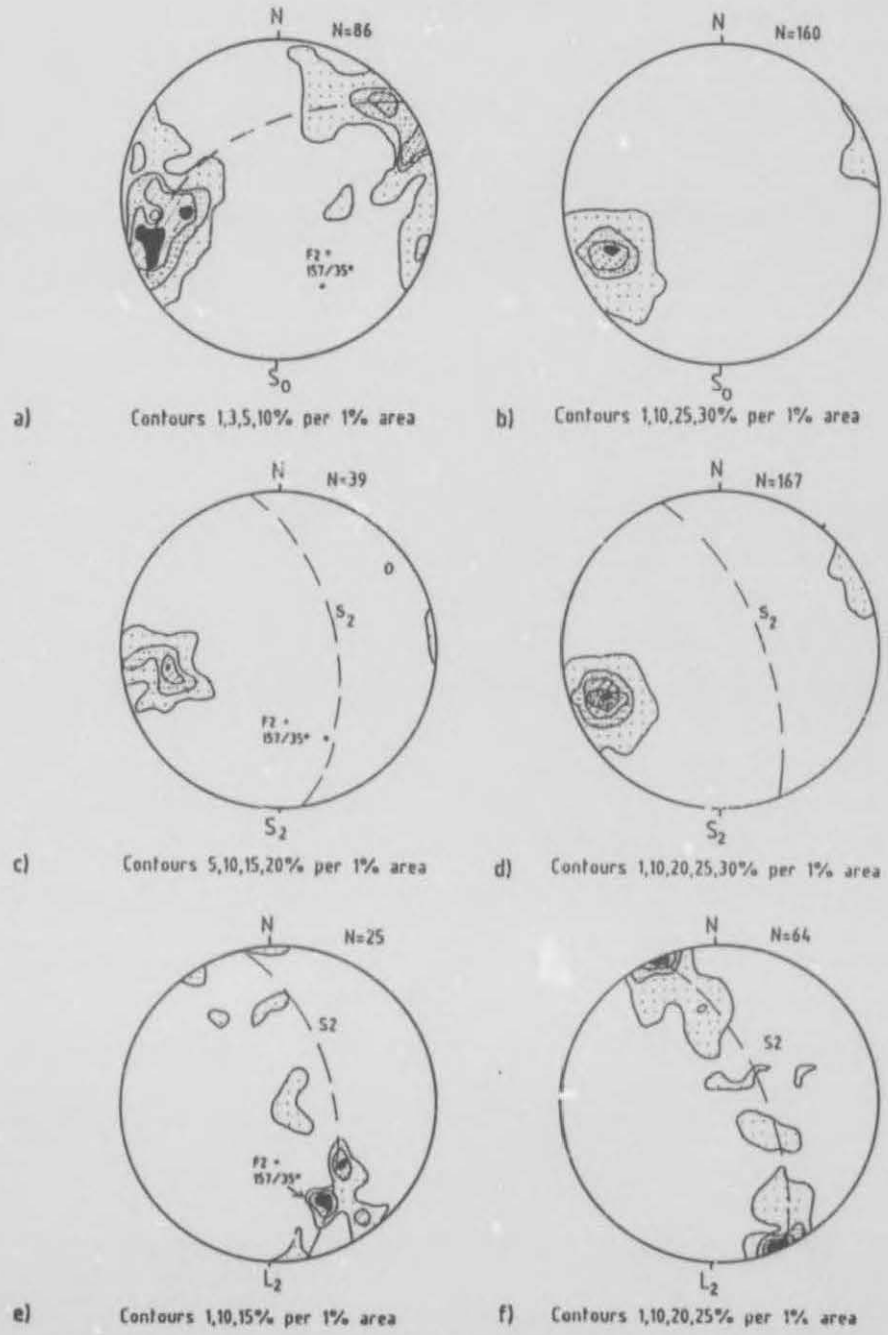

Fig. 59 Fabric data from two areas north-west of the mine in domain 16 (After Hälbich et al., 1972)

Structural studies in the A- and B-mine areas (Annexure 3) (Hälbich, 1971, 1972), also reveals that north-south trending shears have a dextral sense of movement with the north-eastern block having moved obliquely upwards in a south-easterly direction, which is related to the direction of backthrusting.

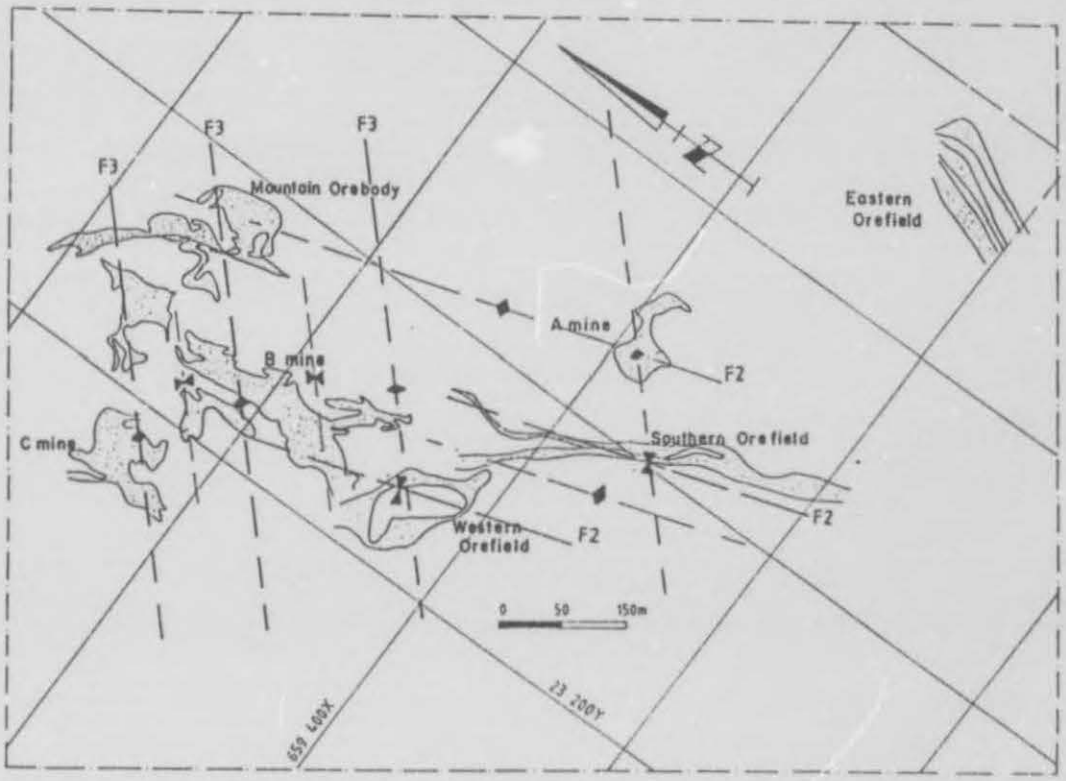

Fig. 60 Distribution of major orebodies relative to F_2 and F_3 regional fold trends within Rosh Pinah Mine Grant Area.

These areas are complexly folded (Fig. 61a), and neither a single great circle nor a small circle girdle fits all data. The single somewhat dispersed cleavage set (Fig. 61b) has a maximum lying on the intersection of two possible S_0 great circles from Fig. 61c and d (data from two nearby areas) respectively. The azimuth of this cleavage is 168° and it dips 48° towards the east-north-east still very nearly parallel to the S_2 cleavage planes of figures 58 and 59.

Hodgson et al. (1972) outline a vague π-pole on 304°/16° for S_0 data for an area near the Rosh Pinah Mine (Fig. 62a). The cleavage is axial planar to the defined folds and is interpreted as S_2 (Fig. 62b).

Here again it is apparent that both cleavage and bedding are also deformed. S_2 are deformed about a π-axis near to the

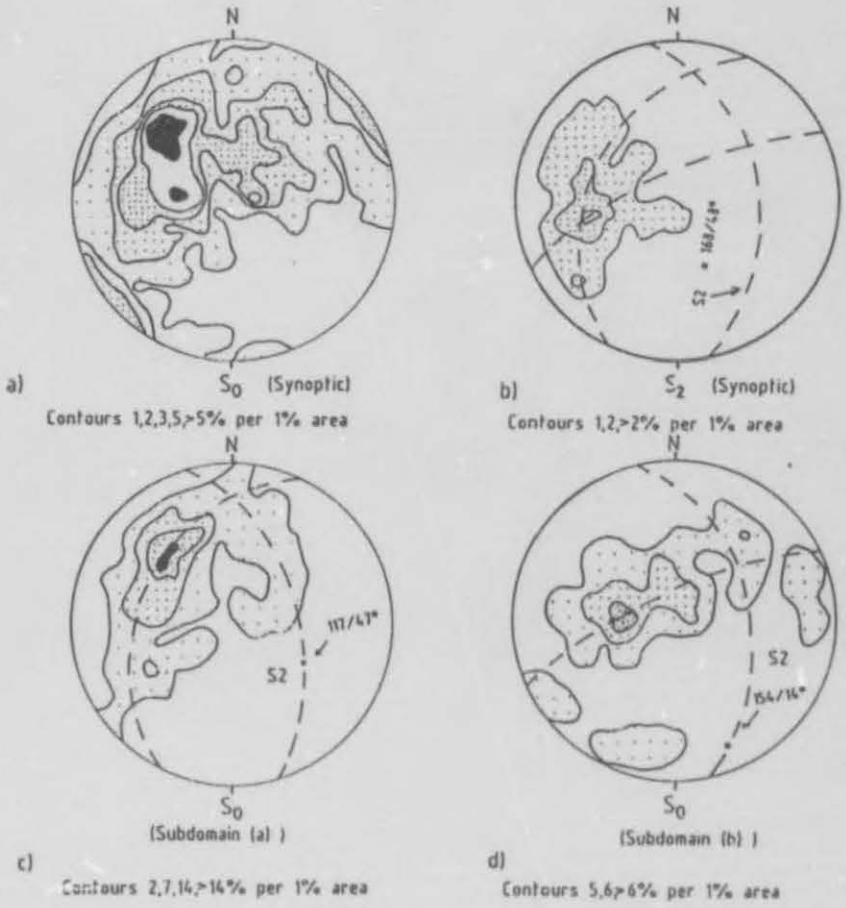

Fig. 61 *Fabric data from the vicinity of B-mine in domain 16 (Annexure 3) (After Hälbich et al., 1973)*

L_1/L_2 stretching lineation and F_2 of Fig. 62a. This indicates that Fig. 62b has components of S_1 as well as S_2, whereas the maximum indicates the S_2 position because the maximum great circle, S_2, passes through 304°/16° and 326°/35°

Lineations were measured on elongate limonite spots and quartz pebbles and define a stretching lineation (L_1, and/or L_2, Fig. 62c) with an attitude of 326°/35°.

Joint data collected by Frankland (1975) in the Rosh Pinah B-mine indicate a strong NNW set, which dips towards the NE and lies parallel to major shearing. A complimentary set has very steep dips both north as well as south and the trend varies between 085° and 077°.

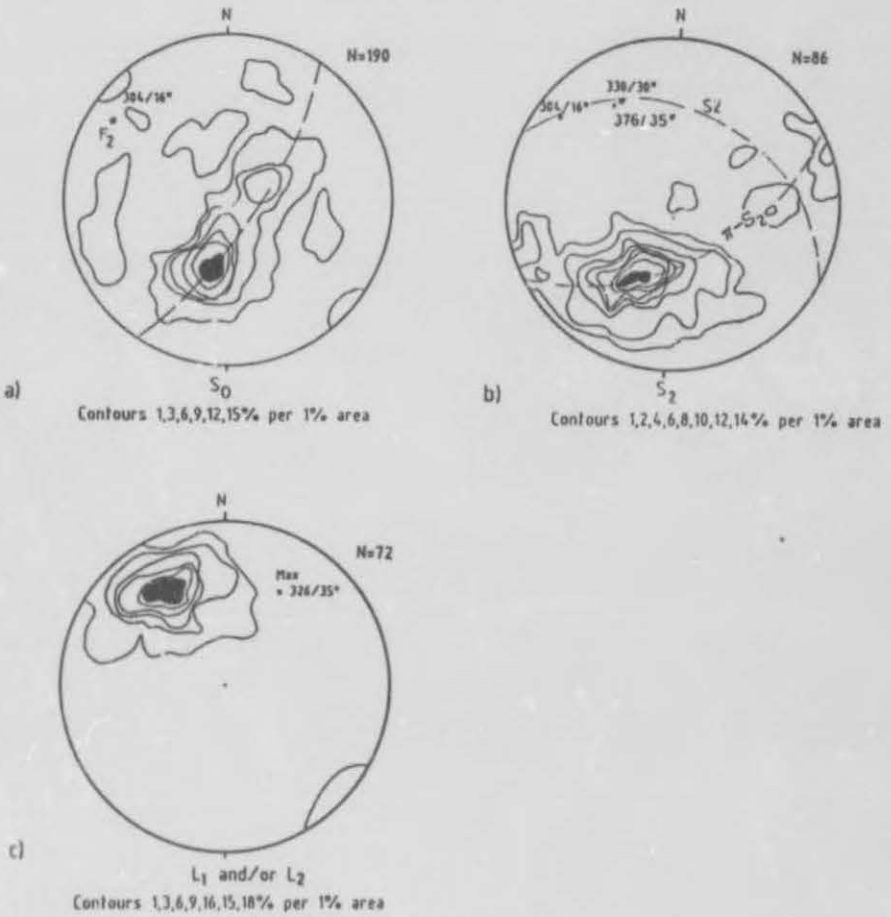

Fig. 62 *Fabric data from domain 16 (After Hodgson et al.,1972). (The locality is towards the west of B-Mine, Annexure 3a)*

Data collected by the author in the area of the Mountain Orebody 470 level adit, outlines bedding data (Fig. 63a) with a near vertical axial plane as well as axial planar cleavage trending NW-SE (Fig. 63b).

In the Pickelhaube Formation of the western part of domain 16 south-easterly striking brittle faults abound. These faults have near-vertical dips and are interpreted as late listric extensional faults that also transect the Rosh Pinah Nappe Thrusts (Annexure 3).

vi) Domain 17

Domain 17 is defined as shown on Annexure 3 to comprise the area just east of the RPNT and west of the Numees Thrust.

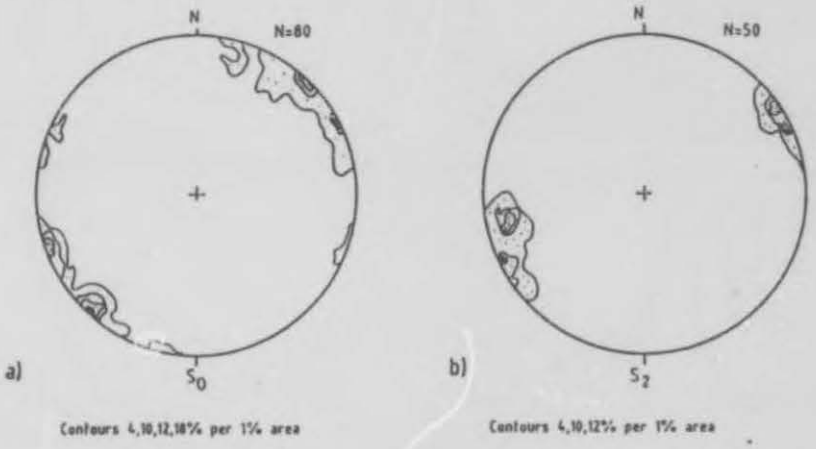

Fig. 63 Fabric data from the Mountain Orebody area in domain 16

The structural data gathered by Hoffmann (1972) in proximity to the Rosh Pinah Nappe thrust are summarized and interpreted in relation to the current study. This domain includes intercalated quartzite and carbonate lithologies, which are correlated with the Rosh Pinah Formation and which lie between the Rosh Pinah Nappe Thrust and the Numees Thrust (Annexure 3c).

The π-pole great circle girdle of S_0 poles (Fig. 64b) in sub-area B some distance away from the RPNT defines an axis plunging at 147°/25°. In sub-area C, closer to the RPNT a similar axis is defined at 145°/58° (not shown). If the pole distributions are interpreted as belonging to slightly conically folded surfaces (Fig. 64b), a cone axes lies at 152°/51° for sub-area B.

The steepening of the fold axes can be explained by shear along the steeply dipping RPNT. The fact that these folds become more steeply plunging in sub-area C, i.e. closer to the thrust and the fact that they are somewhat conical (Fig. 64b) also suggest reorientation of these axes along the fault with a steep dip. The reorientation may be enhanced by the beginning of backfolding.

Lineations measured here as well as some in sub-area D of domain 17 (Fig. 64a) indicate that the fold axes have been

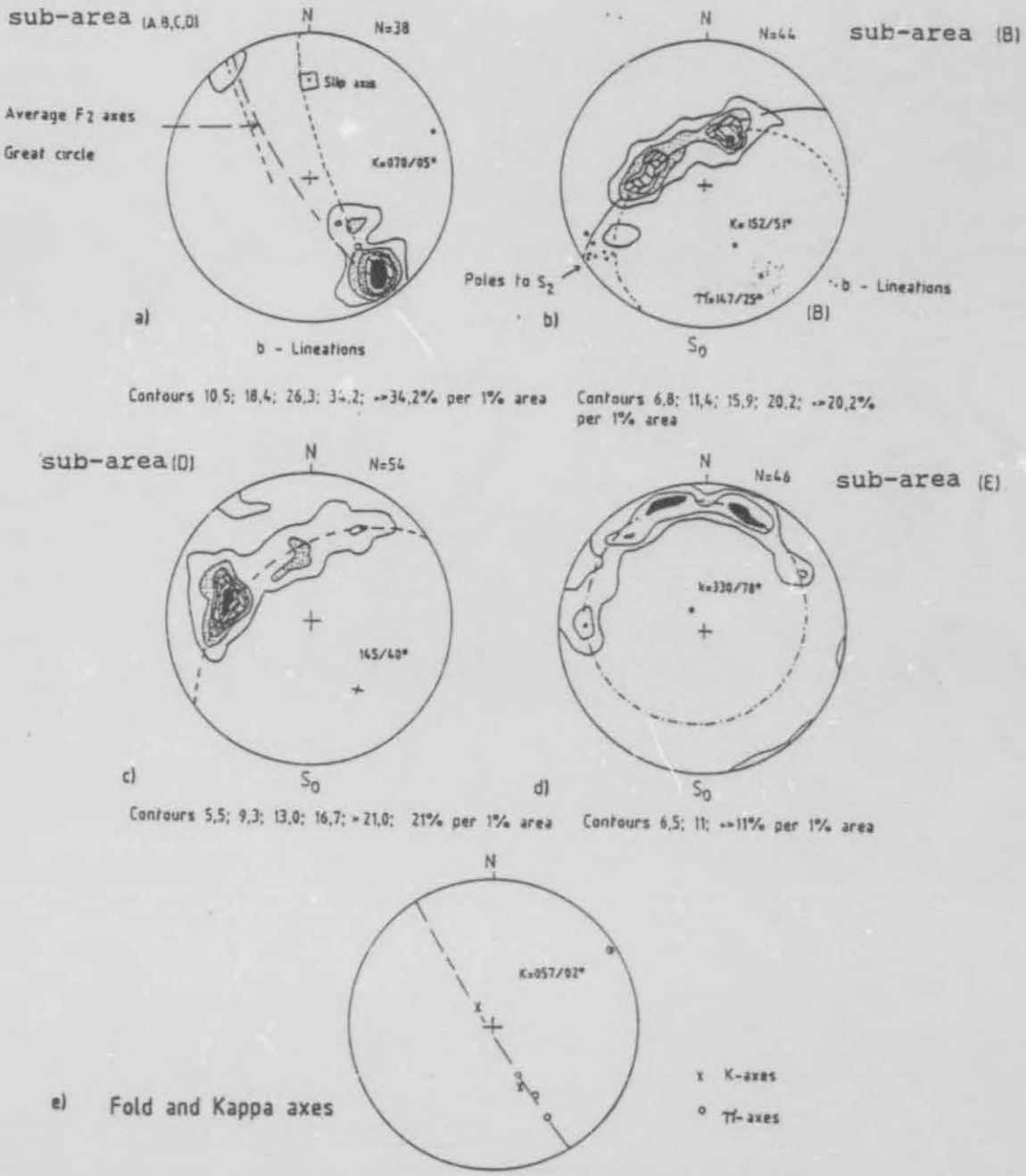

Fig. 64 Fabric data from domain 17 (After Hoffman, 1972). (The data were gathered in the proximity of the Rosh Pinah Nappe Thrust).

rotated around a kappa axis (axis of rotation) lying on 070°/05°, which indicates a phase of cross-folding. The slip axis (Fig. 64a) has been derived from the orientation of long axes of Numees diamictite clasts near Namuskluft farmstead. S_0 data for sub-area D outline a great circle girdle with a

π-axis on 145°/40° (Fig. 64c) which compare closely with data from sub-area B.

The south-east plunging open folds are interpreted as F_2 folds with steep axial planar cleavages (Fig. 64b) which have been slightly rotated off the π-girdle. All these axes lie on a girdle (Fig. 64e) the pole of rotation of which at 057°/02° is close to a kappa rotational axes derived in Fig. 64a for b-lineations at 070°/05° for areas A,B,C and D.

The effect of a third cross folding phase of deformation is shown by the steepening of the b-lineations towards the fold closure in the southwest.

In the field a steepening of the S_2 cleavages towards the east can be observed and the change from cylindrical to conical folds (Fig. 64d) is possibly explained by the presence of a major fault, or as a result of F_3 fold interference, with refolding of the originally cylindrical F_2 folds.

Hoffman (1972) observed two major faults in the area (Annexure 3a), with brecciation in the eastern fault, and mentions that there is a downthrow towards the west along both faults. In this study these faults are rather related to an episode of thrusting of cover rocks over the basement. This is based on the following observations combining the data obtained by Hoffmann (1972) on sub-areas A to E situated west and east of the RPNT.

i) all axes of folds, whether conical or cylindrical, plot on a great circle girdle with a rotational axis at 057°/02°. This could be interpreted as an F_3-axis or as the pole of the RPNT along which all F_2 folds are rotated towards the slip direction on the fault.

ii) B_2 lineations do the same thing (Fig. 64a) converging onto the slip direction.

iii) Refolding along F_3 axes could lead to a very similar result and the question yet to be answered is:

Do F_3 folds actually represent the strain on bedding resulting from forces exerted during slip along the thrust planes?

In the Rosh Pinah Mine, orebodies south of B-mine (Annexure 3) are tightly folded and steeply inclined e.g the Southern and Western Orefield orebodies, whereas north of B-mine they form open domal structures e.g. the C-mine and Mountain Orebodies (Fig. 60). An explanation for this feature may be the possible presence of a major F_3-structure towards the south of the Rosh Pinah Mine (Fig. 2 and Fig. 75).

9. SUMMARY OF THE GARIEPIAN HISTORY

Von Veh (1988) interprets the evolution of the Pan-African Gariep Belt to have taken place on an Atlantic-type passive continental margin, as a progression from an early coarse terrigenous clastic phase of deposition (Stinkfontein Sequence) to a platform carbonate and continental shelf clastic phase (Hilda Sequence), to a deep water clastic phase (Holgat Sequence).

Davies & Coward (1982) see the distribution of the sedimentary facies variations across the Gariep Arc as proof of a plate margin. Further evidence for a plate tectonic origin are comparable sedimentation and deformation patterns (Kröner, 1974) and the association of high-grade metamorphism with large volumes of basic and ultrabasic igneous rocks.

The Gariep Belt evolved during a prolonged period of stretching and thinning of the earth's crust with resultant epeirogenic subsidence. Early listric and block faults formed and rifting was accompanied by large dextral transtensional NW-NNW trending shears (D_2^n) in the basement (Von Veh, 1988), of which remnants are still seen. Gravity gliding featured prominently in the subsiding half graben basins.

Sedimentary filling of basins was rapid and immature sediments were deposited as westward tapering wedges (the Rosh Pinah and Gumchavib Formations of the Stinkfontein

Sequence). Mass-flow and fluvial deposits are represented by lenticular conglomerate units.

In the Trekpoort mountains north of Posh Pinah, large volumes of alkaline acid volcanics extruded through major basement faults, and ore-bearing hydrothermal fluids were exhalated. Subaereal extrusion formed prominent tuff and agglomeratic horizons especially around Spitskop to the north of Rosh Pinah.

Rifting was followed by the opening of the Adamastor Ocean (Hartnady et al., 1985), with widespread outpouring of basaltic lavas on the seafloor during seafloor spreading. Following upliftment and erosion of the Stinkfontein Sequence the continental margin cooled and eventually subsided as it moved away from a spreading centre.

Stable continental shelf conditions followed during which the clastic Hilda Sequence was deposited, followed by a period of worldwide atmospheric and continental instability. The glaciogenic Numees diamictite and accompanying ferruginous lithologies were deposited on a continental slope environment during this period. Finally the fine-grained clastic Holgat quartzites, schists and carbonates were deposited in the deeper parts of the basin while the Witputs Sequence was deposited in shallow water and is time equivalent to the Holgat.

The Adamastor Ocean eventually transgressed over the Congo and the Kalahari Craton (Stanistreet et al., 1991) (Fig. 65a) and the Khomas Sea opened. Glacio-marine and pelagic sediments were deposited in this sea (Stanistreet op. cit.), which subsequently closed during the collision of the Congo and Kalahari Cratons (Fig. 65b). The remnant outlines of the present Gariep basin were established when the Gariep rocks were uplifted during regression and eroded away. During subsequent renewed trangression the shallow water platform deposits of the lower Nama Group overlapped onto the basement.

According to Stanistreet et al. (1991), closure of the Adamastor Ocean followed on the collision of the Kalahari and

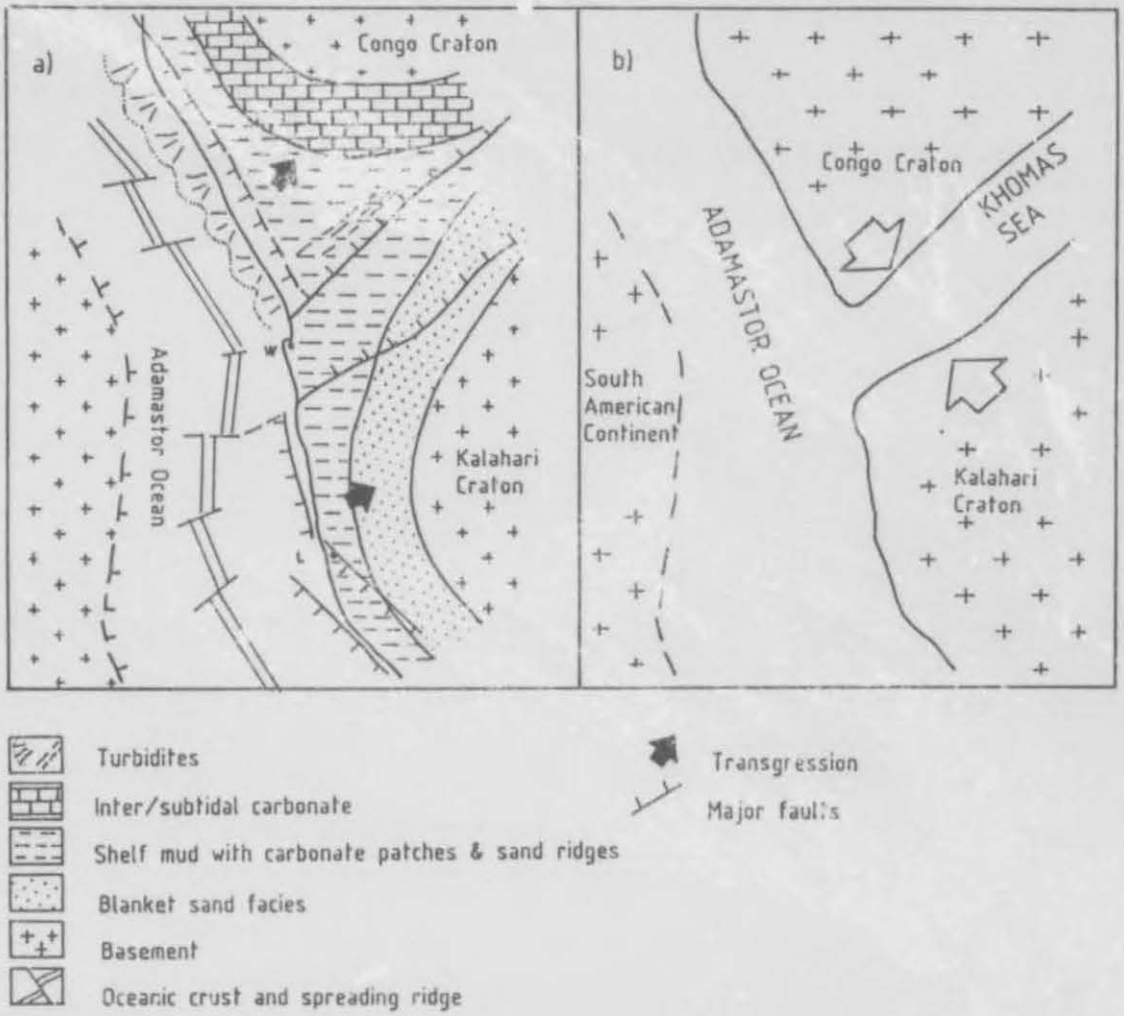

Fig. 65a) Opening of the Adamastor Ocean with subsequent transgression over the Congo and Kalahari Cratons.

b) Formation of the fault controlled Khomas Sea with subsequent closure and collision (after Stanistreet et al., 1991).

Congo Cratons and led to amalgamation of the Southern African and South American Cratons.

The Gariepian orogeny resulted from the oblique southward closure of the NNW-SSE trending proto-Atlantic or Adamastor Ocean as seen in the southeast directed transport vectors along parts of the Pan-African Belt system along the west coast of Southern Africa (Hälbich et al., 1987). Early

gravitational deformation effects were largely obliterated by the subsequent regional contractional tectonic event.

Von Veh (1988) proposes that the rate of southward migration in the Gariep Belt exceeded the rate of closure of the Damara Belt, with the Kalahari Craton arriving at the consuming arc while the main deformation pulse was still proceeding in the central parts of the Damara Belt. The leading edge of the subduction zone consisting of ophiolitic material from an accretionary prism (the Grootderm Suite) and part of a Chilean-type fore-arc basin (the Oranjemund Suite) was obducted in a SE to SSE direction onto the passive margin of the craton.

The Pan-African evolution of the region climaxed with the emplacement of the Kuboos-Bremen line of plutons at about the same time as final closure occurred in the Damara Belt.

10. THE GEOLOGICAL HISTORY OF THE STUDY AREA.

10.1 THE EVOLUTION OF MAJOR STRUCTURES

The structural evolution of the Pickelhaube Peak, Obib Peak, Rosh Pinah and Namuskluft areas was initiated during collision of the African foreland with the obducting tectonic prism of the South American continent.

The master Schakalsberg Thrust emplaced a thick slice (up to 5 km) of dense basic rocks with ophiolitic affinities (see Figs. 73 to 76) onto a foreland situated in the Schakalsberg mountains west of the Obib Mountains during the D_1 transpressive phase (Von Veh, 1988). Gravitational instability was caused in the crust, and an imbricate fan formed by listric splay faults in front of the overlying spreading mass (Fig. 75 episode 7a + 8a).

Transport vectors towards the SE are indicated (Fig. 66). This was accompanied by east-northeast verging F_1 folds with axes aligned parallel or nearly parallel to D_1 thrusts, and a penetrative S_1 shear cleavage dipping SW at moderate to steep angles.

A possible model for the release of bending stress due to loading could have been according to the visco-elastic flexural model of Quinlan and Beaumont (1984), whereby a load emplaced on an originally flat lithosphere would deform the plate as indicated by curve 1 (Fig. 67). If the lithosphere responds elastically, the shape will be maintained although the surface load changes. During loading the flexural profile changes with time according to curves 2 and 3 (Fig. 67) if the bending stresses are released by creep, even if the load remains the same. In the case of the Gariep Belt, however, it is envisaged that bending stresses due to relative fast emplacement of the Grootderm Suite over cover rocks were released by the formation of listric splay faults in front of the overlying mass of high density rocks as the elasticity boundary with regards to shearing was passed.

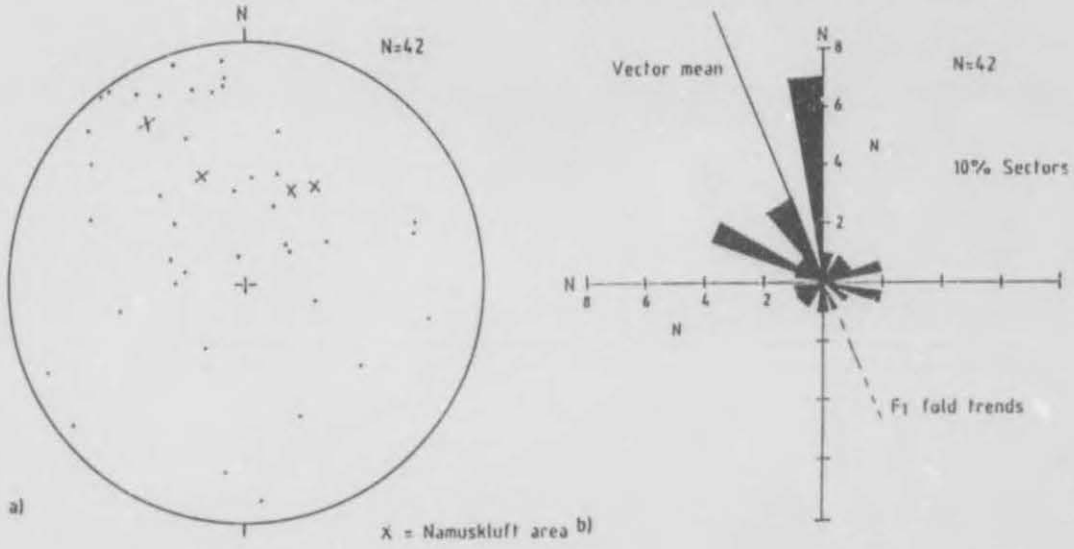

Fig. 66 *Orientation of movement axes displayed on: a) equal area lower hemisphere stereoplot and b) rose diagram. The data consists of striations and corrugations on fault planes in the study area.*

The Gumchavib and Rosh Pinah Formations were duplicated by the Obib Waterhole, Valley and Gumchavib splay thrusts emerging off the footwall of the overlying Schakalsberg Nappe according to Fig. 68a.

The Annisfontein anticlinorium started to form as a ramp structure on the D_1 sole thrust due to continued pressure

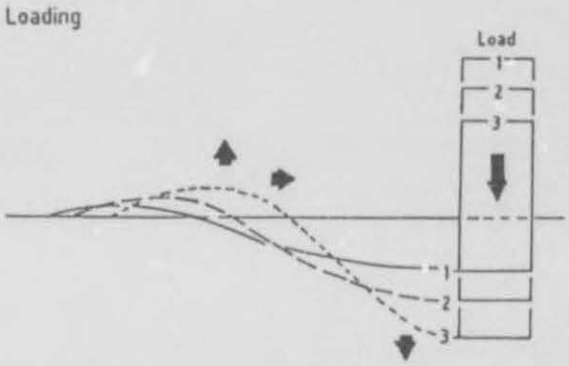

Fig. 67 *Flexural model to illustrate lithosphere response to supracrustal loading, e.g. through overthrusting. (Visco-elastic model after Quinlan and Beaumont, 1984).*

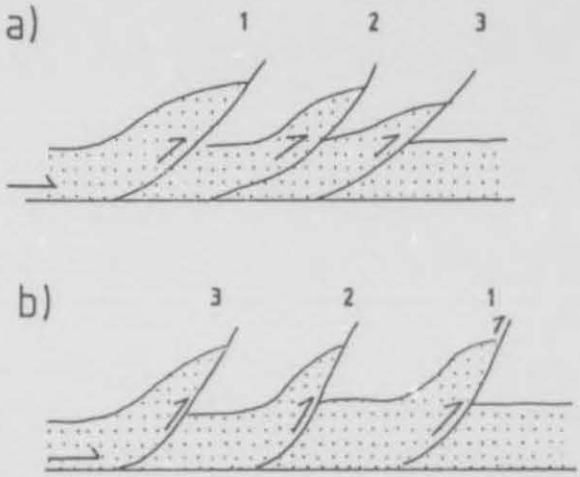

Fig. 68 *Sequential development of different thrust sequences*
a) in-sequence thrusting
b) out-of-sequence thrusting
The thrusts are numbered 1-3 in order of development.

from the SW. The thrusted unit may have acted as a single thrust sheet (Fig. 69), forming a set of intraplate folds (the Sendelingsdrif synclinorium and the Rosh Pinah anticlinorium) evolving from fault propagation folding. The Orange River anticline in the Numees diamictite (east of the Sendelingsdrif synclinorium, Annexure 1) may be interpreted as a minor ramp.

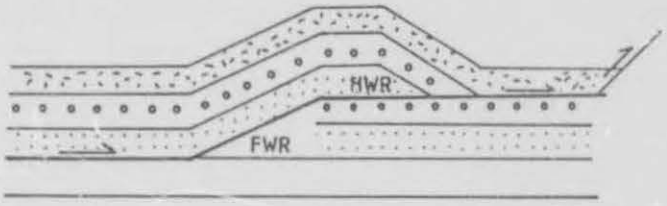

Fig. 69 *The geometry of a single thrust sheet, outlining three types of folds which commonly occur:*
a) ramp anticline (fault-bend fold)
b) intraplate fold (fault-propagation folds)
c) tight folds at leading edge (after Boyer,1986).

At this stage or just before the initiation of the Annisfontein anticlinorium, one of the splay thrusts developed into the Rosh Pinah Nappe, overriding the other splays and possibly even the already initiated Annisfontein anticlinorium. All along the eastern limb of the Annisfontein anticlinorium a hinterland-dipping duplex (the Pickelhaube Duplex Structure) of imbricate fan sheets developed in the overthrust sediments as a result of oblique ramping and sequential steepening of faults against the basement of the foreland.

The Annisfontein anticlinorium was then accentuated, possibly by multiple in-sequence ramping along the footwall. As a result of this part of the RPNT became inactivated where the thrust plane was tilted eastwards. Limited gravitational gliding of the overthrust sediments towards the east into the Sendelingsdrif synclinorium followed contractional deformation and enhanced F_2 backfolding of thrust slices in the duplex zone during D_2 as the units were compressed and steepened against the basement. At this stage the Rosh Pinah anticlinorium may also have formed as a fold/fault controlled

pop-up structure, re-activating and accentuating older graben and horst faults.

Drag according to oblique slip along the various ramps trending NW to NNW is thought to be responsible for conical F_3 folding.

Fig 70(a) F_3 folds with D_3 thrusting along the base. The locality is 2 km north of the Orange River towards Gumchavib Peak (Fig. 2).

Due to differential movement these F_3 folds may be slightly overturned towards the southeast, with slip occurring along cleavage planes to outline minor local thrusting oblique to the previous events (Fig. 70a, b) and trending NE-SW. This folding phase resulted in the present day undulation of the structures and landscape as seen in a N-S section (Fig. 71).

The late lateral transtensive phase D_4-D_5 (Von Veh, 1988) that resulted from the emplacement of the Kuboos-Swartbank plutons is only of very minor and local importance in the present study area. Some small kinks and kinkfolds and E-W trending joints and fractures especially in the Numees synclinorium,

which were not analyzed in detail, represent structures, which are probably related to this event that marks the termination of the Pre-Nama Pan-African orogeny.

Fig 70(b) D_3 thrust contact in Wallekraal grits. The locality is approximately 1,5 km northeast of Pickelhaube Peak.

An attempt is made here to explain the tectonic and sedimentary evolution of the Gariep Belt from observations made in the study area. The model however, does not explain all the intricacies and many questions remain unanswered.

It is also stressed that geological sections have been drawn oblique to the transport direction, but more or less in the direction of compression, i.e. ENE - WSW.

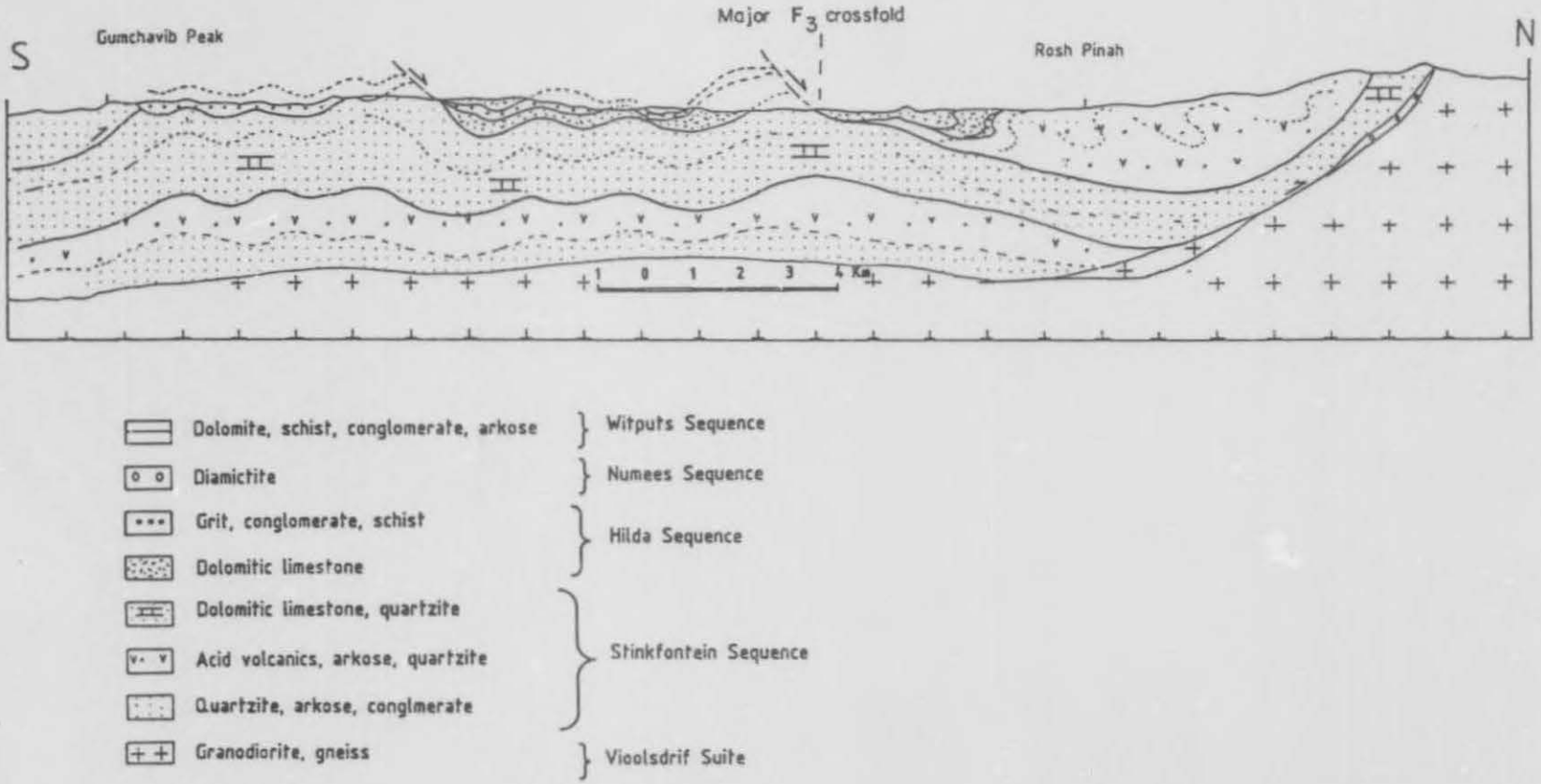

Fig. 71 A north-south profile from north of Rosh Pinah to south of Gumchavib Peak outlining major open F_3 folds and thrusts (See Fig. 2 for profile line).

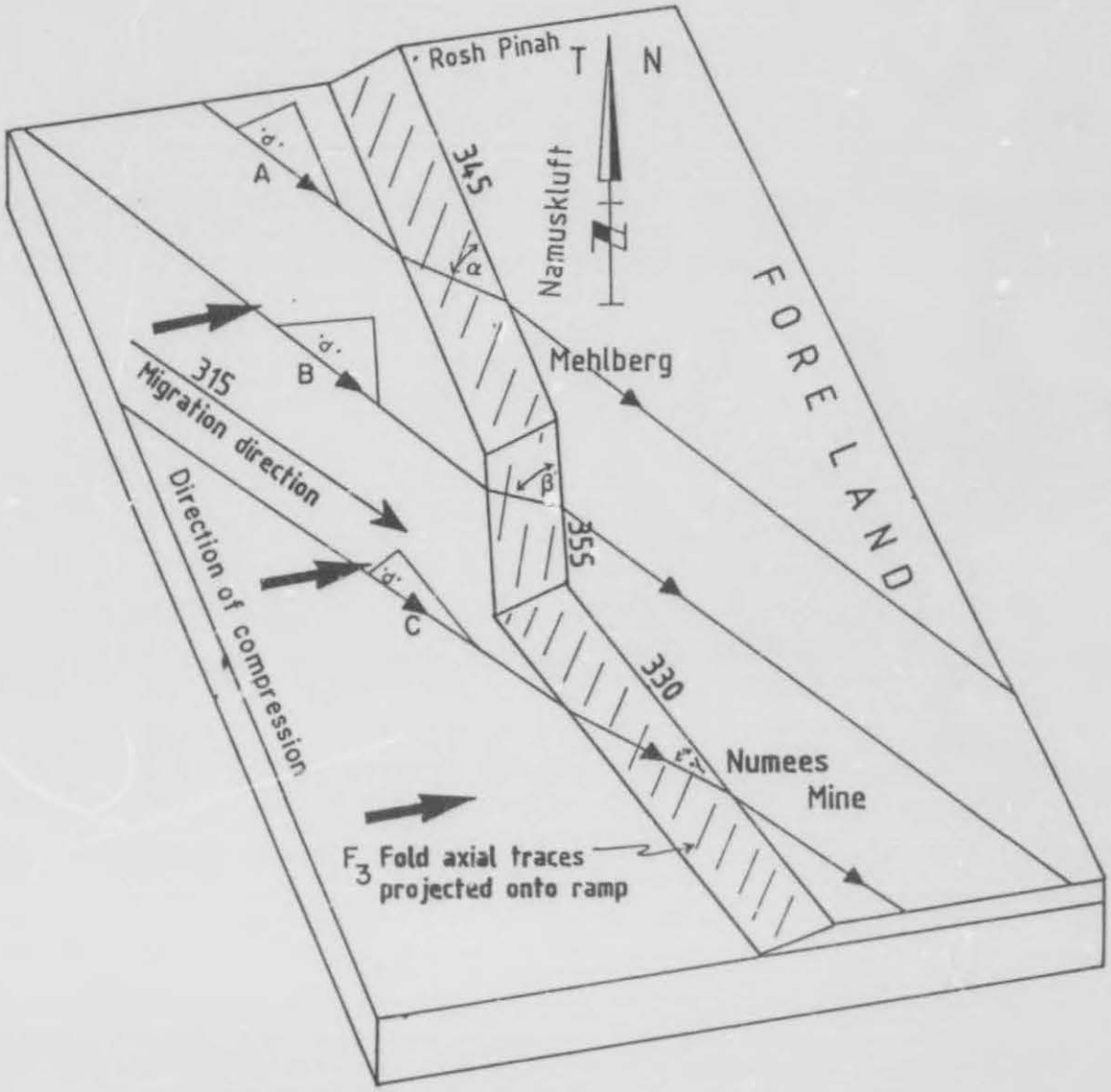

Fig. 72 *The pitch angle of a horizontal slip vector on an oblique ramp depends on the strike of the ramp relative to the slip direction.*

The geometry of a transpressive thrust vector on a foreland is outlined on Fig. 72. A compressional force vector of a transpressional force field produces F_1 overfolds and thrusts during D_1 which verge towards the foreland. The folds axes are finally rotated approximately parallel to NW-SE slip lineations and stretching directions (the migration directions). F_2 folds originate as backfolds co-axial with original F_1 because ramps are frontal ramps for this

compressional vector. Intensive shear zones on ramps reorientate F_1 and F_2 to conical and/or sheath folds by refolding and/or oblique shear respectively.

For unit slip 'd' (as at A, B and C in Fig. 72) the force component at right angles to the strike of the ramp is respectively largest in the middle section (pitch=β), smallest in the southern section (pitch=γ) and intermediate in the northern section (pitch =α). A situation of $\beta>\alpha>\gamma$ applies to this area as indicated by X of the pebble markers (Fig. 31b). This explains the variations of pitch along the northern, middle and southern sections of the eastern boundary faults (or faults close to that boundary) which have trends comparable to the various ramp strikes if the slip vector in the horizontal trends $\pm$ 315° (NW-SE) as shown in Fig. 31a and 31b.

As a crustal segment moves up the oblique ramp it undergoes local compression such that folds may develop with axis trending almost at 90° to the pitching slip vector as shown on Fig. 72. These folds would trend more or less (and somewhat varyingly) NE-SW and would probably be conical, verging SE and plunging at varying angles depending on which limb of an earlier fold they develop. These would be the F_3 folds, which will develop at or near and above every ramp and their intensity would depend on the steepness of the ramp and its strike.

11.2 PHASES OF EVOLUTION

11.2.1 SEDIMENTATION

This is depicted in five episodes (sections approximately 90° to strand line and D_1-D_2 structures, i.e. NE - SW (Fig. 73).

i) Episode 1

Thinning of the crust takes place as an ocean (Adamastor Ocean) opens. This is followed by step faulting and half-graben formation with the Stinkfontein Sequence (Gumchavib Formation) being deposited as fluvial and strandline sediments in a transgressive sea.

This is followed by sandstones, grits and conglomerates (clastic deposition) and acid lavas and tuffs of the Rosh Pinah Formation (volcanism) with contemporaneous deposition of fumarolic precipitated hydrothermal orebearing fluids. These rocks were finally intruded by basic dykes and sills. Reef carbonates develop along the coast during the final stages of transgression.

ii) Episode 2

Uplift of the craton and erosion of the craton and early shelf carbonates follow. A period of regression follows. The Hilda Sequence is deposited unconformably on the shelf on top of the tilted Stinkfontein as clastic carbonates, (Pickelhaube Formation) followed by deposition of shales, grits and conglomerates of the Wallekraal Formation.

All these rocks are inverted erosion products of the Stinkfontein Sequence and the basement rocks (first clastic carbonates then siliceous clastics). Hilda sedimentary breccias thinning rapidly westwards across fault steps are proof of such features on subbasins parallel to main structures.

iii) Episode 3

Further regression follows because of widespread evenly distributed uplift of the shelf with some further horizontal extension. Finally erosion of the Hilda occurs and towards the end of this episode deposition of banded iron formations takes place in shallow depressions of a marginal epicontinental sea or brackish to fresh water lake environment subjected to evaporation cycles and some differential basining along fault bounded long shore basins.

The BIF deposition is a world wide feature related to global tectonics (Rapitan-type iron formations) and varying thicknesses of the latter overlie different fault blocks, because old lineaments are briefly reactivated as syn-sedimentary faults extending upwards through the Hilda Sequence.

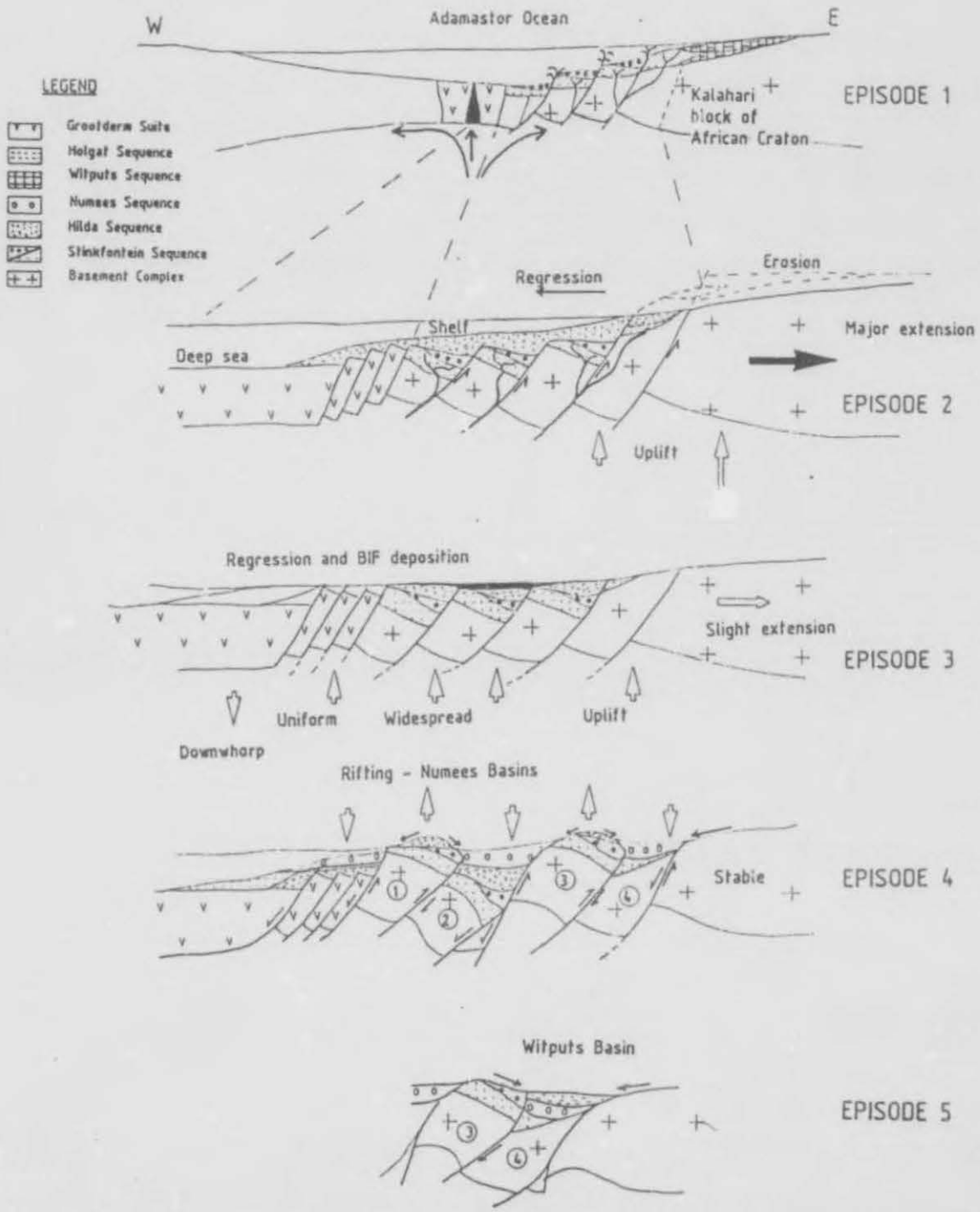

Fig. 73 *The sedimentary history of the Gariep Belt as dispicted in five episodes.*

iv) Episode 4

Rifting, horst and graben formation takes place. Glacial activity leads to filling of grabens with mainly basement material derived from the east, while horsts are

partly eroded to provide minor clasts of Gariep lithologies. Numees sediments transgress over graben edges and thin rapidly.

The three grabens and two horsts are schematic. Their exact width and trend considerably influence the final (and present) distribution of basement thrust slices between cover sediments during the final episode.

v) Episode 5

The Witputs graben forms closest to the craton edge or between the easternmost faults. The Holgat Formation (not shown) which is possibly contemporaneous is deposited west of the westernmost horst above the Numees diamictite shown in episode 4 of Fig. 73.

11.2.2 **TECTOGENESIS PROPER** (Subduction on South American side

i) Episode 6

Beginning of D_1 compressional phase. Decoupling and overfolding (F_1) takes place with thrusting to the east, and deformation and slip of horst-graben blocks over each other. Merging of toes of thrusts towards a common sole takes place. Blocks may plunge into and out of section because of differential upward gliding across their trend, and influenced by SE-directed migration somewhat oblique to the section.

From here on several deformation histories can be envisaged. Three different paths are treated and an attempt is made to conserve volume from here.

a) **PATH 1 (Fig. 74)**

i) Episode 7

D_1 intensified, with much near surface gliding, nappe thrusting and recumbent folding. Upthrusts first steepen and then shallow out in depth to coalesce at the Moho into a single sole thrust. Overthrusting onto a rigid continental

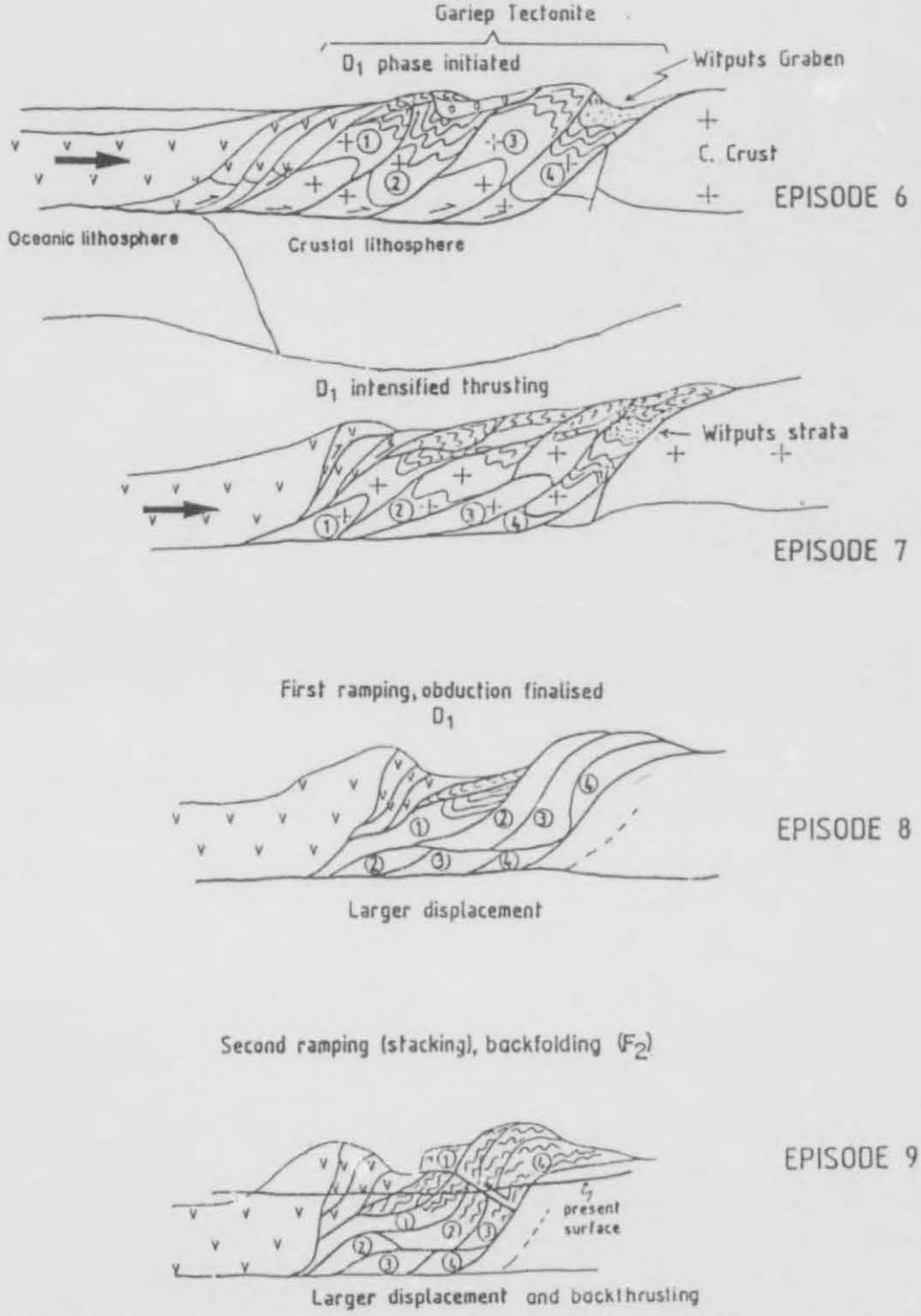

Fig. 74 *The tectonogenesis of the Gariep Belt. Episodes 6,7,8 and 9 outlines the first of three possible deformation paths envisaged.*

block that was never thinned during the sedimentation phase, takes place. Except for boundary faults of blocks, all structures are near horizontal far

from the craton block but flattening is dominant near the craton.

Four blocks are numbered to coincide more or less with the two grabens and two horsts formed during episode 4. This part is very schematic because no exact boundaries of blocks are known. Obduction has now started.

ii) Episode 8

Ramping occurs above the sole and obd[illegible] finalized.

iii) Episode 9

A second ramp has developed with stacking at depth. Backfolding (F_1) takes place in the eastern parts mainly above but also below a backthrust verging west. Original thrusts steepen against the undeformed craton and become backfolded too. Relaxation is not considered here.

An erosion surface shows that certain features are reminiscent of the surface geology in Annexures 1 to 4. However, the RPNT is a backthrust here and the Annisfontein anticlinorium is not recognisable as such.

This model (Path 1) is fairly deficient in many respects. Note that no details of lithologies inside blocks 1-4 are given, because backfolding is highlighted in episode 9 of the figure.

The amount of sliding during two ramp episodes is here also assumed to be large relative to the spacing between the floor ramp and the craton ramp.

b) **PATH 2 (Fig. 75)**

i) Episode 7a

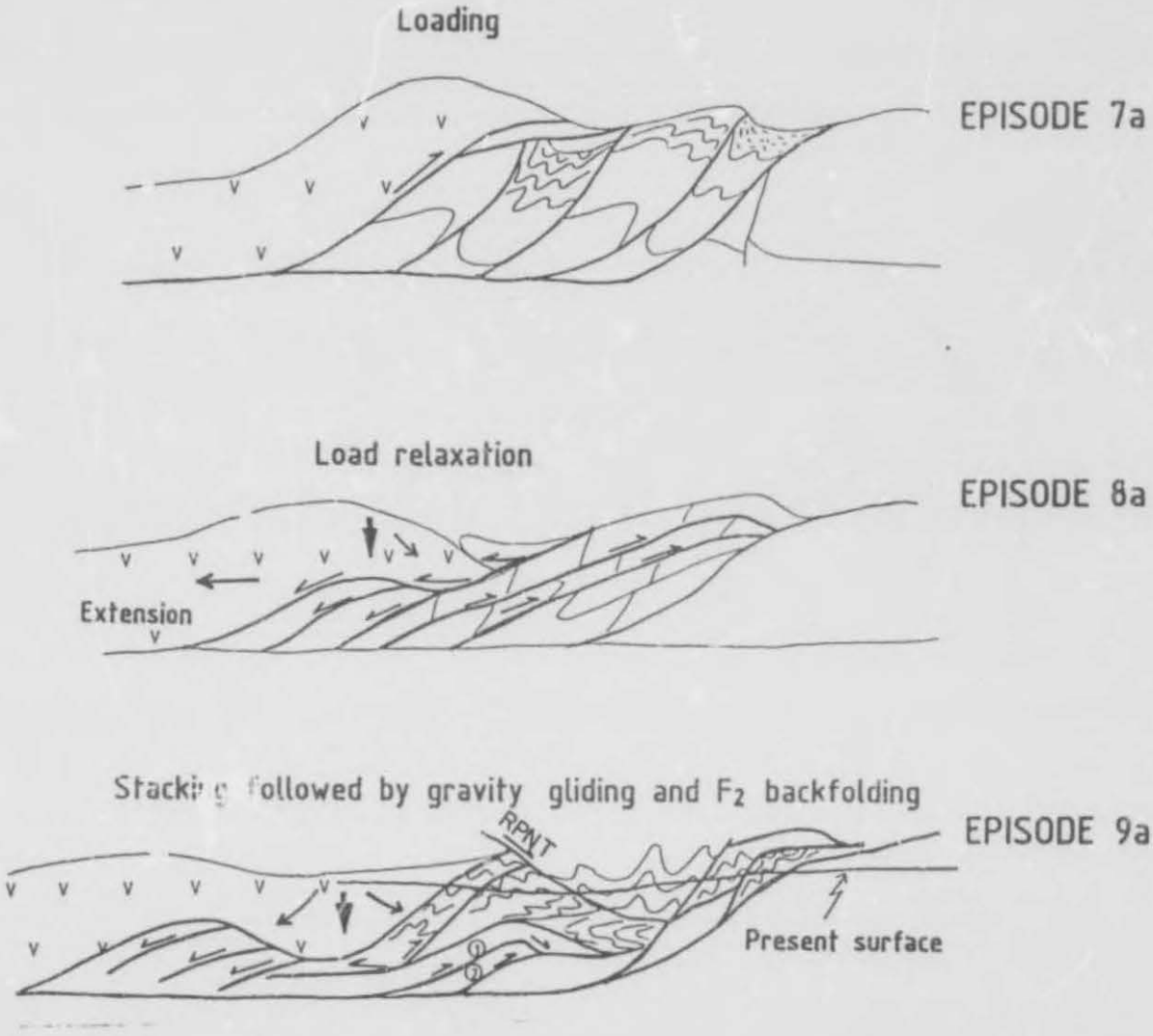

Fig. 75 The tectonogenesis of the Gariep Belt. The second possible deformation path is outlined in episodes 7a, 8a and 9a.

Following episode 6, there is assumed to have been a much farther eastward obduction of the oceanic crustal slab.

ii) Episode 8a

Relaxation occurs after loading according to the visco-elastic flexural model of Quinlan and Beaumont (1984). The

tectonite extends horizontally away from the craton, but new foreland directed thrusts develop, slicing the 4 blocks.

Some gravitative back folding and thrusting takes place near the top of the column. Underthrusting develops to the west below the load.

iii) Episode 9a

Gravitational collapsing of the cover below the load. An antiformal stack (or a multiple ramp) develops on the foreland side of the collapse structure and steepened foreland directed upthrusts (the Gumchavib, Obib Waterhole and Valley Thrusts) occur overriding the antiformal stack.

Gravitative gliding towards the foreland develops the RPNT, the sharp Rosh Pinah anticlinorium, the eastern synclinoria and backfolds (F_2). Steep thrusts slice some of these structures.

The Annisfontein anticlinorium is distinctly developed and has F_1 recumbents and F_2 backfolds. The Pickelhaube Duplex is not shown but it is possible to visualise.

The major problem with path 2 is that the model will not develop enough shortening to produce the antiformal stack (or the multiple ramp) as well as the steep thrusts closer to the craton together with the gravitational slide on the RPNT. It is also difficult to visualise how an F_3 can develop west of the RPNT in such a model where the steep thrusts close to the craton are decoupled from the RPNT, which has mainly a gravitational origin.

c) **PATH 3 (Fig. 76)**

i) Episode 8b

After episode 7 the first ramp occurs above the sole. Block one thrusts over block two but the displacement is much less than in model 8. Note that the obduction pile is not as thick as in 8.

ii) Episode 9b

A second ramp develops in foreland propagating fashion (i.e. in sequence - Fig. 68). Again the displacement is taken to be small relative to the spacing of the two ramps. All the various lithologies are shown.

iii) Episode 10

After some backthrusting and F_2 backfolding, an erosion surface exposing the Witputs strata close to the craton reveals granites close to surface on both sides of a possible Annisfontein anticlinorium which, however, is not in the correct position relative to other structures.

The Pickelhaube Duplex Structure is not a gravitational feature but part of the D_1 phase deformed by backfolding. Steepened thrusts near the craton have been flattened above the backthrust. Backfolding is possible here. A deeper erosion profile exposes too much granite near the surface, but this is very much a consequence of the assumptions made initially in episode 4 where overschematization fouls the picture.

11.3 A FINAL MODEL ?

The above exercise shows that various possibilities exist. In general too many unknowns occur to be able to reconstruct a balanced cross section for such a complicated tectonite with three partly non-colinear phases of deformation and compression across, as well as slip along, oblique ramps.

A model combining overfolding and thrusting with obduction, relaxation and renewed compression in that order to develop an antiformal stack (or multiple ramp) above the sole is probably the best one. The obliquity of the transport direction (migration direction) to the cratonic margin accounts for the varying pitch of stretches and different slip directions along craton ramps as well as for variation in the direction and plunge of F_3 folds.

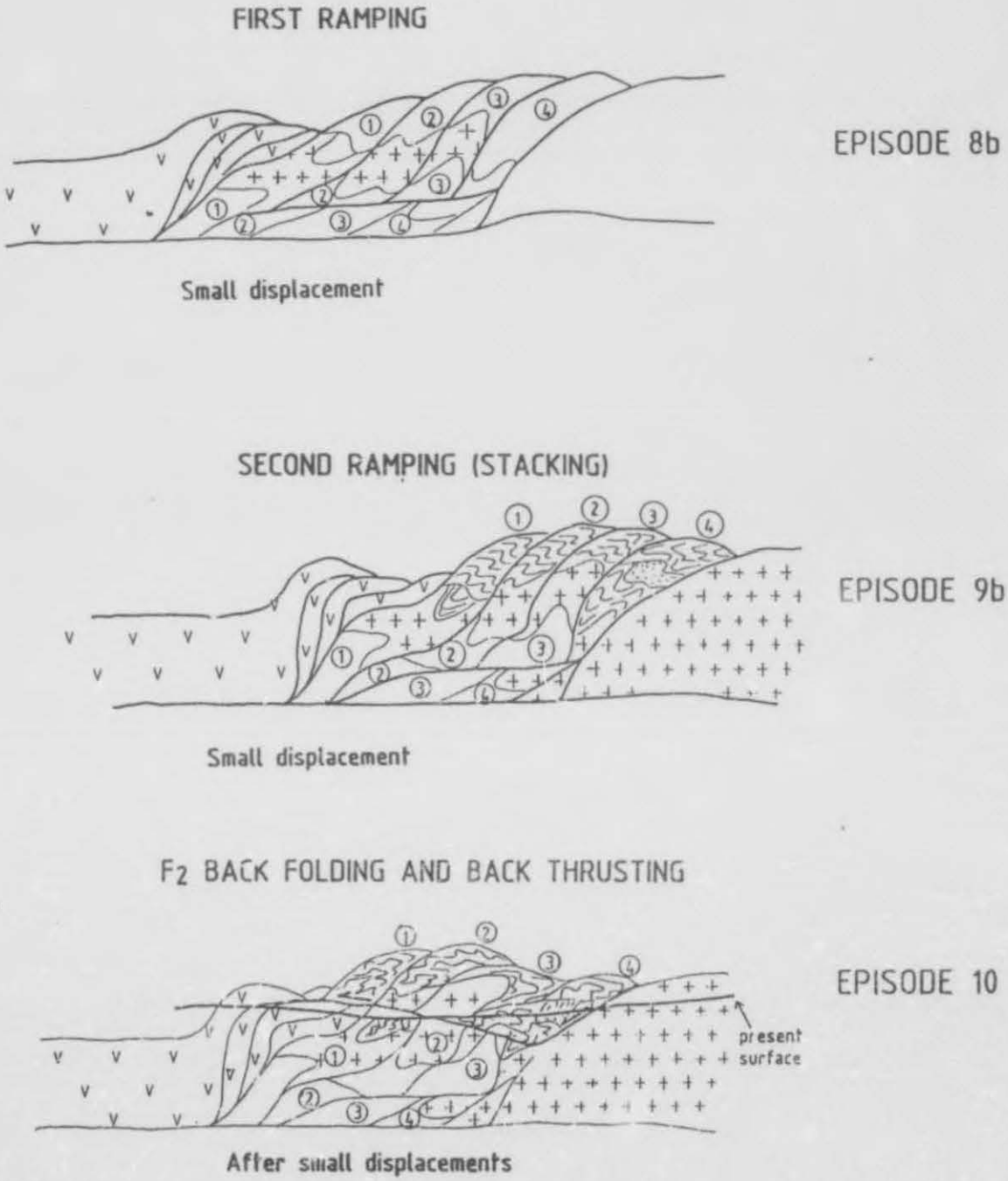

Fig. 76 The tectonogenesis of the Gariep Belt. A third possible deformation path is outlined in episodes 8b, 9b and 10.

The RPNT probably has a complex history which is closely associated with the origin of the Rosh Pinah anticlinorium and the Sendelingsdrif synclinorium. Gravity gliding of sediments towards the foreland followed by hinterland directed backfolding are feasible. Compressional backthrusts of F_2 age are indeed found in the field (Annexure 4) to affect the Pickelhaube Duplex Structure.

12. ACKNOWLEDGEMENTS

I wish to acknowledge my gratitude to the following persons and institutions for help during the project:

The Board of Imcor Zinc for permission to undertake the study and for some financial aid.

Dr H.J. Lüthy for help and encouragement.

My supervisor, Prof I.W. Hälbich for his guidance and encouragement during the duration of the project.

The geological staff of the Rosh Pinah Mine and especially to Mr R.P. Randel for help with proofreading the script. Dr C. Stowe of the Precambrian Research Unit kindly provided the computer program used in conducting the fabric analysis.

The thin sections were prepared by Iscor staff and Mr Donald Hendrikse of the University of Stellenbosch, while Mrs L. Hatton helped with draughting. Mrs C.P. Visser of Iscor supplied the photo of the biotite twin.

My wife Marthina and children are thanked for love and support under often difficult circumstances.

Finally but above all I wish to thank my Maker.

13. REFERENCES

Ahrendt, H., Hunziker, J.C., and Weber, K. (1978). Age and degree of metamorphism and time of nappe emplacement along the southern margin of the Damara Orogen/Namibia (SW Africa). *Geol. Rdsch.*, **67**, 719-742.

Allsopp, H.L., Köstlin, E.O., Welke, H.J., Burger, A.J., Kröner, A., and Blignault, H.J. (1979). Rb-Sr and U-Pb geochronology of Late Precambrian/Early Paleozoic igneous activity in the Richtersveld (South Africa) and southern South West Africa. *Trans. geol. Soc. S. Afr.*, **82**, 185-204.

Arguden, A.T. and Rudolfo, K.S. (1986). Sedimentary facies and tectonic implications of lower Mesozoic alluvial-fan conglomerates of the Newark basin, northeastern United States. *Sediment Geol.*, **51**, 97-118.

Beetz, W. (1926). Die Konkip- und Namaformation. *In: Kaiser, E.* (Ed.) *Die Diamantenwuste Sudwest-Afrikas*. D. Reimer Verlag, Berlin, 92-122.

Bertrand, J.M. (1976). Granitoids and deformation sequence in the Goodhouse-Henkries area. A new interpretation of the relationship between rocks in the Vioolsdrif-Goodhouse area and the Namaqualand and Bushmanland gneisses. *A. Rep. Precambr. Res. Unit, Univ. Cape Town*, **13**, 61-71.

Bjornerud, M. (1989). Towards a unified conceptual framework for shear-sense indicators. *J. Struct. Geol.*, **11**, 1045-1049.

Blignault, H.J. (1974). Aspects of the Richtersveld Province: *In: Kröner, A. (Ed) Contribution to the Precambrian geology of southern Africa*. Bull. Precambr. Res. Unit, Univ. Cape Town, **15**, 49-56.

Blignault, H.J. (1977). Structural-metamorphic imprint on part of the Namaqua Mobile Belt in South West Africa. *Bull. Precambr. Res. Unit, Univ. Cape Town*, **23**, 197pp.

Bryant, B., and Read, J.C. (jnr.) (1969). Significance of lineations and minor folds near major thrust faults in the

southern Appalachians and the British and Norwegian Caledonides. *Geol. Mag. Vol.*, **106**, No. 5, 412-429.

Booth, P.W.K. (1987). The relationship between the Richtersveld and Bushmanland Subprovince in the Namaqualand coastal belt. In: Hartnady, C.J.H. (Ed.) Proceedings and Abstracts of the Alex. L. Du Toit Golden Jubilee Conference on Tectonostratigraphic Terrane Analysis. *Precambr. Res. Unit, Univ. Cape Town,* 34-35.

Boyer, S.E. (1986). Styles of folding within thrust sheets: examples from the Appalachian and Rocky Mountains of the U.S.A. and Canada. *J. Struct. Geol.*, **8**, 325-340.

Borraidaile, G.J. (1984). Strain analysis of passive elliptical markers: success of de-straining methods. *J. Struct. Geol.*, **6**, 433-437.

Cahen,l., Snelling, N.J., Delhal, J., Vail, J.R., Bonhomme , and Ledent, D., (1984). *The geochronology and evolution of Africa*. Clarendon Press. Oxford, 512pp.

Clifford, T.N. (1967). The Damaran episode in the Upper Proterozoic/Lower Paleozoic structural history of Southern Africa. *Spec. Pap. geol. Soc. Am.*, **92**, 100pp.

Davies, C., and Coward, M.P. (1982). The structural evolution of the Gariep Arc in Southern Namibia. *Precambr. Res.*, **17**, 173-198.

De Villiers, J. (1968). *Ann. Rep. Precambr. Res. Unit, Univ. Cape Town*, **6**, 36pp.

De Villiers, J., and Söhnge, P.G. (1959). The geology of the Richtersveld. *Mem. geol. Surv. Dep. Min. S. Afr.*, **48**, 295pp.

Downing, K.N., and Coward, M.P. (1981). The Okahandja lineament and its significance in Damaran tectonics in Namibia. Geol. Rdsch., **70**, 972-1000.

Eisenbacher, G.H. (1970). Deformation mechanism of mylonitic rocks and fractured granites in Cobequid Mountains, Nova Scotia, Canada. *Geol. Soc. Am. Bull.*, **81**, 2009-2020.

Etheridge, M.A., and Hobbs, B.E. (1974). Chemical and deformational controls on recrystallization of micas. *Contr. Mineral trol.*, **43**, 111-124.

Frankland, H. (1975). *Structure of the Rosh Pinah mine area. Unpublished data.* Imcor Zinc Pty (Ltd), 4pp.

Frimmel, H.E., and Hartnady, C.J.H. (1992). The significance of blue amphiboles for the metamorphic history of the Pan-African Gariep Belt, Namibia. *Inf. Circ. Precambr. Res. Unit, Univ. Cape Town,* **5**, 27pp.

Germs, G.J.B. (1972). The stratigraphy and paleontology of the lower Nama Group, South West Africa. *Bull. Precambr. Res. Unit, Univ. Cape Town*, **12**, 250pp.

Germs, G.J.B. (1974). The Nama Group in South West Africa and its relationship to the Pan-African geosyncline. *J. Geol.*, **82**, 301-307.

Germs, G.J.B. (1983). Implication of a sedimentary facies and depositional environment analysis of the Nama Group in South West Africa/Namibia. In: *Miller, R. Mcg. (Ed.) Evolution of the Damara orogen, South West Africa/Namibia.* Spec. Publ.. geol. Soc. S. Afr., **11**, 409 - 429.

Gresse, P.G. (1993). Strain partitioning in the southern Gariep Arc as reflected by sheath folds and stretching directions. In press. *S. Afr. J. Geol.*

Hälbich, I.W. (1971). *Verslag oor strukturele kartering in die onmiddelike omgewing van Rosh Pinah Myn.* Summ. of Unpubl. B.Sc. (Hons.) projects. Univ. Stellenbosch, 4pp.

Hälbich, I.W. (1972). *Rosh Pinah myn. 1:1000 kartering.* Summ. of Unpubl. BSc. (Hons.) projects. Univ. Stellenbosch, 6pp.

Hälbich, I.W. (1973). *1:1000 kartering.* Summ. of Unpubl. B.Sc. (Hons) projects. Univ. Stellenbosch, 4pp.

Hälbich, I.W., Gresse, P.G., Freyer, E.E., and Horstmann, U. (1987). Evidence for oblique southward subduction along the west coast of Southern Africa in Pan-African times. In: *Hartnady, C.J.H. (Ed.) Proceedings and Abstracts of the Alex. L. Du Toit Golden Jubilee Conference on Tectonostratigraphic Terrane Analysis.* Precambr. Res. Unit, Univ. Cape Town, 36pp.

Hartmann, O., Hoffer, E., and Haack, U. (1983). Regional metamorphism in the Damara orogen: Interaction of crustal motion and heat transfer. *Spec. Publ. geol. Soc. S. Afr.*, 11, 233-241.

Hartnady, C.J.H., Joubert, P., and Stowe, C.W. (1985). Proterozoic crustal evolution in southwestern Africa. *Episodes*, 8, 234-244.

Haughton, S.H. (1961). Discussion of "The Gariep System" by J.de Villiers. *Publ.C.C.T.A.* 80,89.

Haughton, S.H. (1963). *Stratigraphic history of Africa south of the Sahara.* Oliver and Boyd, Edinburgh, 365pp.

Henry, G., Stanistreet, I.G., and Maiden, K.J. (1986). Preliminary results of a sedimentological study of the Chuos Formation in the Central Zone of the Damara Orogen: evidence for mass flow processes and glacial activity. *Comm. geol. Surv. S.W.A./Namibia*, 2, 75-92.

Hodgson, I., Knight, J., Martin, R. (1972). *Report to accompany map of an area north of Rosh Pinah, S.W.A.* Unpubl. B.Sc. (Hons) project. Univ. Cape Town, 14pp.

Hoffmann, K.H. (1983). Lithostratigraphy and facies of the Swakop Group of the Southern Damara Belt. S.W.A./Namibia. In: *Miller, R. Mcg. (Ed.) Evolution of the Damara orogen, South West Africa/Namibia*. Spec. Publ. geol. Soc. S. Afr., **11**, 09 409 - 429.

Hoffmann, K.H. (1972). *Geological report on an area north-east of Rosh Pinah in South West Africa*. Unpubl. B.Sc. (Hons.) project. Univ. Cape Town, 26pp.

Hoffmann, K.H. (1989). New aspects of lithostratigraphic subdivision and correlation of late Proterozoic to early Cambrian rocks of the southern Damara Belt and their correlation with the central and northern Damara Belt and Gariep Belt. *Communs. geol. Surv. Namibia*, **5**, 59-67.

Horstmann, U.E. (1987). Die metamorphische Entwickelung im Damara Orogen, Sudwest Afrika/Namibia, abgeleitet aus K/Ar Datierungen an detritischen Hellglimmern aus Molassesedimenten der Nama Group. *Gottinger Arb. Geol. Paleont.*, **32**, 78-86.

I'ons, M.I., and Light, M.P.R. (1971). *A geological report on a small area in the Kapok east of Rosh Pinah*. Unpubl. B.Sc. (Hons) project, Univ. Cape Town, 15pp.

Joubert,P., and Kroner, A., 1972. The Stinkfontein Formation south of the Richtersveld. *Trans. geol. Soc. S. Afr.*, **75**, 47-54.

Kennedy, W.Q. (1964). The structural differentiation of Africa in the Pan -African (+ 500 m.j.) tectonic episode. 8th *Ann. Rep. Research Inst. African Geol., Univ. Leeds*, **48-49**

Köppel, V. (1987). Lead-isotope studies of stratiform deposits of the Namaqualand, N.W. Cape Province, South

Africa, and their implication on the age of the Bushmanland Sequence. *Proc. Fifth I.A.G.O.D. Symp.*, **1**, 195-207.

Kröner (1972). Preliminary resume of the geology of the Gariep geosyncline in the Orange River area. *In*: De Villiers, J. (Ed.) *A. Rep. Precambr. Res. Unit, Univ. Cape Town*, **7-9**, 51-57.

Kröner, A. (1974). The Gariep Group, Part 1: Late Precambrian formations in the western Richtersveld, northern Cape Province. *Bull. Precambr. Res. Unit, Univ. Cape Town*, **13**, 115pp.

Kröner, A. (1975). Late Precambrian formations in the western Richtersveld, northern Cape Province. *Trans. R. Soc. S. Afr.*, **41**, 375-433.

Kröner, A. (1977a). Non-synchroneity of late Precambrian glaciation in Africa. *J. Geol.*, **85**, 289-300.

Kröner, A. (1977). The Sinclair aulacogen as a late Proterozoic volcano-sedimentary association along the Namib desert of southern Namibia. *Abstr. Colloq. Afr. Geol. Göttingen*, **9**, 83pp.

Kröner, A. (1982). Rb-Sr geochronology and tectonic evolution of the Pan-African Damara Belt of Namibia, Southwestern Africa. *Am. J. Sci.*, **282**, 1471-1507.

Kröner, A., and Blignault, H.S. (1976). Towards a definition of some tectonic and igneous provinces in western South Africa and southern South West Africa. *Trans. geol. Soc. S. Afr.*, **79**, 232-238.

Kröner, A., and Germs, G.J.B. (1971). A re-interpretation of the Numees/Nama contact at Aussenkjer, South West Africa. *Trans. geol. Soc. S. Afr.*, **74**, 69-74.

Kröner, A., and Hawkesworth, C.J. (1977). Late Pan-African emplacement ages for Rössing alaskite granite (Damara Belt) and Rooi Lepel bostonite (Gariep Belt) in Namibia and their

significance for the timing of metamorphic events. *A. Rep. res. Inst. Afr. Geol., Univ. Leeds*, **20**, 14-17.

Kröner, A., and Jackson, M.P.A. (1974). Geological reconnaissance of the coast between Luderitz and Marble point, South West Africa. *Bull. Precambr. Res. Unit, Univ. Cape Town*, **15**, 79-103.

Kroner, A., McWilliams, M.O., Germs, G.J.B., Reid, A.B. and Schalk, K.E.L. (1980). Paleomagnetism of late -Precambrian mixtite-bearing formations. Am. J. Sci., 280, 942-968.

Kröner, A., and Rankama, R. (1972). Late Precambrian sedimentary rocks in southern Africa: A compilation with definitions and correlations. *Bull. Precambr. Res. Unit, Univ. Cape Town*, **11**, 37pp.

Kröner, A., and Welin, E. (1973). Evidence for a +500my old thermal episode in southern South West Africa. *Earth Planet Sci. Lett.*, **21**, 149-152.

Lisle, R.J. (1977). Estimation of the tectonic strain ratio from the mean shape of deformed elliptical markers. *Geologie Mynb.*, **56**, 140-144.

Lisle, R.J. (1979). Strain analysis using deformed pebbles: The influence of initial pebble shape. *Tectonophysics*, **60**, 263-277.

Lisle, R.J. (1985). *Geological strain analysis: A manual for the R_f/θ method*. Pergamon Press, 99pp.

Lindström, M. (1961). Beziehungen zwischen Klein faltenuergenzen und Gefügemerkmalen in den Kaledoniden Skandinaviens. *Geol. Rdsch.*, **51**, 144-180.

Martin, H. (1965). The Precambrian geology of South West Africa and Namaqualand. *Precambr. Res. Unit, Univ. Cape Town*, **15**, 153-165.

McMillan, M.D. (1968). The geology of the Witputs-Sendelingsdrif area. *Bull. Precambr. Res. Unit, Univ. Cape Town*, **4**, 177pp.

Minnit, R.C.A. (1992). Trace-element models for the evolution of the Vioolsdrif Suite, Richtersveld Province, Southern Namibia. *Econ. Geol. Res. Unit. Inf. Circ.* No. **246**. 24pp.

Middlemost, E.A.K. (1964). Petrology of the plutonic and dyke rocks of the south-eastern Richtersveld. *Trans. geol. Soc. S. Afr.*, **67**, 227-261.

Middlemost, E.A.K. (1966). The genesis of the Stinkfontein Formation. *Trans. geol. Soc. S. Afr.*, **69**, 87-98.

Nicholayson,L.A., and Burger, A.J. (1965). Note on an extensive zone of 1000 million-year old metamorphic and igneous rocks in southern Africa. *Sci. de La Terre*, **10**, 497-516.

Onstott, T.C., Hargraves, R.B., and Reid, D.L. (1986). Constraints on the tectonic evolution of the Namaqua Province 111: paleomagnetic and Ar^{40}/Ar^{39} results from the Gannakouriep dyke swarm. *Trans. geol. Soc. S. Afr.*, **89**, 171-183.

Page, D.C., and Kindl, S. (1978). *The Zinc-Lead-Copper deposits of the Rosh Pinah Mine, South West Africa*. Unpubl. Rep., Imcor Zinc (Pty) Ltd., Rosh Pinah, 17pp.

Page, D.C., and Watson, M.D. (1976). The Pb-Zn deposit of Rosh Pinah Mine, South West Africa. *Econ. Geol.*, **71**, 306-327.

Park, R.G. (1989). *Foundations of Structural geology* 2nd ed. Blackie; Glasgow and London, 148pp.

Pickering, K.T. (1987). Wet-sediment deformation in the Leamington Formation. In: *Jones, M.E. and Preston, R.M.F. (Ed.) Deformation of Sediments and Sedimentary rocks*. Geol. Soc. Spec. Publ. No 29. Blackwell Scientific Publications, London, 350pp.

Quinlan, G.M., and Beaumont, C. (1984). Appalachian thrusting, lithospheric flexure, and the Paleozoic stratigraphy of the eastern interior of northern America: *Can. J. Earth Sci.*, **21**, 973-996.

Ramsay, J.G. (1967). *Folding and Fracturing of Rocks.* McGraw-hill, New York, 568pp.

Ramsay, J. G., and Huber, M.I. (1983). *The Techniques of modern Structural Geology. Vol. 1: Strain Analysis.* Academic Press, London, 307pp.

Reid, D.L. (1974). Preliminary report on petrologic studies of volcanic and intrusive rocks in the Vioolsdrif region, lower Orange River. In: *Kröner, A. (Ed.) Contributions to the Precambrian geology of Southern Africa.* 1. Precambrian Res. Unit, Univ. Cape Town, **15**, 57-68.

Reid, D.l. (1977). Geochemistry of Precambrian igneous rocks in the Lower Orange River Region. *Bull. Precambr. Res. Unit, Univ. Cape Town*, **22**, 397pp.

Reid, D.L. (1979). Age relationships within the Mid-Proterozoic Vioolsdrif batholith, lower Orange River Region. *Trans. geol. Soc. S. Afr.*, 82, 305-311.

Reid, D.L. (1982). Age relationships within the Vioolsdrif batholith, lower Orange River region II. A two stage emplacement history and the extent of Kibaran overprinting. *Trans. geol. Soc. S. Afr.*, **85**, 105-110.

Reid, D.L., Ransome, I.G.D., Onstott, T.C. and Adams, C.J. (1991). Time of emplacement and metamorphism of Late Precambrian mafic dykes associated with the Pan-African Gariep orogeny, Southern Africa: implications for the age of the Nama Group. *Journal of African Earth sciences*, **13**, 531-541.

Ritter, U. (1978). The southwestern Richtersveld between Eksteenfontein and Klein Helskloof, its relationship to Gariep metamorphism and tectonism and to the Namaqua

Metamorphic Complex. *A. Rep. Precambr. Res. Unit, Univ. Cape Town*, 14-15.

Ritter, U. (1980). The Precambrian evolution of the Eastern Richtersveld. *Bull. Precambr. Res. Unit, Univ. Cape Town*, **26**, 276pp.

Rogers, A.W. (1915). The geology of part of Namaqualand. *Trans. geol. Soc. S. Afr.*, **18**, 72-101.

Sassi, F.P., and Scolari, A. (1974). The b_o value of the potassic white micas as a barometric indicator in low grade metamorphism of pelitic schist. *Contr. Miner. Petrol.*, 45, 143-152.

Shack Pedersen, S.A. (1987). Studies of gravity tectonics In: *Jones, M.E. and Preston, R.M.F. (Ed.) Deformation of Sediments and Sedimentary rocks*. Geol. Soc. Spec. Publ. No 29. Blackwell Scientific Publications, London, 350pp.

Shimron, A.E. (1987). Proterozoic orogenesis and crustal evolution in the Richtersveld Subprovince. *A. Rep. Precambr. Res. Unit, Univ. Cape Town*, **21-23**, 58-66.

Siegfried, P.R. (1990). *Aspects of the geology of the Mountain orebody, Rosh Pinah mine, Namibia*. Unpubl. Msc. thesis , Univ. Cape Town. 130pp.

Stannistreet, I.G., Kukla, P.A., and Henry, G. (1991). Sedimentary basinal responses to a late Precambrian Wilson Cycle: The Damara Orogen and Nama Foreland, Namibia. Jnl. of African Earth Sci.,**13**, 141-156

Stowe, C.W. (1988). A pascal program for plotting and rotating stereographic projections. *S. Afr. J. Sci.*, **91**, 527-542.

Stowe, C.W., Hartnady, C.J., and Joubert, P. (1984). Proterozoic tectonic provinces of Southern Africa. (Abs). *Precambr. Res.*, **25**, 229-231.

South African Committee for Stratigraphy (SACS), 1980. The Gariep Complex. *In: Kent, L.E. (Comp) Stratigraphy of Southern Africa. 1. Lithostratigraphy of the republic of South Africa, South West Africa/Namibia, and the Republics of Bophuthatswana, Transkei and Venda. Handb. geol. Surv. Dep. Min. S. Afr.*, **8**, 690pp.

Söhnge, P.G., and De Villiers, J. (1948). The Kuboos pluton and its associated line of intrusives. *Trans. geol. Soc. S. Afr.*, **51**, 1-31.

Spry, A. (1969). *Metamorphic Textures*. Pergammon Press. Oxford, London, New York. 350p.

Spry, A. (1963). The origin and significance of snowball structure in garnets. *J. Petrol.*, **4**, 211-222.

Tankard, A.J., Eriksson, K.A., Hobday, D.K., Hunter, D.R., Minter, W.E.L. (1982). *Crustal evolution of Southern Africa*. Springer Verlag, New York, 480pp.

Theart, H.F.J. (1980). The geology of the Precambrian terrane in parts of western Namaqualand. *Bull. Precambr. Res. Unit, Univ. Cape Town*, **30**, 103pp.

Turner,F.J., and Weiss, L.E. (1963). *Structural analysis of metamorphic tectonites*. Mcgraw-Hill, New York, 545pp.

Van Biljon, S. (1939). The Kuboos batholith in Namaqualand, South Africa. *Trans. geol. Soc. S. Afr.*, **42**, 123-219.

Van Vuuren, C.J.J. (1986). Regional setting and structure of the Rosh Pinah Zinc-Lead deposit, South West Africa/Namibia. *In: Anhaeusser, C.R., and Maske, S. (Eds.) Mineral Deposits of Southern Africa Vol II. Geol. Soc. S. Afr.*, 1593-1607.

Visser, C.P. (1993). *'n Mineralogiese ondersoek op gesteente monsters vanaf die Rosh Pinah omgewing*. Ongepubl. Verslag., Navorsing en ontwikkeling, Analitiese dienste, Mineralogie, YSKOR, Pretoria, 8 pp.

Von Veh, M.W. (1988). *The stratigraphy and structural evolution of the Late Proterozoic Gariep Belt in the Sendelingsdrif-Annisfontein area, north-western Cape Province*. Ph.D. thesis (unpubl.), Univ. Cape Town, 174pp.

Watson, M.D. (1980). *The geology, mineralogy and origin of the Zinc-Lead-Copper deposit at Rosh Pinah, South West Africa*. Unpubl. Ph.D. thesis, Univ. Pretoria, 250 pp.

Welke, H.J., Burger, A.J., Corner, B., Kröner, A., and Blignault, H.J. (1979). U-Pb and Rb-Sr age determinations on middle Proterozoic rocks from the Lower Orange River area, South West Africa. *Trans. geol. Soc. S. Afr.*, **82**, 205-214.

Winkler, H.G.F. (1976). *Petrogenesis of metamorphic rocks* (Fourth edition). Springer-Verlag. New York, Heidelberg, Berlin, 334pp.

Whitten, E.H.T. (1966). *Structural geology of folded rocks*. Rand McNally, Chicago, 663pp.

Young, G.M. (1982). The late Proterozoic Tindir Group, east-central Alaska - Evolution of a continental margin. *Bull. geol. Soc. Am.*, **93**, 759-783.

APPENDIX

1. FINITE STRAIN ANALYSIS

1.1. Introduction to techniques used

One of the objects of this study has been to quantify the pervasive finite strain of the area. To achieve this the magnitudes and orientations of the three principal axes of the strain ellipsoid had to be established.

Three basic methods have been devised to quantify strain and are described by Park (1989):

a) individual strain ellipsoids can be measured using various "strain markers" and an average result obtained

b) total shortening or elongation is estimated by scanning the geometry of folds or faults

c) a regional homogeneous strain is assumed and it is inferred that the statistical arrangements of all planar and linear structural elements throughout the area reflect both the orientation as well as size of the bulk finite strain axes.

The principal strain axes of the strain ellipsoid (Fig. 1) can be located if the rock possesses a new planar or linear fabric which reflects the finite strain geometry. A planar flattening fabric (slaty cleavage, schistosity or gneissosity) will lie in the XY plane of the strain ellipsoid, enabling the Z strain axis to be found. If a "stretching direction" (i.e. an elongation lineation) is present the orientation of the X-axis can also be obtained.

Strain data measurements have been obtained by measuring initially spherical objects, but certain reservations as summed up by Park (1989), have to be taken into account:

1) a more sophisticated technique has to be employed if a non-random variation in initial shape is suspected, e.g. controlled by bedding

2) the degree of homogeneity of strain has to be taken into account

3) Strain markers may have different competencies than their matrix.

Measurements may be made directly in the field, or from thin sections, polished slabs or on enlarged photographs.

The lengths of the long axes are plotted against the lengths of the short axes on graphs, and the slope of the best-fit straight line through the origin gives the mean value of the strain ratio Y'/X', in that plane (Fig. 2).

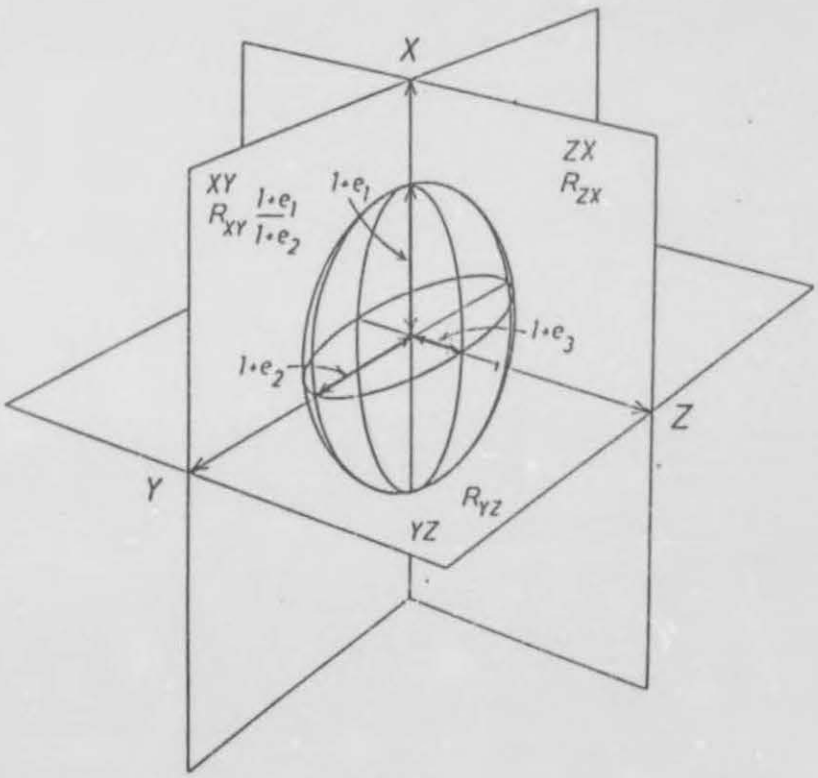

Fig. 1 *The strain ellipsoid (after Ramsay and Huber, 1983). Principal strains are given by e^1, e^2, and e^3, principal strain directions by X, Y, and Z, and the principal planes by XY, YZ, and XZ. The principal plain strain ratios are given by RXY, RYZ and RZX.*

If there is a large difference in ductility between the measured objects and the matrix, the measured strain will not apply to the whole rock, as in the case of the Wallekraal conglomerates, where quartz and quartzite pebbles are located within a sandstone or mudstone matrix. Much higher strain would occur in the matrix as compared to the pebbles.

The centre to centre method avoids this problem. It relies on the fact that originally randomly arranged spheres are

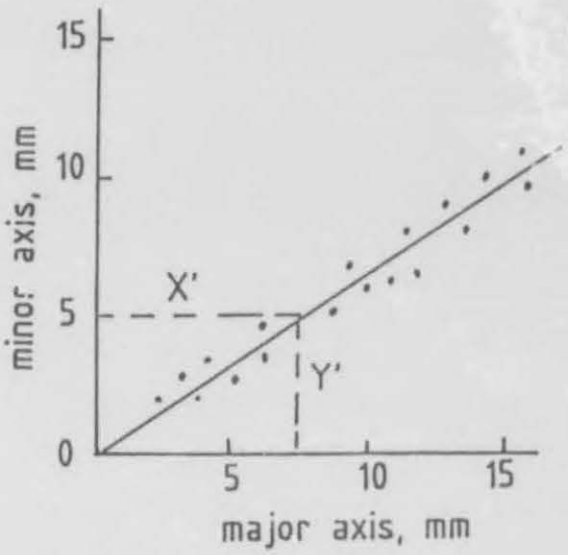

Fig. 2 *A graph to illustrate the method to determine the principal strain ratio in two dimensions from deformed circular objects. The slope of the line gives the Y'/X' (after Ramsay and Huber, 1983).*

systematically altered during strain in such a way that the changes are related to the distance between them. The ratio between the minimum and maximum mean distances is equal to the strain ratio Y'/X'.

To determine the ratio, a plot is made of the distances between adjacent centres against the orientation of the line between the centres. An $m_1 + m_2$ value (minimum and maximum mean distance) is obtained for the distance, which is subsequently used to calculate the strain ratio and two

corresponding values of α (αy + αx) for the orientation of Y′ and X′ (Fig. 3).

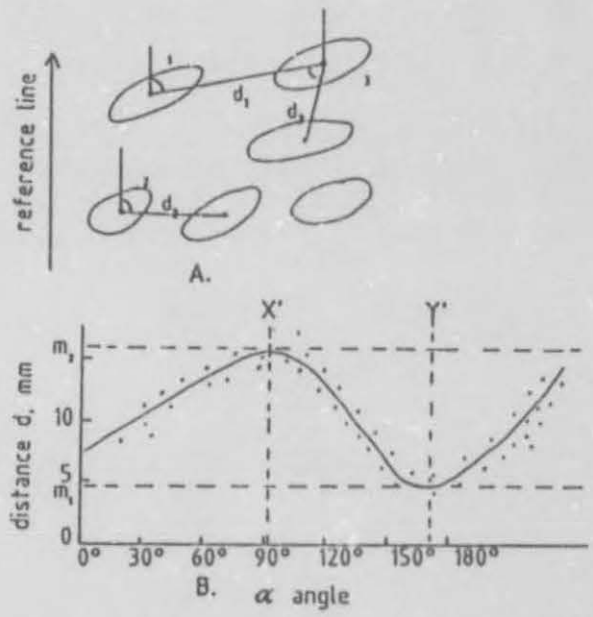

Fig. 3 *Determining the principal strain ratio in two dimensions by using the centre to centre method:*
A. measurements of distances and angles between adjacent centres
B. Plots of d and α to determine X′ and Y′.
Sketch after Park (1989) Fig 8.2

The centre to centre method can be applied to any rock with randomly distributed particles as the respective ductilities play no role. The method is however, only applicable if the particles are matrix supported and the distribution of pebbles not too heterogeneous. However, it is not an easy task to accurately determine the centres of the particles.

Deformed clasts within the Numees Sequence were measured in several areas to obtain a large number of approximate results rather than measure a single pebble bed that may be atypical for the area. The use of pebbles rests on the assumption that they originally possessed an elliptical shape, and the final shape which is measured is a compromise between two ellipses with regard to both direction and axial ratio.

1.2. Strain measurements using elliptical deformed objects (The R_f/θ technique)

Ramsay (1967 p. 202-211) has indicated that a set of elliptical markers with identical initial eccentricity but variable orientation will show a characteristic pattern if their deformed axial ratios (R_f) and orientations (θ) are plotted graphically. This method has become known as the R_f/θ technique and allows the effects of the initial shape of the markers to be distinguished from those due to tectonic strain.

Lisle (1977) describes a method to define a theta curve on the R_f/θ diagram. With varying initial orientations a whole set of theta-curves are produced which radiate from the point ($\theta=0$, $R_f=R_s$). They are drawn by substituting the appropriate values of R_s and θ into the equation.

When the family of θ and R_i curves are plotted together, they form a net on the R_f/θ diagram. Lisle (1985) has compiled a range of such marker deformation nets, which if placed on a R_f/θ data set, allows us to read off the axial ratios and orientations we would obtain by de-straining the rock by an amount corresponding to the R_s value of the grid.

The method makes use of elliptical, sub-elliptical or parallelogram shaped inclusions but caution should be exercised to see that the boundaries have not migrated i.e. significant boundary slip of pebbles has not occurred during metamorphism or pressure solution phenomena are not present. Such pebbles should be avoided.

Measurements have been taken on planar surfaces e.g. joints or bedding planes and their geographical orientation carefully recorded. The R_f value was obtained by measuring the dimensions of the long and short axes of inclusions and the ratio calculated. The θ angles are obtained by measuring the orientation of the long axis with respect to a chosen reference line. These angles will therefore fall in the range $+90^\circ$, to -90° with respect to the reference line.

Markers were carefully inspected to avoid sampling heterogeneously deformed specimens, which are indicated by widely varying long axis orientations. Fifty to eighty readings were collected at one site which, according to experiments, give the best results (Borradaille, 1984).

Measurements on individual markers were then plotted as points on a transparent overlay on a graph of R_f against θ. The data point distributions are then compared to the standard curves of Lisle (1985) and results are evaluated by means of several tests. Results are verified by subjecting them to a number of criteria.

The degree of symmetry of markers is evaluated with the Symmetry Test (Lisle, 1985), as randomly orientated markers will tend to show a symmetrical R_f/θ pattern after straining. The vector mean θ, and the harmonic mean, H are calculated from the following equations:

Vector mean θ or $\theta - = \frac{1}{2}$ arctan $(\{\Sigma \sin 2\theta\}/\{\Sigma \cos 2\theta\})$

Harmonic mean $H = N/(R_{f1}^{-1} + R_{f2}^{-1} + R_{f3}^{-1} \ldots\ldots\ldots R_{fn}^{-1})$

The means are plotted and they divide the graph into four areas labelled A, B, C, D, and the number of points occurring in each area are subsequently counted. A typical plot of data from near Dreigratberg illustrates the distribution of markers (Fig. 4).
The symmetry of the markers can then be established using the following equation:

$$I_{SYM} = 1 - (|n_A - n_B| + |n_C - n_D|)/N$$

where n_A, n_B, n_C, n_D, are the number of points in areas A, B, C, D and N is the total number of data points.

High values of I_{SYM} outline a highly symmetrical pattern of data points while low values may indicate that an initial fabric has been present.

Rs \ Sample Size N	20	35	60	100	200
1.5	0.3 (0.4)	0.51 (0.63)	0.60 (0.67)	0.74 (0.78)	0.82 (0.85)
2.0	0.5 (0.5)	0.63 (0.63)	0.73 (0.77)	0.80 (0.82)	0.86 (0.88)
3.0	0.5 (0.6)	0.63 (0.63)	0.73 (0.77)	0.80 (0.82)	0.87 (0.88)
5.0	0.5 (0.6)	0.63 (0.63)	0.73 (0.77)	0.82 (0.82)	0.87 (0.88)
10.0	0.6 (0.6)	0.63 (0.63)	0.73 (0.77)	0.82 (0.84)	0.87 (0.89)

Table 1 *Critical values of I_{SYM} used in the Symmetry Test (after Lisle, 1985). Values given are the 5% (10%) percentage points of the I_{SYM} distribution.*

Lisle (1985) has established a range of critical values for the test, and if I_{SYM} is lower than the appropriate critical values (Table 1) we can conclude that the markers did not come from an uniform orientation distribution (however, there is a 1 in 20 chance of being wrong).

The symmetry test, however, cannot be used to differentiate between a rock without an initial fabric and one in which the strain has been symmetrically superimposed on an initial fabric. A symmetrical R_f/ϕ plot could be interpreted either way.

The θ distribution Test

If the I_{SYM} test values indicate a symmetric pattern, the data points are compared to the shape of the R_i/θ curves on the standard charts of Lisle (1985). The chart where the θ points are most evenly distributed gives us the strain rate value R_s, which is the best estimate of the strain ratio (Fig. 5).

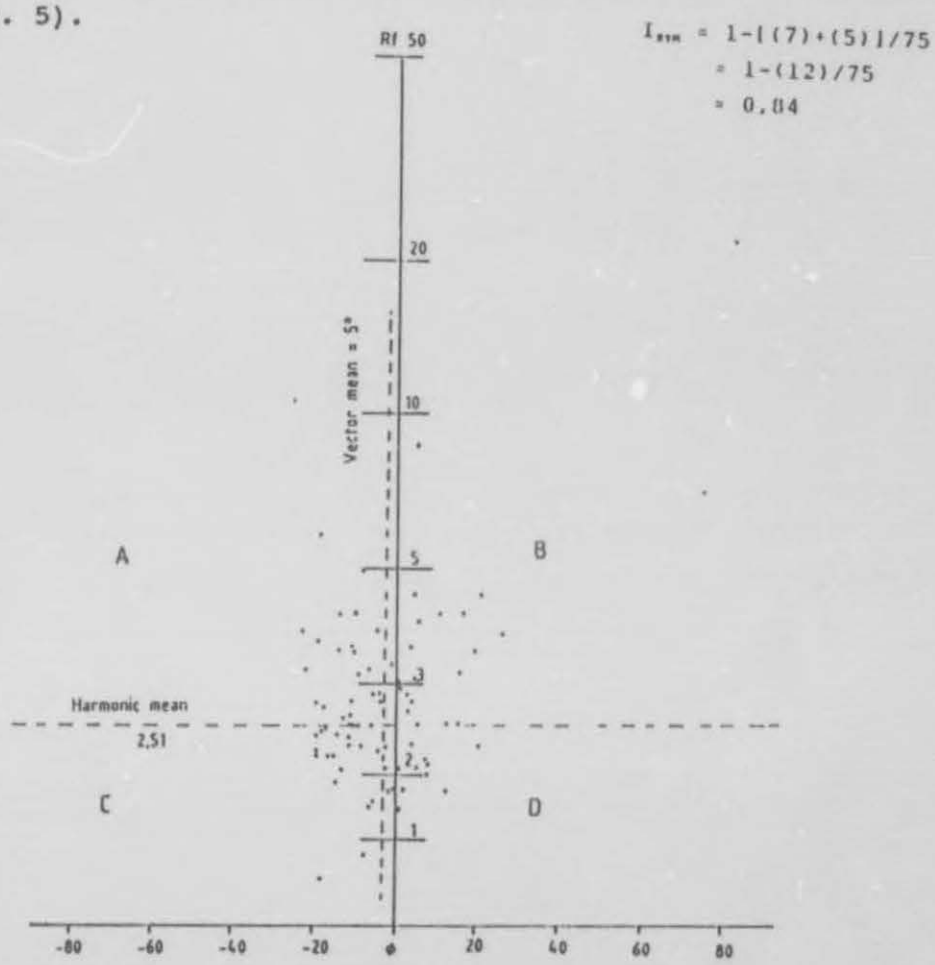

Fig. 4 *A R_f/θ plot of Numees diamictite clasts of an area east of Dreigratberg beacon (Q/19, Annexure 1). The I_{sym} test value indicates a highly symmetrical pattern for originally unorientated clasts.*

The approximate values of the strain ratio can also be established by several other methods, the first of which uses the harmonic mean also used in the symmetry test (Lisle, 1977, and 1979). This value may approximate or slightly overestimate the strain ratio. Fig. 6 (Lisle, 1985) can be used to establish the estimated R_s from the harmonic mean.

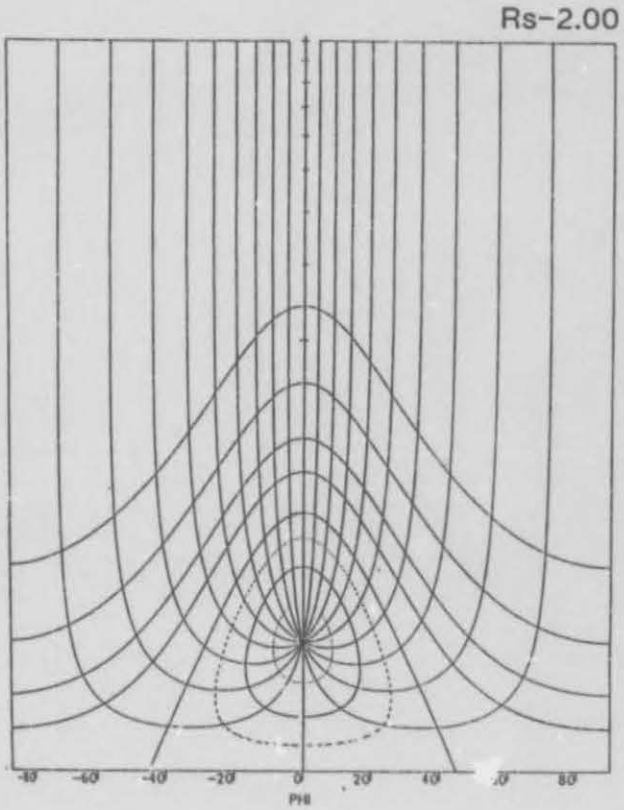

Fig. 5 A standard R_i/θ chart of Lisle (1985).

Further estimates can be made by using the $R_{f\ max}$. and $R_{f\ min}$. values or the orientation and axial ratios of markers with extreme orientations. The statistical X^2 test allows an objective assessment of the goodness of fit to be made. The equation for the test is as follows:

$$X^2 = \{(O-E)^2/E$$

Where O is the observed number of points occupying a cell bounded by two theta curves and E is the number expected in the cell.

The results of these measurements are discussed under 6.9 and 7.7.

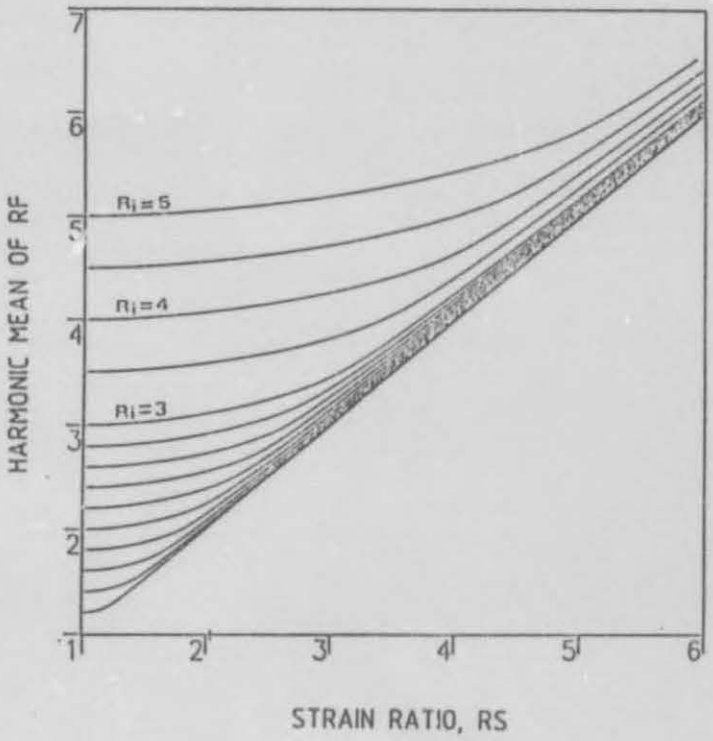

Fig. 6 *A diagram to establish the estimated R_s from the harmonic mean (after Lisle, 1985).*

SHORT DISCRIPTION OF SAMPLES IN THESIS

SAMPLE NO	APPROX. LOCALITY	DESCRIPTION
N 11	1 Km SW of Namuskluft Farmstead	Numees diamictite
N 13	1 Km SW of Namuskluft Farmstead	Numees diamictite
N 14	1 Km SW of Namuskluft Farmstead	Dark sandstone (BIF)
N 16	1 Km SW of Namuskluft Farmstead	Brown grit
NT 2	2 Km NE of Namuskluft Farmstead	Grey-green chlorite schist
NT 5	2 Km NE of Namuskluft Farmstead	Calcareous argillite
NT 6	2 Km NE of Namuskluft Farmstead	Dark-brown carbonate band in black argillite
NT 7	2 Km NE of Namuskluft Farmstead	Dark grey dolomite
NT 9	2 Km NE of Namuskluft Farmstead	Cream-coloured dolomite
NT 10	2 Km NE of Namuskluft	White carbonate
NT 11	1,8 Km NE of Namuskluft Farmstead	Dark-grey dolomite
NT 12	1,8 Km NE of Namuskluft Farmstead	Blue-grey carbonate
NT 17	2 Km SE of Namuskluft	Arkosic grit
NT 19	2 Km SE of Namuskluft Farmstead	Dark-grey to black schist
NT 24	5,5 Km SE of Namuskluft Farmstead	Dark-grey dolomite (brecciated)
NT 39a	Near Orange River	Pisolitic dolomite
NT 39	Dreigratberg	Synsedimentary carbonate breccia
NT 41	Dreigratberg	Quartz-chlorite schist
NT 44	6 Km SE of Namuskluft	Chlorite schist
NT 51	3,5 Km SE of Namuskluft	Cream-coloured carbonate
NT 52	3 Km SE of Namuskluft	Pink dolomitic limestone
NT 53	2,5 Km SE of Namuskluft Farmstead	Light-grey quartzite
NT 55	Orange River	Altered green-grey granodiorite
NT 61	Dreigratberg	Cream-coloured dolomite
NT 62	Dreigratberg	Cream-coloured dolomite
NT 67	3,3 Km NE of Namuskluft Farmstead	Pink quartzite
NT 69	Orange River	Brown gossanous dolomite rock encorporated in ORG
NT 70	Orange River	Chlorite-schist (ORG)
NT 71	Orange River	Coarse-grained sheared volcanic rock
NT 74	Orange River	Chlorite-schist (ORG)
NT 75	Lorelei Mine	Light-brown leucogranite
NT 76	Lorelei Mine	Dark-green amphibolite
NT 77	3 Km west of Rosh Pinah	Brown, sandy quartzite
NT 82	3,5 Km west of Rosh Pinah	Fine-grained, micaceous quartzite
NT 83	6 Km SW of Rosh Pinah	Blue-grey grit
NT 84	6 Km SW of Rosh Pinah	Pebble conglomerate
NT 85	3,5 Km west of Rosh Pinah	Blue-grey dolomite
NT 86	5 Km west of Rosh Pinah	Micaceous feldspathic quartzite
NT 88	5 Km west of Rosh Pinah	Fine-grained, light-brown calcareous quartzite
NT 90	5 Km west of Rosh Pinah	Blue-grey dolomite
NT 91	5 Km west of Rosh Pinah	Quartz-sericite schist
NT 92	5 Km west of Rosh Pinah	Fine-grained, light-brown calcareous quartzite
NT 93	4 Km of Rosh Pinah	White limestone
NT 94	7,5 SW of Rosh Pinah	Micaceous feldspathic quartzites
NT 95	5 Km E of Obib	Light-brown quartzite
NT 97	8 Km west of Rosh Pinah	Black shale
NT100	3 Km NE of Obib	Quartz-sericite schist
NT101	3 Km NE of Obib	Quartz-sericite schist
NT102	3 Km NE of Obib	Biotite-quartz schist
NT103	3 Km NE of Obib	Fine-grained quartzite
NT105	3 Km NE of Obib	Biotite-quartz schist
NT111	2,5 Km NE of Obib	Biotite-chlorite-quartz schist
NT113	2 Km E of Obib	Spotted light-grey quartzite
NT116	5 Km west of Rosh Pinah	Calcareous quartzite
NT128	3,5 Km SW of Pickelhaube Peak	Wallekraal schist - silvery blue-grey, laminated rock
NT136	2,5 Km NW of Dreigratberg	Banded iron formation
NT139	Obib Peak	Hornblende-chlorite schist
NT141	Obib Peak	Small pebble conglomerate
NT143	Valley Thrust-1km west of Obib	Fine-grained, blue-grey dolomite
NT149	500m west of Obib	Light blue-grey dolomite
NT150	Obib Peak	Quartz-biotite-muscovite schist.
NT154	Gumchavib granite inlier	Epidotized grey granite
NT155	Gumchavib granite inlier	Micaceous granite
NT156	Gumchavib granite inlier	Blue-grey granite
NT161	2,5 Km SW of Pickelhaube Peak	Quartz-muscovite-biotite schist
NT162	2,5 Km SW of Pickelhaube Peak	Quartz-muscovite-biotite schist